Taphonomy, palaeoecology and taxonomy of an ophiuroid-stylophoran obrution deposit from the Lower Devonian Bokkeveld Group, South Africa

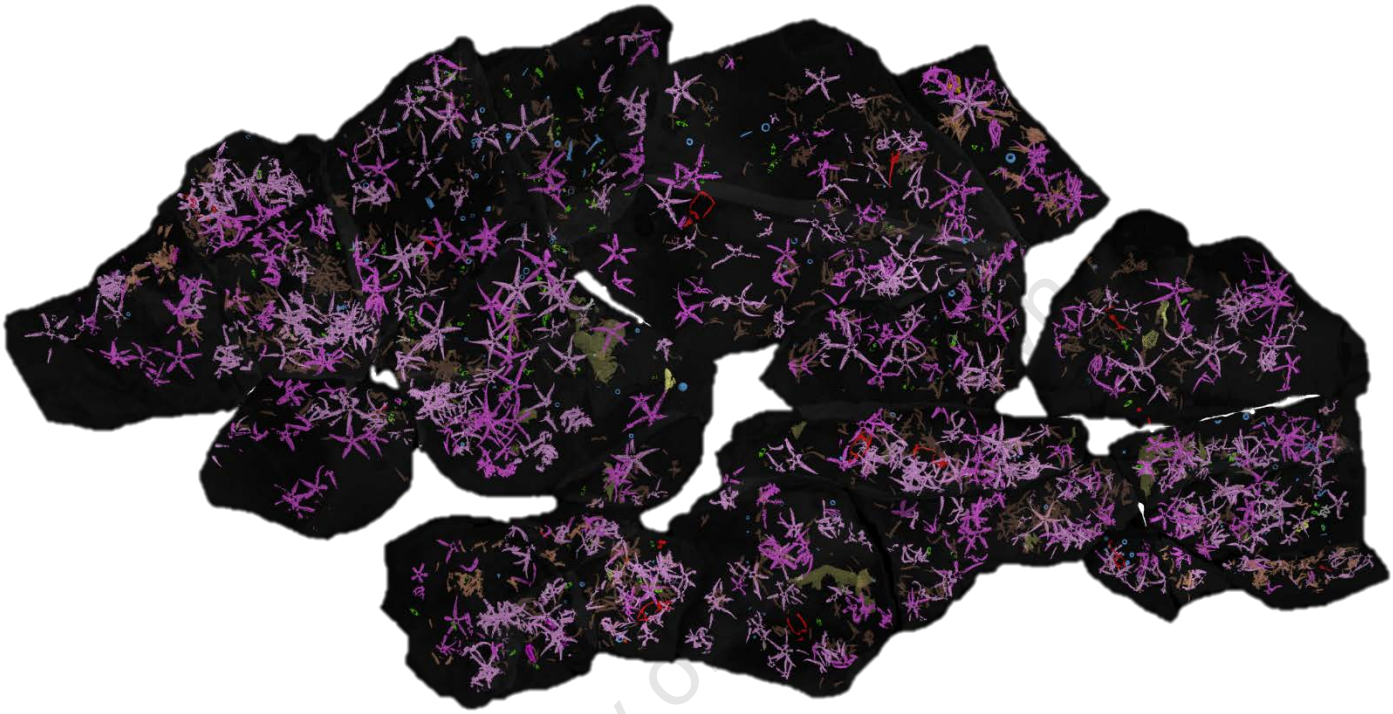

by

Mhairi Reid

Supervisors: Dr Wendy Taylor and Dr Emese M. Bordy

Dissertation presented for the degree of Master of Science in Geology in the Department of Geological Sciences, University of Cape Town

January 2017

DECLARATION

I, Mhairi Reid, hereby declare that the work on which this dissertation/thesis is based is my original work (except where acknowledgements indicate otherwise) and that neither the whole work nor any part of it has been, is being, or is to be submitted for another degree in this or any other university.

Signed by candidate
Signature removed

18 January 2017

ACKNOWLEDGEMENTS

First of all, I would like to express my deepest gratitude to my supervisors for this project, Dr Wendy Taylor and Dr Emese Bordy, whose unwavering guidance, advice, meticulous feedback, support and time, has been invaluable. This research project would not have been possible without funding from the NRF/DST Centre of Excellence in Palaeosciences (CoE-Pal), thank you for the generous funding. My gratitude is extended to Dr. Aaron Hunter for being so kind as to let me be a guest in his home in Australia and for teaching me the intricacies of Paleozoic ophiuroid taxonomy. As well as, Bertrand Lefebvre for his detailed discussion, thoughts and help on the stylophorans. I would like to thank Claire Browning form the Council of Geoscience for helping me whenever I visited and viewed the fossil collections housed there. Further, I would like to thank Dr. Roger Smith for allowing me to use the fossil preparation tools from the Iziko South African Museum. Thank you to the Robles family for use of their farm Karbonaatjies during fieldwork. I would like to thank Cameron Penn-Clarke for his many years of support, helpful discussions and his never ending passion for the fossils of the Bokkeveld Group.

I would like to thank my fantastic team of excavators Bianca Harrison, Claire Browning and Tanya Deyer for all their support. And finally, Michael for wielding the pickaxe like a champion and for being so caring and patient during this time.

ABSTRACT

The Lower Devonian Voorstehoek Formation is a fossil-rich, siliciclastic unit (Ceres Subgroup, Bokkeveld Group, Cape Supergroup) in South Africa. This Emsian unit contains a highly endemic benthic fossil biota characteristic of the cool to cold water Malvinokaffric Realm of southwestern Gondwana. The palaeontological and sedimentological investigations of the Voorstehoek Formation suggest that deposition took place in a shallow marine environment within the storm influenced, proximal part of an offshore transition zone.

A relatively diverse, ophiuroid–stylophoran assemblage, well-preserved in the Karbonaatjies obrution bed, was excavated at the study site in the Hex River Pass, Western Cape. In this study the taphonomy, taxonomy and the palaeoautecology of Palaeozoic ophiuroids and stylophorans was investigated using micro CT scans. Over 60 samples were scanned, manually segmented and stitched together to create a virtual 3D model of a portion of the Karbonaatjies obrution bed. This method allowed for the determination of the degree of fossil articulation, fossil orientation and faunal counts, without damaging the delicate echinoderm fossils. Furthermore, the ability to digitally analyse the fossil-rich bed has revealed an echinoderm assemblage composed of over 700 articulated ophiuroids dominated by a proposed new genus and species *Gamiroaster tempestatis*, over 145 articulated mitrate stylophorans *Paranacystis cf. petrii* Caster, 1954 and eight *Placocystella africana* (Reed, 1925).

Taphonomic analysis of this ophiuroid–stylophoran assemblage indicates this obrution deposit formed due to rapid burial that smothered a potentially gregarious community during a single storm event. Additionally, the admixture of skeletal debris and intact echinoderms present in the Karbonaatjies obrution bed reflects a complex history with significant time-averaging. This unique assemblage provides a taphonomic window into the marine ecosystems of the Early Devonian, including the structure of an unusual, echinoderm-dominated benthic community that forms part of a much wider fossil biota from the Falkland Islands and Precordillera of Argentina, which formed part of SW Gondwana.

TAXONOMIC DISCLAIMER

This thesis is not deemed nor intended to be a valid publication for the naming of new taxa as stipulated in the International Code of Zoological Nomenclature, Article 8.2.

Table of Contents

Supplementary data available from figshare.com: https://figshare.com/s/cefe3dd5fcc4cb8b46d4

CHAPTER 1 INTRODUCTION

Obrution beds are deposits attributed to sudden smothering of benthic communities by rapidly deposited sediments and provide insightful snapshots of offshore marine life on the seabed. They often display unusual or exceptional preservation that provides a glimpse into the ecology of an ancient community. Such deposits are characterised by exceptional fossil abundance (concentration *Lagerstätten*) or preservation quality (conservation *Lagerstätten*) and provide information that would otherwise be removed from the fossil record by taphonomic processes (Seilacher *et al.*, 1985). *Konservat* or conservation *Lagerstätten* are responsible for a large proportion of Palaeozoic metazoan marine diversity, and iconic examples include the Burgess Shale of British Columbia (e.g., Gould, 1989; Butterfield, 1990), Hunsrück slate of Germany (e.g., Bartels *et al*., 1998; Glass and Blake, 2002) and Mazon Creek of northern Illinois (e.g., Baird *et al*., 1985). These famous *Lagerstätten* are known for having exceptionally preserved soft tissues, while obrution deposits such as the Rochester Shale of western New York preserve articulated multielement skeletons (only hard parts) that, as a consequence, are often overlooked and yet are an invaluable source of taphonomic, palaeoecological and taxonomic data (e.g., Taylor and Brett, 1996). Taphonomy, the study of processes of preservation and how they affect information in the fossil record, was originally recognised by a Russian palaeontologist Ivan Efremov in 1940 and unites aspects of both paleoecology and sedimentology (Behrensmeyer and Kidwell, 1985; Behrensmeyer *et al*., 2000). Modern research in taphonomy is associated with the documentation of information loss and bias in the fossil record and relies heavily on actualistic comparisons. This is a challenge for many taphonomists studying ancient fauna such as stylophorans, with little or no modern affinities. Echinoderm taphonomy is a somewhat different approach to the more traditional invertebrate taphonomic studies that have often concentrated on molluscs, brachiopods and bivalves (for extensive reviews on echinoderm taphonomy see Lewis, 1980; Donovan, 1991; Brett *et al*., 1997; Ausich, 2001; Nebelsick, 2004). Echinoderms are unique in having multielement endoskeletons consisting of individual calcium carbonate plates connected to each other with soft tissue and thus more akin to arthropods and vertebrates in that disarticulation of the skeletons is the rule and not the exception (Nebelsick, 2004). Preservation varies widely between different echinoderm groups as rates of disarticulation of echinoderm skeletons is dependent on the constructional morphology of the specific group. Brett *et al*. (1997) divided echinoderms based on the time required for complete disarticulation and classified both

ophiuroids and stylophorans as 'Type 1' which consists of weakly articulated forms with plates (ossicles) bound together by ligaments and other soft tissues. Ophiuroid and stylophoran skeletons can only be preserved intact if buried very rapidly (within hours to days) after death and in rare cases, as seen in this study, buried alive by obrution events (*sensu* Brett, 1990). Rapid and deep burial of benthic communities shields them from decay and scavengers, but also prevents the escape of mobile taxa (Brett and Baird, 1986; Speyer and Brett, 1991; Brett *et al*., 1997). Echinoderm decay and disarticulation processes have been demonstrated by many field and lab studies (e.g., Meyer, 1971; Kidwell and Baumiller, 1990; Gorzelak and Salamon, 2013). Specific to this study Kerr and Twitchet (2004) investigated modern ophiuroids that displayed several stages of disarticulation related to post-mortem burial. It was found that at 6° C, dead ophiuroids begin disarticulation within 15 hours due to rapid decay of connective tissue (rate doubles with each 10° C rise in temperature), thus rapid burial must occur to preserve fully articulated specimens (Kerr and Twitchet, 2004). Therefore, it is all the more remarkable to find well preserved ophiuroids (and stylophorans) with their community structure intact, giving snap shots of the ancient seafloor community. Thus, inferences about the paleoecology of echinoderms can be made and aid in understanding the living ophiuroids of today.

In a previous study conducted by Reid *et al*. (2015), a well-preserved ophiuroid–stylophoran assemblage, the Karbonaatjies obrution bed, was reported in a thin, fossiliferous bed from the Lower Devonian (Emsian ~400 Ma) Voorstehoek Formation. The main focus of this preliminary report resulted in a detailed assessment of the small-scale vertical and lateral facies changes of the sedimentary architecture at the main field site. Fossil and sedimentary evidence at this site indicate that storm deposits (tempestites) rapidly buried benthic communities living on a shallow marine shelf environment. Conventional palaeontological analysis of this deposit posed problems due to the fragile state of the fossils caused by the deep chemical weathering of the originally calcitic fossils, leaving voids or moulds. To retrieve more useful data, selected samples from the Karbonaatjies obrution bed were micro-CT scanned resulting in extraordinary resolution of the specimens. This powerful technique allowed the visualisation of not only the degree of articulation and types of taxa present (that otherwise would have been missed), but also the orientation of fossils within the rock. This presented an excellent opportunity for both taphonomic and taxonomic analysis and for further understanding of the palaeoautecology of Palaeozoic ophiuroids and stylophorans. Therefore, the purpose of this research project is to:

1) Resolve whether the ophiuroid–stylophoran associations represent a distinct palaeoecological association or are the result of taphonomic bias.

2) Understand the paleoecology of ophiuroid–stylophoran associations providing insights into the original community structure and organism interactions.
3) Determine the depositional environment and conditions that facilitated the rapid burial and extraordinary preservation.
4) Add to and revise existing taxonomic descriptions for Devonian ophiuroids of South Africa.

This is achieved by microCT scanning of a larger section of the Karbonaatjies obrution bed and conducting semi-quantitative taphonomic analysis of the three dimensionally reconstructed fossil bed. Finally, by integrating the taphonomic and sedimentological findings, a more accurate understanding of Early Devonian marine communities as well as a detailed reconstruction of the paleoenvironment of the Voorstehoek Formation will emerge.

To date, the taphonomy of echinoderm assemblages within the Voorstehoek Formation has received little attention as previous studies have focused on systematic palaeontology and biostratigraphy. The unique preservation of Bokkeveld invertebrate assemblages has often been associated with obrution beds (Hiller and Theron, 1988). Such beds contain crinoid calyces, arms and stems found from the Gydo Formation, as well as exquisitely preserved bryozoans, complete trilobites and adult to immature ophiuroids found from the Waboomberg Formation (Hiller and Theron, 1988; Jell and Theron, 1999). These “starfish beds” have often been associated with large numbers of infaunal bivalves preserved at high angles to the bedding. Stylophorans within this formation are often associated with ostrocod fauna and *Lingula* brachiopods (Ruta and Theron, 1997). Both well-preserved ophiuroids and stylophorans are known to occur in the Voorstehoek Formation (Ruta and Theron, 1997; Jell and Theron, 1999), but abundant, fully-articulated remains of both ophiuroids and stylophorans within the same bed have not been formally described from the Devonian of South Africa.

Ophiuroids, commonly known as brittle stars, are the most diverse living class within the phylum Echinodermata and make an important component of present-day marine benthic communities (Stöhr *et al*., 2012). Modern ophiuroids are characterised by their stellate shape with a well-defined disk separated by five (but in some cases six or more) long slender arms and are found across all modern environments from the Arctic regions to the Equator (Stöhr *et al*., 2012) (Fig. 1A). Their fossil record can be traced back at least to the Early Ordovician. Palaeozoic ophiuroids are fundamentally different in the organisation of the skeleton very

different in form from their Mesozoic to modern relatives: the disks are much larger; arms broader and are made up of unfused opposite or alternating ambulacrals (as opposed to fused ambulacrals) thus making their overall appearance more asteroid-like (Fig. 1B). However, Palaeozoic ophiuroids do have clear affinities to modern ophiuroids even though they are only distantly related to living ophiuroid species. Consequently, they have rather different morphologies and, presumably, taphonomic pathways. Stylophorans are an extinct Palaeozoic group of asymmetrical, non-pentaradiate calcite plated marine fossils that lived from the Middle Cambrian to the Late Carboniferous (Lefebvre, 2003) (Fig. 1C). The class Stylophora (Gill and Caster, 1960) comprises the two orders Cornuta (Jaekel, 1901) and Mitrata (Jaekel, 1918), which includes over 120 species. Stylophorans are characterised by an asymmetrical to nearly bilaterally symmetrical theca and a long flexible appendage (the aulacophore) inserted into the theca (Lefebvre, 2003). Both stylophorans found within this study belong to the order Mitrata, which have a nearly bilaterally symmetrical theca that comprises robust marginal plates. The theca shows two surfaces: flat or slightly concave surface and a slightly convex surface. The appendage (aulacophore) has been subject to much controversy over the years: it is seen as a muscular stalk (e.g., Philip, 1979; Kolata and Jollie, 1982), a chordate tail (e.g., Jefferies, 1967; Cripps and Daley, 1994), a muscular locomotory organ (Clausen and Smith, 2005); a feeding arm (e.g., Ubaghs, 1961; Parsley, 1988; David *et al*., 2000); or a combined feeding and locomotory structure (e.g. Parsley, 1988 ; Ruta, 1999) . Stylophorans in this study are treated as echinoderms, there are however, many debates on whether stylophorans are basal chordates (calcichordate model, e.g., Jefferies, 1968; Cripps, 1989), stem group echinoderms (echinoderm I model, e.g., Chauvel, 1941; Ubaghs, 1975; Paul and Smith, 1984) or derived echinoderms (echinoderm II model, e.g., Sumrall, 1997; David *et al.,* 2000).

To be noted throughout the paper, the term “Karbonaatjies obrution” bed is often substituted for the “fossiliferous bed” and the “obrution bed”. All terms should be considered synonymous.

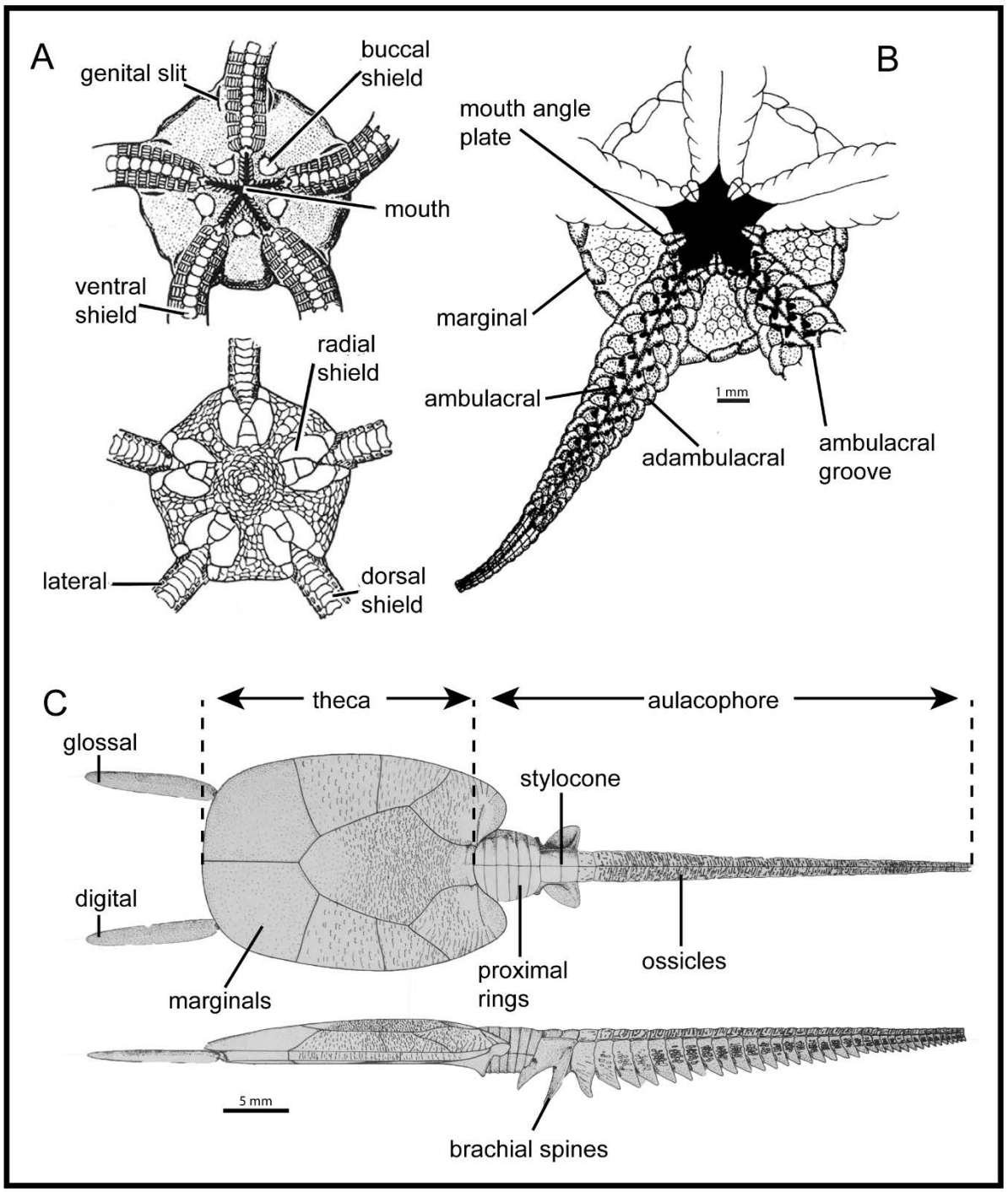

Figure 1. (**A**) Morphology of a modern ophiuroid showing the central disk and long thin arms with vertebrae and enclosing plates (Taken from Spencer and Wright, 1966). (**B**) *Crepidosoma wenlocki* Spencer, 1930; partial reconstruction of oral surface, an example of a Palaeozoic ophiuroid (taken from Lewis *et al*., 2007). (**C**) Reconstruction of the mitrate stylophoran *Placocystella africana* (Reed, 1925), top and bottom figure view of the flattened thecal surface (taken from Ruta and Theron, 1997). Reconstructions are not to scale.

1.1 GEOLOGY OF THE BOKKEVELD GROUP

1.1.1 Geological context

The study area is located within the southern part of the north-south trending Clanwilliam Sub-basin of the Cape Basin and the exposed rocks lithostratigraphically belong to the Voorstehoek Formation (Rust, 1973), one of the lowermost units of the Bokkeveld Group (Figs. 2-4). The studied outcrop is located ~80 km E of Ceres near the Hex River Pass in the Western Cape Province (GPS: 33°24003.600S, 19°52042.700E Karbonaatjies Farm) (Fig. 2). The outcrop is an E–W orientated road cutting of ~80 m in length and ~2 m in height along the N1 highway. Situated within the northern limb of an E-W striking syncline in the Cape Fold Belt, the beds of the outcrop dip 20" S and show evidence of E-W faulting and shearing. The Karbonaatjies obrution bed forms part of a succession of medium to fine-grained sandstones interbedded with siltstones and sandy mudstones from the lower half of the Voorstehoek Formation. Typical sedimentary features are summarised in figure 3.

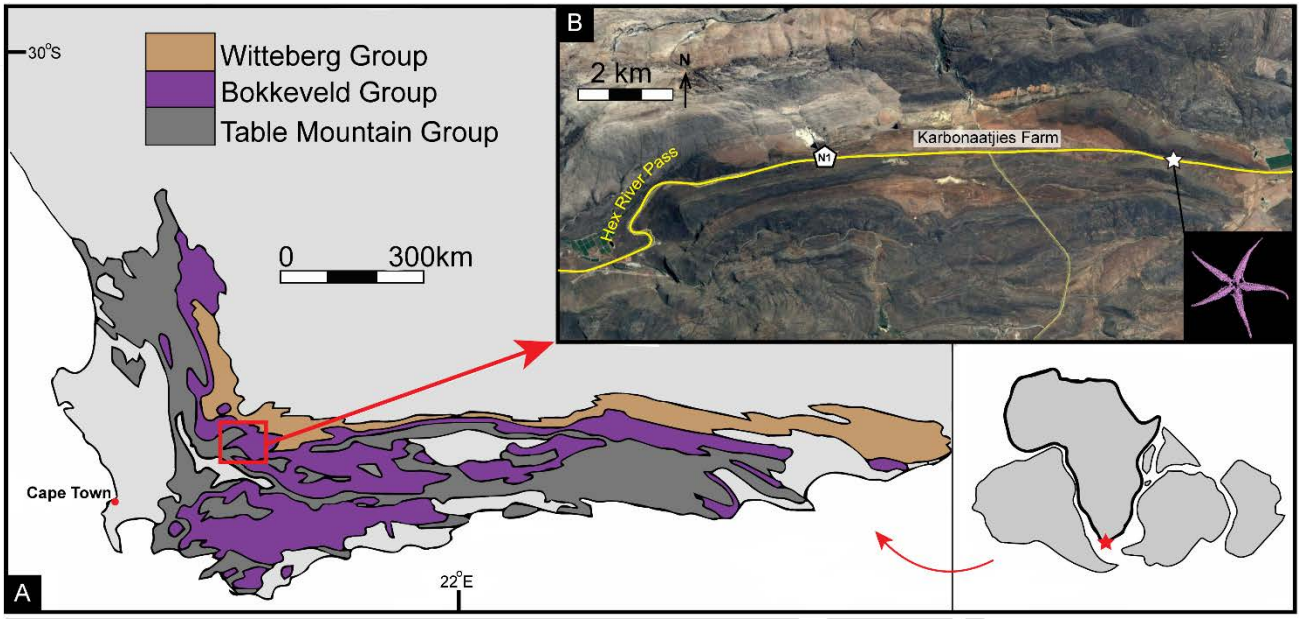

Figure 2. (**A**) Simplified geological map of the Cape Supergroup in South Africa. Location of the fossil locality (red square) within the Cape Fold Belt, ~145 km NE of Cape Town, insert shows Africa's position within Gondwana (redrawn and modified from Reid *et al*., 2015; Theron and Loock, 1988). (**B**) Arial photograph of approximate location of the Karbonaatjies obrution bed (pink 3D image of ophiuroid), along the N1 national road (yellow line) on the Western Cape Province (South Africa).

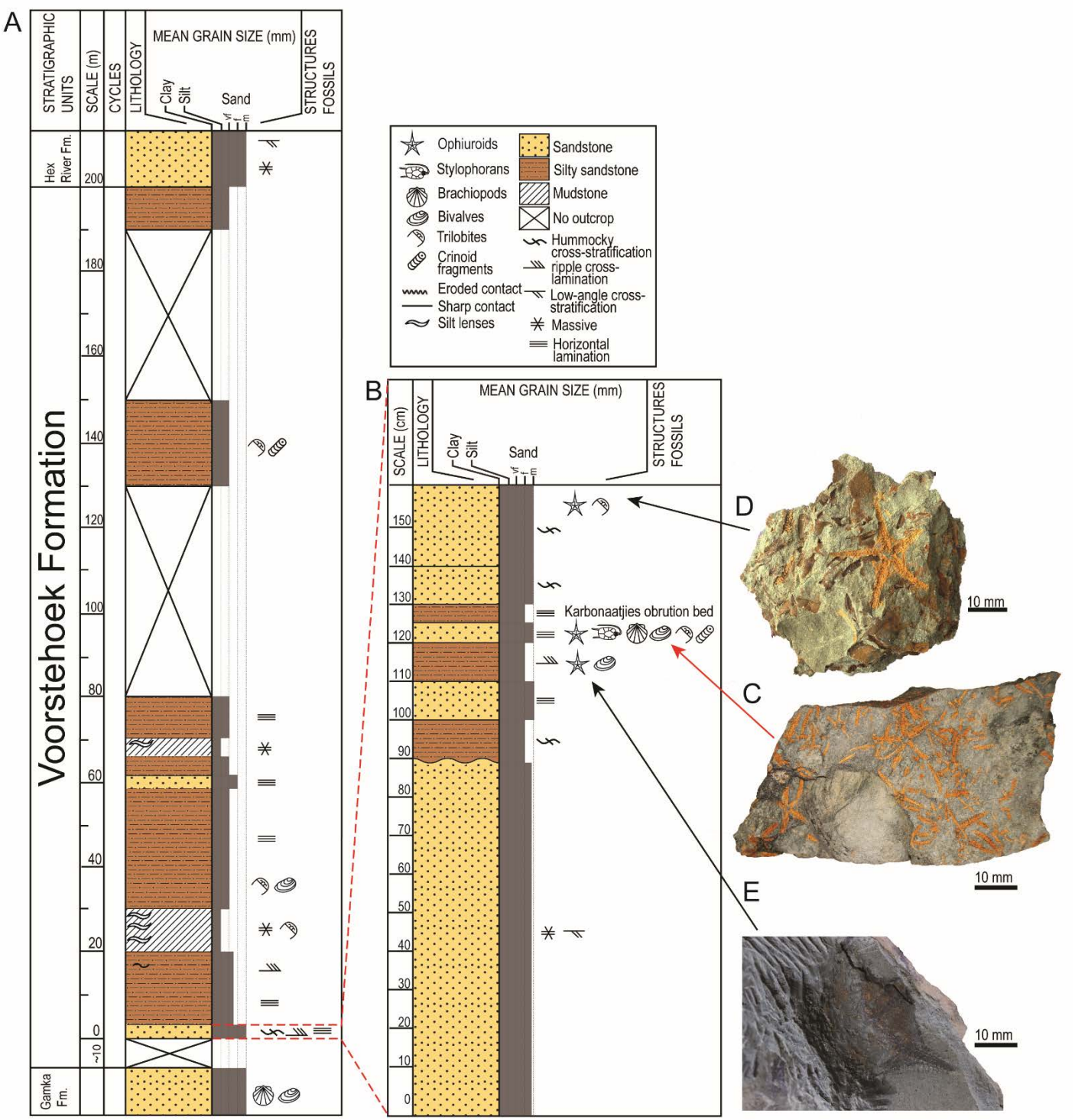

Figure 3. (**A**) Stratigraphic section of the Voorstehoek Formation showing the location of the Karbonaatjies obrution bed (dashed red lines). (**B**) High resolution sedimentary log of the investigated section with features indicative of an offshore transition zone in a storm-dominated shelf. (**C**) Arrow marks location of the Karbonaatjies obrution bed from the lower Voorstehoek Formation. (**D**) and (**E**) Location of other ophiuroid specimens found and described in this study.

Forming the middle unit of the clastic Cape Supergroup, the distinctly argillaceous Bokkeveld Group conformably overlies the Table Mountain Group and underlies the Witteberg Group (see legend in Fig. 2). The Bokkeveld Group is a ~0.7–3.5 km thick succession of Lower to Middle Devonian siliciclastic, mostly marine sedimentary rocks, ranging in age from Lochkovian (~419 Ma) to Givetian (~382 Ma; e.g., Theron, 1970; Boucot *et al*., 1983; Hiller and Theron, 1988; Theron and Johnson, 1991; Fourie *et al*., 2011). Age determination is based on faunal associations within different units; the occurrence of *Proboscidina arcei* on the Gydo Formation restricts the Bokkeveld Group to the Emsian (Lower Devonian) (Boucot and Theron, 2001), while the occurrence of terebratuloid brachiopod *Rhipidothyris* in the Karoopoort Formation restricts it to the Givetian (Middle Devonian) (Boucot and Theron, 2001).

The Bokkeveld Group crops out within the Permo-Triassic Cape Fold Belt of the Western and Eastern Cape Provinces of South Africa (Fig. 2). The six lowermost Bokkeveld formations, collectively referred to as the Ceres Subgroup (Fig. 4), extend across the entire Cape Fold Belt from east to west. The Ceres Subgroup consists of three laterally continuous, upward-coarsening successions of mudstones, siltstones and sandstones (Fig. 3) that have been interpreted as evidence for: a) deposition in muddy offshore to sandy nearshore settings on a stable, storm-dominated marine shelf; and b) repeated basinward shifts of an E–W striking shoreline after major transgressive events (Theron and Johnson, 1991). Found in the middle part of the Ceres Subgroup, the mudstone-rich Lower Devonian (Emsian) Voorstehoek Formation is sandwiched between the sandstones of the underlying Gamka Formation and the overlying Hex River Formation. The thickness of the Formation varies widely from east to west, but in this study area, it is estimated to be ~100 m thick (Theron, 1972, 2003). The Voorstehoek Formation is dominated by dark grey to olive grey siltstones (up to 65%), mudstones (up to 60%) and minor sandstones. When unweathered, these rocks are dark grey to olive grey in colour, however in most outcrops, they have been heavily weathered to pale yellow brown, grey, orange and red, and are often covered by a red, ferruginised crusty layer. The lower part of the Formation is made up of dark grey mudstones with thin calcareous lenses, which up-sequence, give way to siltstone and thin sandstone lenses. Common features found in the upper part of the Formation are storm deposits (tempestites or event beds) comprising wave ripple cross-lamination and hummocky cross-stratification that increase in frequency indicating a shallowing upward succession (Theron, 2003). The sedimentary features in these

heterolithic tempestite-dominated successions suggest that the Formation was deposited in a predominantly shallow marine environment.

The rocks of the Bokkeveld Group have a well-developed cleavage that formed during the Permo-Triassic deformation of the Cape Supergroup (Johnson, 1976). This tectonic overprint increases southward and eastwards of the Cape Fold Belt, however metamorphism has only reached lower greenshist facies throughout (Theron, 1999). Fossil deformation within the Voorstehoek is minimal.

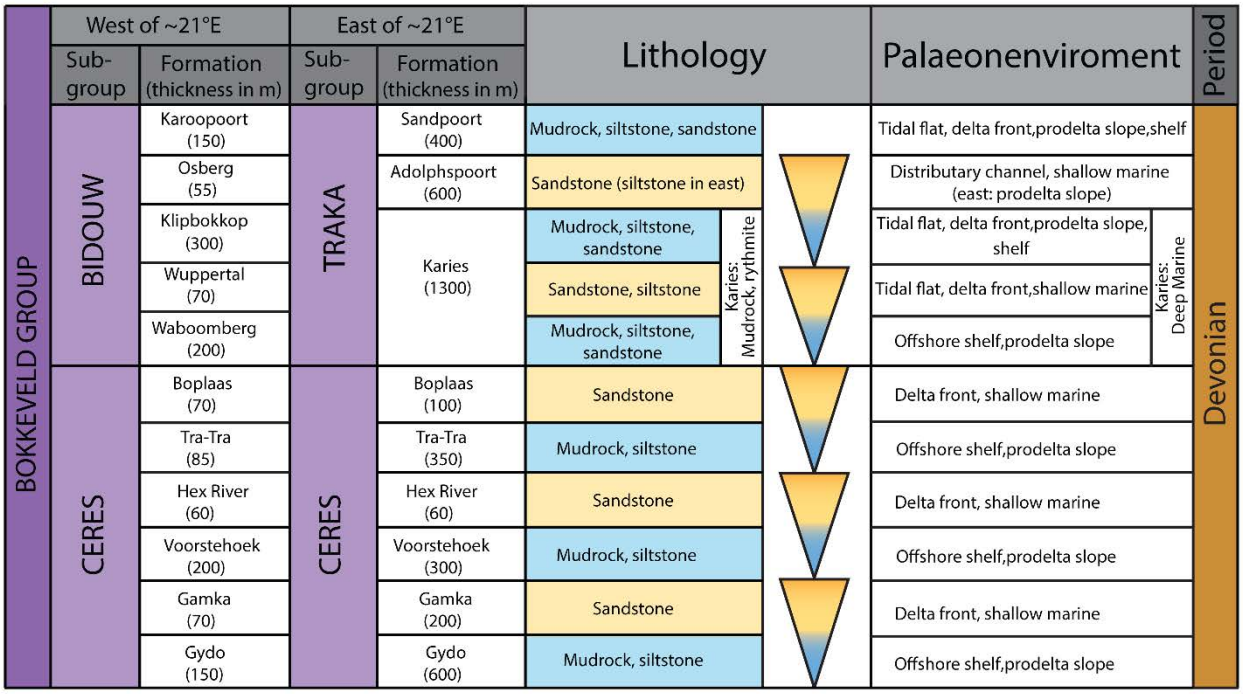

Figure 4. Stratigraphy of the Devonian Bokkeveld Group. Triangles indicate large-scale, upward-coarsening cycles, which represent shallowing upwards successions. Age of the Voorstehoek Formation is Emsian (~400 Ma old) (figure taken from Reid *et al*., 2015).

1.1.2 Depositional environment

Sedimentary controls within the Cape Basin are largely unresolved (Broquet, 1992), although the depositional environment in which the Bokkeveld Group rocks formed is unambiguously marine as is evident from the fossil content. The alternating argillaceous and arenaceous formations that make up the group represent vertical stacking of five coarsening-upward sequences which imply a history of either tectonically or eustatically controlled regressive and transgressive cycles and thus record the most dynamic phase of the Cape basin development (Theron, 1972; Rust, 1973; Tankard and Barwis, 1982; Theron and Loock, 1988). These five major cycles have been envisaged as a number of lobate, wave-dominated deltas prograded south and south-eastwards into a wave and storm dominated epeiric sea (Theron, 1972; Tankard and Barwis, 1982) (Fig. 5). Initially, transgressions were possibly induced by an increase in tectonic subsidence, and eustatic rise in sea levels which resulted in a rapid basin-wide deepening and marked the deposition of Gydo Formation into deeper water. Following this, regression resulting in the deposition of the more arenaceous Gamka Formation indicative of a gradual shallowing. The series of regressions and transgressions are marked by the alternating pelites and arenites that continue throughout the Bokkeveld (Theron, 1999).

The tabular and lateral continuity of the sandstone deposits in the Voorstehoek Formation and the occurrence of marine invertebrate fossil assemblages are all indicative of a shallow clastic marine environment. The Voorstehoek Formation forms the basal part of the second coarsening-upward deltaic cycle of the Bokkeveld Group. The vertical increase in abundance of sandstones, their grain size and the prevalence of storm deposits are indicative of a shallowing-upward (shoaling) succession. This has been interpreted as evidence for a large scale, basin-wide regressive episode in the southern part of the Clanwilliam sub-basin in the Emsian (Theron, 2003). Furthermore, in the north–south trending Clanwilliam sub-basin, the abundance of the sandstone facies increases from south to north, and this, together with other sedimentological evidence (Theron, 2003), suggests that in the north, the basin was shallower and deposition occurred above the fair-weather wave-base. For the northern region, ancient delta-slope to inner shelf as well as tidal flats (based on some structures indicative of brief exposure) are suggested as potential depositional environments (Theron, 2003) (Fig. 5). In summary, the Voorstehoek Formation was deposited in a shallow marine, inner shelf setting (with potential deltas and tidal flats) in the north, whereas in the south, near to the location of the outcrop, the sedimentation occurred in a deeper water setting closer to the outer shelf (Fig.

5). In this southern region of the Clanwilliam Sub-basin, the older strata of the Voorstehoek Formation were initially deposited in the offshore zone, and then, as the overall shallowing of the sub-basin occurred, in the offshore transition zone (Reid *et al*., 2015).

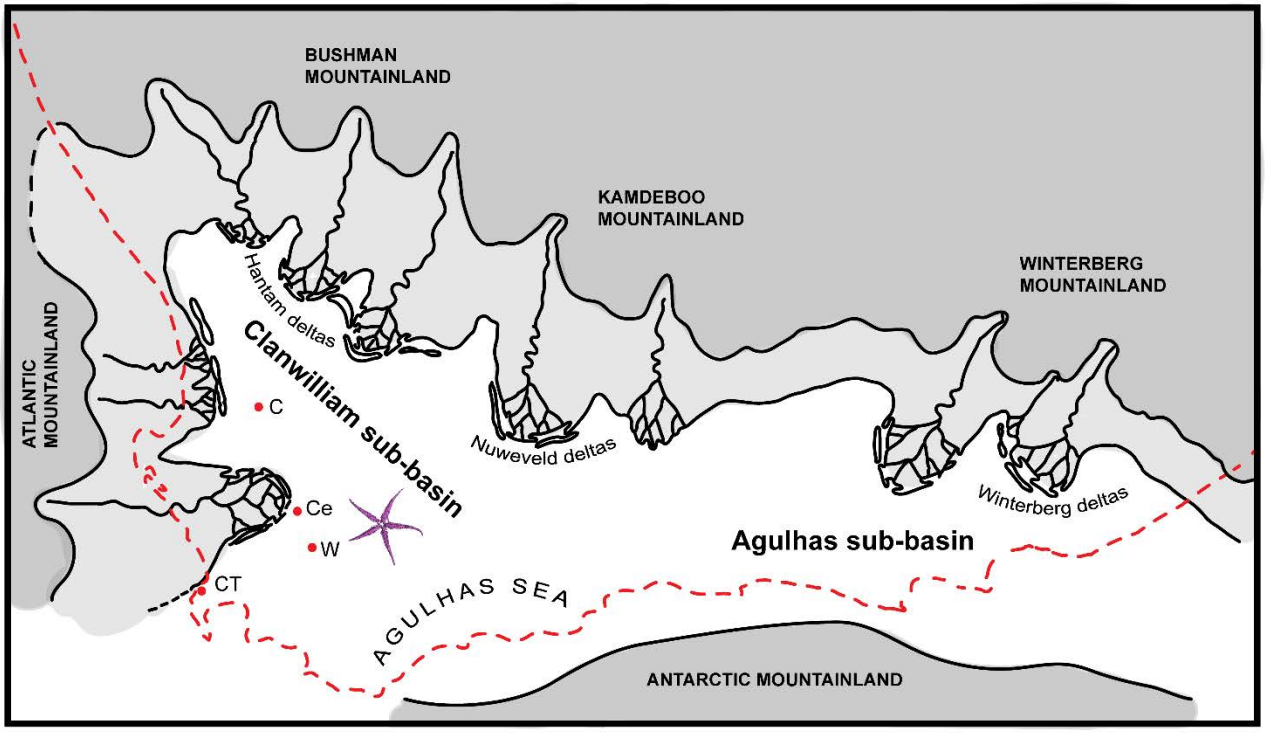

Figure 5. Interpretative model of SW Gondwana during the Bokkeveld Deposition**.** Theron (1972) proposed four large depocenters to have existed within the Bokkeveld Basin at the time of sedimentation; the shallow Clanwilliam sub-basin contained the Hantam and Saldanha Deltas, whilst in the East the deeper Agulhas sub-basin contained the Nuweveld and Winterberg Deltas. Detailed palaeocurrent analysis as well as isopath maps complied by Theron (1972) revealed a predominantly south to south-western palaeoslope and thus a north to eastern provenance area (Bushman, Kamdeboo and Winterberg Mountainlands), as well as a western provenance (Atlantic Mountainlands) where progradation was directed westward. C = Clanwilliam; Ce = Ceres; W = Worcester; CT = Cape Town (redrawn and modified from Theron, 1972).

1.1.3 Previous study on the depositional environment of the Karbonaatjies obrution bed

In a preliminary report conducted by Reid *et al*. (2015), the sedimentary successions were identified as proximal storm deposits or event beds as they displayed a characteristic facies succession ranging from massive conglomerate beds with reworked brachiopod fossil fragments (storm erosion) at the base, to amalgamated beds of fine sandstone with hummocky cross-stratification (main storm deposition). This succession is overlain by minor wavy lamination and wave ripple cross lamination (waning storm deposition) which gives way to

fair weather mud deposits at the top. It was concluded based on these sedimentary features that the fossiliferous bed formed in a shallow marine environment, within the storm influenced, proximal part of an offshore transition zone (Fig. 6).

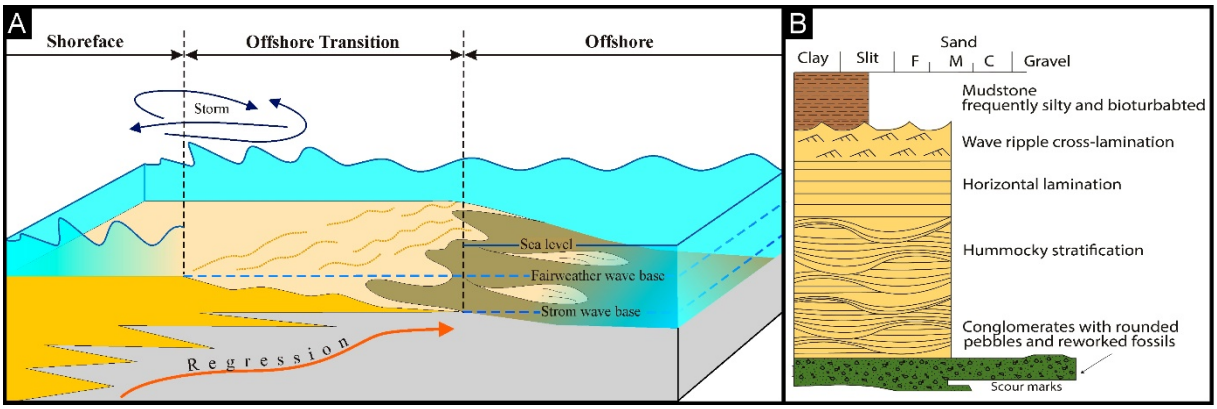

Figure 6. (**A**) Generalized depositional model of a storm-influenced shelf setting within the southern part of the Clanwilliam Sub-basin during the deposition of the Voorstehoek Formation (taken from Reid *et al*., 2015). (**B**) Schematic illustration of a proximal storm deposit (tempestite) showing basal conglomerates beds with fossils and mudstone pebbles; amalgamated beds of hummocky cross-stratified sandstones and minor wavy lamination and wave ripple cross-lamination (taken from Reid *et al*., 2015).

1.2 PALAEONTOLOGY OF THE BOKKEVELD GROUP

The fossiliferous nature of the Lower Devonian Bokkeveld Group was first recorded in 1830 (e.g., Grisbrook, 1830; Thom, 1830; Salter, 1856; Wyley, 1859) and in a comprehensive review by Reed (1925). Faunal lists have been compiled by Du Toit (1956) and Oosthuizen (1984). The Ceres subgroup is characterised by a wide variety of benthic invertebrate fossils. These fossil assemblages are dominated by trilobites (most common is *Burmeisteria* Salter, 1865), brachiopods (most common are *Australocelia* Boucot and Gill, 1956; *Australospirifer* Caster, 1939 and *Pleurochonetes* Isaacson, 1977) and bivalves (most common are *Nuculites* Conrad, 1841 and *Palaeoneilo* Hall and Whitfield, 1869). Less common taxa include molluscs (bivalves, gastropods, orthocone nautiloids) and echinoderms (asteroids, ophiuroids, crinoids, stylophorans) with minor taxa including corals, conulariids, tentaculitids, fish remains; in addition, there is a richly diverse association of trace fossils of the *Cruziana* ichnofacies (Theron 1972, 2003; Cooper, 1982; Oosthuizen, 1984; Theron and Loock, 1988; Hiller and Theron, 1988; Gresse and Theron, 1992; Almond *et al.,* 1996). These shelly fossil assemblages are generally preserved as moulds and are abundant within the mudrock dominated units such as the Gydo, Voorstehoek and Waboomberg Formations (Bidouw Subgroup). Unweathered

fossil samples often display pyritic encrustations, the most well preserved fossils occurring within concretions (Oosthuizen, 1984; Theron, 1972; Theron, 1999). Invertebrate assemblages of the Voorstehoek Formation are often disarticulated and concentrated in shell lenses and coquinites, which further suggest strong current action, created by storm waves in nearshore environments (Hiller and Theron, 1988). Compared to the collections of marine invertebrate faunas from the underlying Gydo Formation, the collections from the Voorstehoek Formation are smaller with sparser, less diverse (possibly due to collection bias) and poorly studied fossil material (Oosthuizen, 1984; Hiller and Theron, 1988). There appears to be a distinct difference in size and faunal composition of invertebrate fossils in the western Bokkeveld Group brachiopods and bivalves (such as *Australocoelia* and *Australospirifer*), which appear to much larger than that in the eastern Bokkeveld Group. In addition, echinoderms and trilobites are more common in the west while in the east conularians, anthozoans and hyolthids are more common (Oosthuizen, 1984). Overall the invertebrate fossil content of the Bokkeveld Group decreases northwards as the argillaceous units become sandier (Hiller and Theron, 1988).

Certain taxa within the Bokkeveld Group appear to be limited to particular lithologies (Theron, 1972; Oosthuizen, 1984; Cooper, 1982). Trilobites and cephalopods are generally confined to the argillaceous formations, while gastropods, bivalves and brachiopods are found in the arenites. Crinoids occur throughout the succession and are generally preserved as stem fragments and isolated columnals with rare well-preserved crowns occurring within the finer grained sediments. Ophiuroids, stylophorans and blastoids appear mainly in the dark grey mudstones and shales. However, the ophiuroids and stylophorans discovered in this study are found within the silty sandstone units of the Voorstehoek Formation.

1.2.1 Malvinokaffric Realm Biota

The Devonian Bokkeveld Group of South Africa comprises invertebrate fossil assemblages that belong to the unique cool to cold water, high latitude Malvinokaffric Realm, a biogeographic term first introduced by Richter (1941) and originally used to denote the highly endemic, benthic marine, Devonian invertebrate faunas of the Southern Hemisphere (Fig. 7). Initially defined based on the distribution of endemic Devonian trilobites and brachiopods (Clarke, 1913; Richter and Richter, 1942; Boucot *et al.,* 1969; Eldredge and Ormiston, 1979), this polar biogeographic unit now encompasses the Early Palaeozoic (Late Ordovician to Middle Devonian (Eifelian) invertebrate fossil assemblages of south-western Gondwana which extend from South America, southern Africa, Falkland Islands and Antarctica (Boucot, 1985, 1988; Melo, 1988). The Devonian Malvinkaffric Realm, a time of high level provincialism (Boucot, 1988), is recognised as a major palaeogeographic division based on evidence from the endemic distribution of trilobites (Clarke, 1913, Richter and Richter, 1942 ; Eldredge and Ormiston, 1979) and brachiopods (e.g., Boucot *et al.,* 1969). Generally, the Malvinokaffric Realm is characterised by a low-diversity fauna with abundant conulariids and hyolithids and the absence of certain major groups such as stromatoporoids, conodonts, nautiloids, and graptolites, with almost no thermophilic reef-building corals or bryozoans (Oliver, 1980; Bigey, 1985; Boucot, 1985, 1988; Hiller and Theron, 1988; Meyerhoff *et al.*, 1996). The Malvinokaffric biota of the Bokkeveld Group comprises both highly endemic species (e.g., certain bivalves and brachiopods) as well as several widespread taxa (e.g., *Australospirifer* sp., *Australocoelia* sp., *Burmeisteria* sp.) that are also found in the Devonian of the Falkland Islands and southern parts of South America (Ponta Grossa Formation in the Parana Basin) (e.g., Reed, 1906; Clarke, 1913; Richter and Richter, 1942; Melo, 1988; Almond *et al.,* 1996; Boucot, 1999).

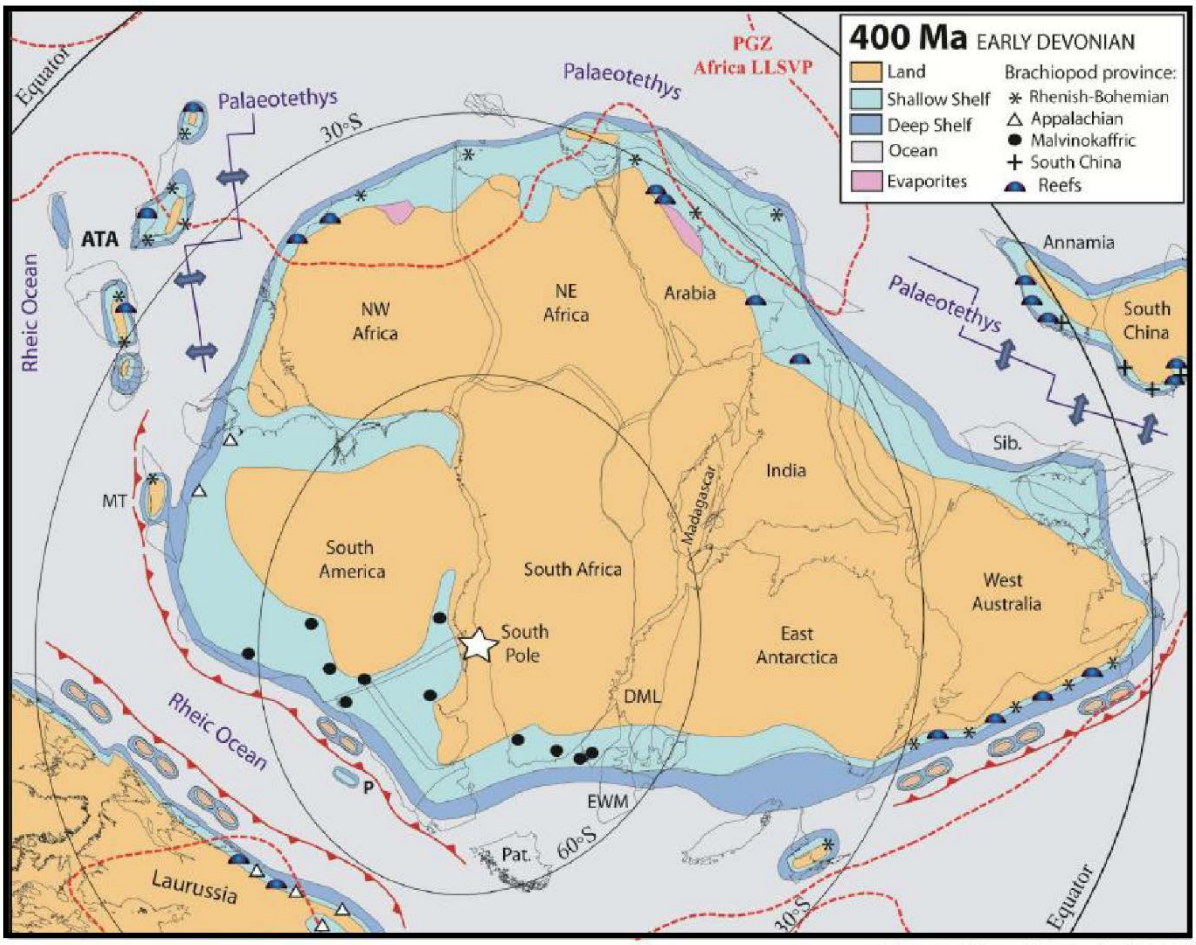

Figure 7. Gondwana and nearby palaeocontinents at 400 Ma, in the Early Devonian (Emsian). Showing the distribution of the highly provincial brachiopod faunas (black dots = Malvinkaffric Realm Biota) (taken from Torsvik and Cocks, 2013).

1.2.2 Paleoecology of the Voorstehoek Formation

Hiller and Theron (1988) correlated Bokkeveld benthic communities with the depositional sub-environments of the deltaic complexes proposed by Theron (1972). Four benthic communities are recognised within the deltaic sequence: the tidal flat community represented by the Weltevrede Formation (Witteberg Group) that is dominated by inarticulate brachiopods (e.g., *Lingula*) and infaunal bivalves that inhabited the sheltered, back barrier environment; the distributary mouth bar community (the highest energy environment) represented by the Gamka Formation, overwhelmingly dominated by brachiopods, in particular *Australospirifer* that occupy the turbulent shallow water setting of the deltaic fringe; the delta slope environment represented by the Gydo Formation and to some extent the Voorstehoek Formation, which consists of a much more diverse community of brachiopods, infaunal bivalves, gastropods,

cricoconarids, crinoids and trilobites; the shelf community represented by the Voorstehoek Formation (Fig. 8), lower parts of the Gydo Formation and western outcrops of the Waboomberg Formation, which contains the most diverse community, with brachiopods (making up less than half of the assemblage), abundant trilobites, bivalves and gastropods and a significant proportion of echinoderms, hyoliths, corals, bryzoans, conulariids and cephlaopods. The shelf community occupied a deeper water environment beyond the effects of wave and tidal activity. Most forms were adapted for living unattached on a soft substrate (e.g., free-living brachiopods like *Schuchertella*). *Australospirifer* specimens are found to be much smaller than specimens within the shallow water communities and were adapted to live either attached to the substrate by a pedicle in turbulent water or free-living on the substrate in more quiet water (McGhee, 1976). Notably, this community contains a high number of deposit feeders such as the infaunal bivalves *Nuculites* and *Palaeoneilo* (both found within the studied outcrop) and possibly some trilobites, ophiuroids and stylophorans.

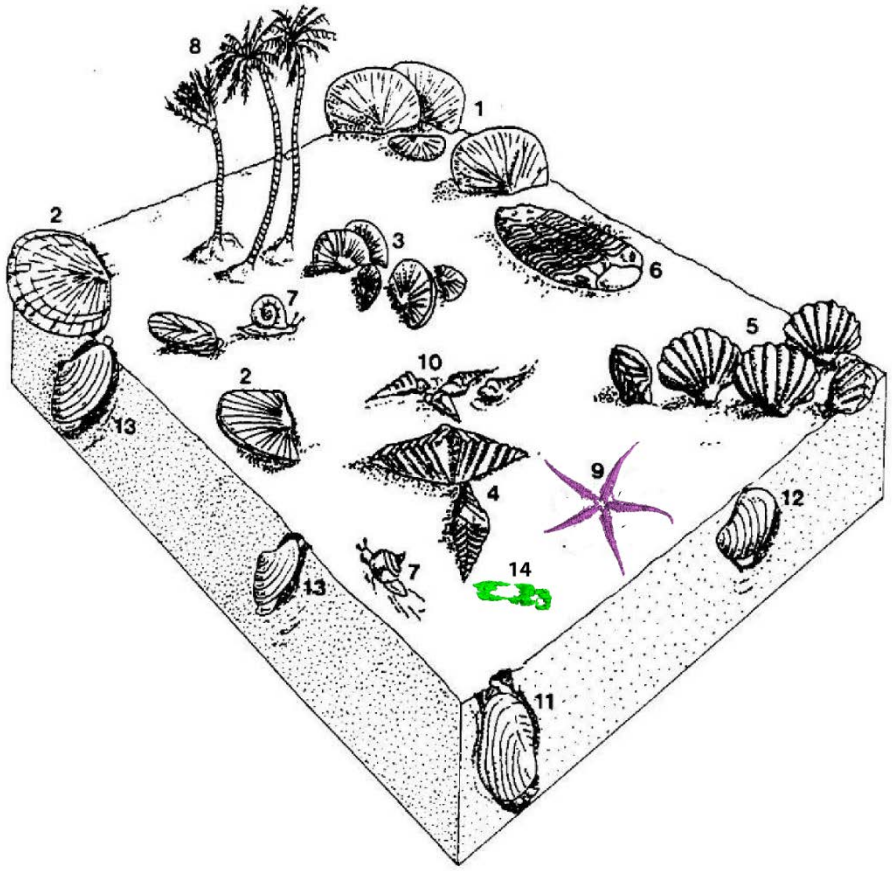

Figure 8. Reconstruction of the shelf community from the Voorstehoek Formation (Lower Bokkeveld Group): (1) *Australostrophia*; (2) *Schuchertella*; (3) *Pleurochonetes*; (4) *Australospirifer*; (5) *Australocoelia*; (6) the trilobite *Metacryphaeus*; (7) the gastropod *Pleurotomaria*; (8) crinoids; (9) ophiuroids; (10) hyoliths; (11) bivalves *Sanguinolites*; (12) *Palaeoneilo*, (13) *Nuculites*; (14) stylophorans (modified from Hiller and Theron, 1988).

CHAPTER 2 MATERIALS AND METHODS

2.1 EXCAVATION AND PREPARATION

Fieldwork for this project was undertaken in a road cutting on Karbonaatjies farm, which is situated ~145 km northeast of Cape Town (Fig. 9A and B), under the excavation permit #15060901GT0610E obtained from the Heritage Western Cape (Appendix 9). A section of the fossiliferous bed, approximately 2 m long by 1 m wide, was excavated. The fossiliferous bed was systematically removed using a flat brick chisel and geological hammer. Due to the highly-weathered nature of the outcrop, the fossiliferous bed broke up into approximately 55 smaller sections (15 cm wide by 8 cm long on average) during removal. Effort was made to collect all fossiliferous rock fragments, even if they only contained fragmentary and disarticulated fossils. These sections were subsequently reassembled in the lab (Fig. 9C) and imaged via computer tomography (CT) scanning.

2.2 MICRO COMPUTED TOMOGRAPHY

Micro computed tomography (micro-CT) is a scanning technology used to acquire internal information for objects non-destructively by producing a series of cross-sectional images (tomographic images), representing X-ray attenuation maps (Sutton, 2008). The method, which is described in more detail in Appendix 1.1, was originally developed as a medical diagnostic tool, however CT has been used as a routine tool for investigation in many other fields such as geology and palaeontology. Generally, in palaeontology, CT studies have focused on describing the internal anatomy and morphology of fossils with the aid of a 3D digital reconstructions (e.g., Abel *et al.* 2012). In this study, however, micro-CT scanning is predominantly used as an aid for taphonomic analysis.

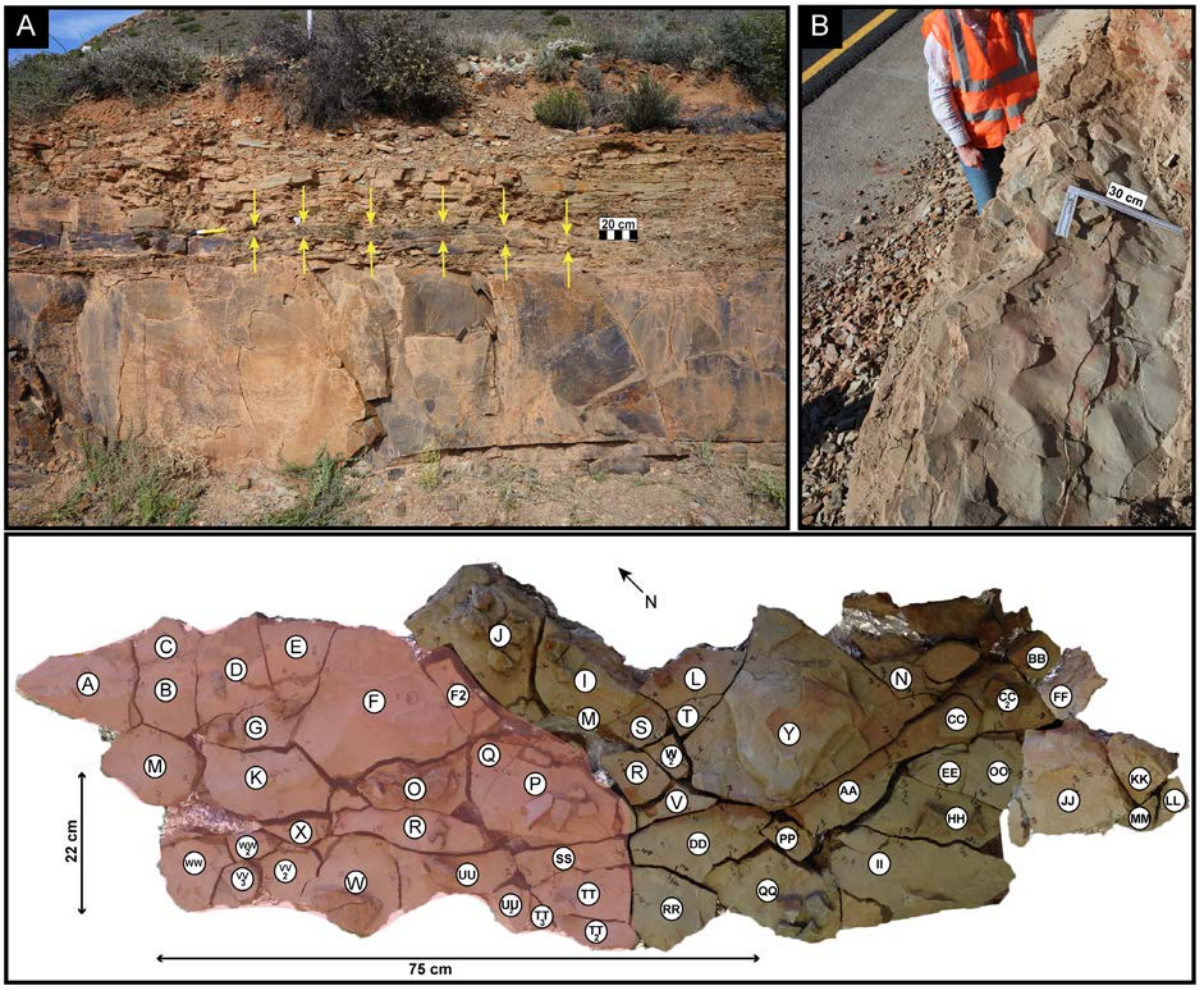

Figure 9. (**A**) Location of the Karbonaatjies obrution bed within the outcrop (indicated by yellow arrows). (**B**) Top surface of the fossiliferous bed, note the interference ripple marks. (**C**) Excavated Karbonaatjies obrution bed. Each individual rock fragment was given a reference letter in the field and subsequently reassembled in the lab. The entire fossil bed was CT scanned however only the red shaded area was digitally rendered in 3D (see Appendix 1.2 for details on problems encountered in digital analysis).

The micro-CT scanning was performed at the Stellenbosch University Central Analytical Facility (CAF), with the aid of a walk-in microfocus X-ray CT scanner. This is a General Electric Phoenix V|Tome|X L24 model with additional NF180 option and contains two X-ray tubes; a reflection-type target (max voltage of 240 kV) and a transmission target (max voltage of 180 kV). The CAF micro-CT instrument has a typical minimum voxel size of between 1 and 100 µm and can be used for samples that are up to 300 mm long and 200 mm wide. Source spot size, specimen size and detector dimensions are the main controls on scan resolution, which is the ability to resolve objects as separate forms (Sutton *et al.,* 2014). To ensure that the X-ray spot size did not exceed the selected scan resolution, optimal X-ray scan parameters were chosen while using live digital X-ray images (e.g., for ideal X-ray penetration, we

monitored the high transmitted brightness values). X-ray settings ranged for voltage from 160 kV to 240 kV (for larger samples) and for current from 200 μA to 220 μA, respectively. Detector shift was activated and background calibration was performed before each scan in order to minimize ring artefacts and achieve high image contrast. To reduce potential beam hardening artefacts, a 0.1 mm copper beam filter was used in all the scans. The samples in this study are relatively dense, rigid rock fragments with an average length of 200 mm. To obtain sharp images of larger samples, the voltage had to be pushed up to 240 kV on the high-power tube allowing for more beam filtration (less beam hardening) and limiting the generation of other artefacts (du Plessis *et al*., 2016). Scan time averaged from approximately 40-60 minutes per scan depending on the size of the sample. Longer samples were scanned in sections (allowing for magnification based on the medium axis). Rock samples were scanned one at a time and had to be fixed to the stage firmly to prevent movement during scanning. For this purpose, the samples, contained in a plastic bottle that was sliced in two and filled with florist foam crumbles, were placed onto a plastic rod and mounted onto the platform. A small wax ball was stuck to the upper surface of each sample in order to indicate right way up orientation in the scans. Using an exposure time of 500 ms per image, 1400-2600 images were acquired in each 360° rotation, averaging two images and skipping one image. The acquired images (tomograms) were reconstructed using system-supplied Datos reconstruction software, which uses a filtered back projection algorithm to convert raw attenuation images into computed tomograms. The tomograms that contained no data (or only surrounding air) were cropped in order to reduce the size of the images or volume.

2. 3 DIGITAL ANALYSIS

The reconstruction dataset obtained from the scanning was visualised and analysed using the Volume Graphics VG StudioMax 2.2 software package (http://www.volumegraphics.com). This software was also used to produce images (i.e., screen shots) and animations, which were then exported into the animation package Adobe After Effects (CS6), and subsequently to Adobe Illustrator and Adobe Photoshop for final editing.

The scanned dataset was studied both directly from the tomographs (as a set of 2D cross-sectional slices) and with the use of three dimensional (3D) visualisations. Generally, when a fossil is scanned, it is the minerals that make up the rock and the fossil itself that are differentiated allowing interior and exterior structures to be digitally visualised in 3D. This highlights one of the major problems with CT scanning of fossiliferous rock samples, because

the shape and composition of the fossils are often lacking contrasts between the specimen and the sedimentary rock matrix (Sutton et al., 2014). However, the fossils of this study are external moulds (i.e., large voids in the rock) with no internal mineralogical information, this made segmentation easier in that the contrast between the fossil (air) and surrounding rock are very high. For step by step details on the virtual preparation and recreation of the fossiliferous bed in 3D, please see Appendix 1.3.

2.4 TAPHONOMIC ANALYSIS

2.4.1 Echinoderms

All measurements and observations of the fossil echinoderms in this study were made from the 2D slices and the 3D reconstructions with the aid of digital instruments of the VGStudioMax 2.2 software (e.g., indicator, distance and calliper tools). These digital tools allowed not only the 3D (x-y-z) positioning of each fossil relative to one another, but also the direct measurement of their individual sizes on the 2D scans. It is important to note that a slight error in all measurements must be assumed due to the resolution of the scans (additionally, digital artefacts as explained in the Appendix 1.2) and limitations of the segmentation process, which is somewhat subjective (Abel, *et al*., 2012). Considering that the distance between each successive slice is 0.099 mm, a slight error must be assumed when measuring specimens directly from the 2D slices. In addition to CT scans, high-resolution, close-up photographs have been taken of several fossil specimens to facilitate their taphonomic analysis. The latter, together with silicone rubber moulds (see Appendix 1.4 for casting method), were used to describe the morphology of specimens.

Ophiuroids

Taphonomic measurements and observations undertaken in this study include the following: specimen counts (only counted if disk fully visible); counts of arm fragments; disk diameter (measured from the base of the arm to the opposite interradius); arm length (measured in relation to the disk diameter); orientation of specimens (oral side up, oral side down or oblique) (Dornbos and Bottjer, 2001; Twitchett *et al*., 2005; Zatoń *et al*., 2008; Stöhr *et al*., 2012); as well as the level at which the ophiuroids occur in the fossiliferous bed (upper, lower or middle part of the bed).

Ophiuroids with different arrangements of the arms were also documented largely using the method of Ishida and Fujita (2001), who compared the behaviour and posture of living individuals of *Ophiura sarsii sarsii* Lütken that were experimentally buried in sediment to a Miocene deposit of *O. sarsii sarsii*. Because the Miocene ophiuroids were preserved in postures similar to those of the extant ophiuroids escaping experimental burial, the following four posture categories were erected by Ishida and Fujita (2001) (Fig. 10): 1) *resting posture*: radially arranged arms, extended straight with a slight curve at the tips; 2) *walking posture*: bilaterally symmetrical arms, lateral arms are bent at an angle, leading arm stretched out; 3) *escape posture*: oral side down (normal position) one or two leading arms raised, disk tilted upwards, trailing arms extended straight back, lateral arms curved backward, tips bent in a "u" shape; oral side up (inverted position) one or two leading arms raised, lateral arms curved downward and trailing arms extended downward; 4) *irregular posture*: arms irregularly positioned, asymmetrical arranged.

In order to better understand the taphonomy of fossilised ophiuroids, Kerr and Twitchett (2004) also undertook a series of experiments on extant ophiuroids (*Ophiura texturata*) that were decayed for 14 days at temperatures ranging from 15° to 25° C and subjected to tumbling to stimulate the turbidity of currents in sedimentary depositional environments. Furthermore, these authors distinguished between ophiuroids that were buried alive and those that had died prior to burial by assessing the degree of disarticulation of the fossil remains, which is assumed to indicate the length of time between death and final burial (Kerr and Twitchett, 2004). Using this approach, various semi-quantitative decay stages were established that range from full articulation to complete disarticulation. The ophiuroids in this study are classified into three different taphonomic groups (analogous to decay stages) following a modified procedure from Kerr and Twitchett (2004) (Table 1).

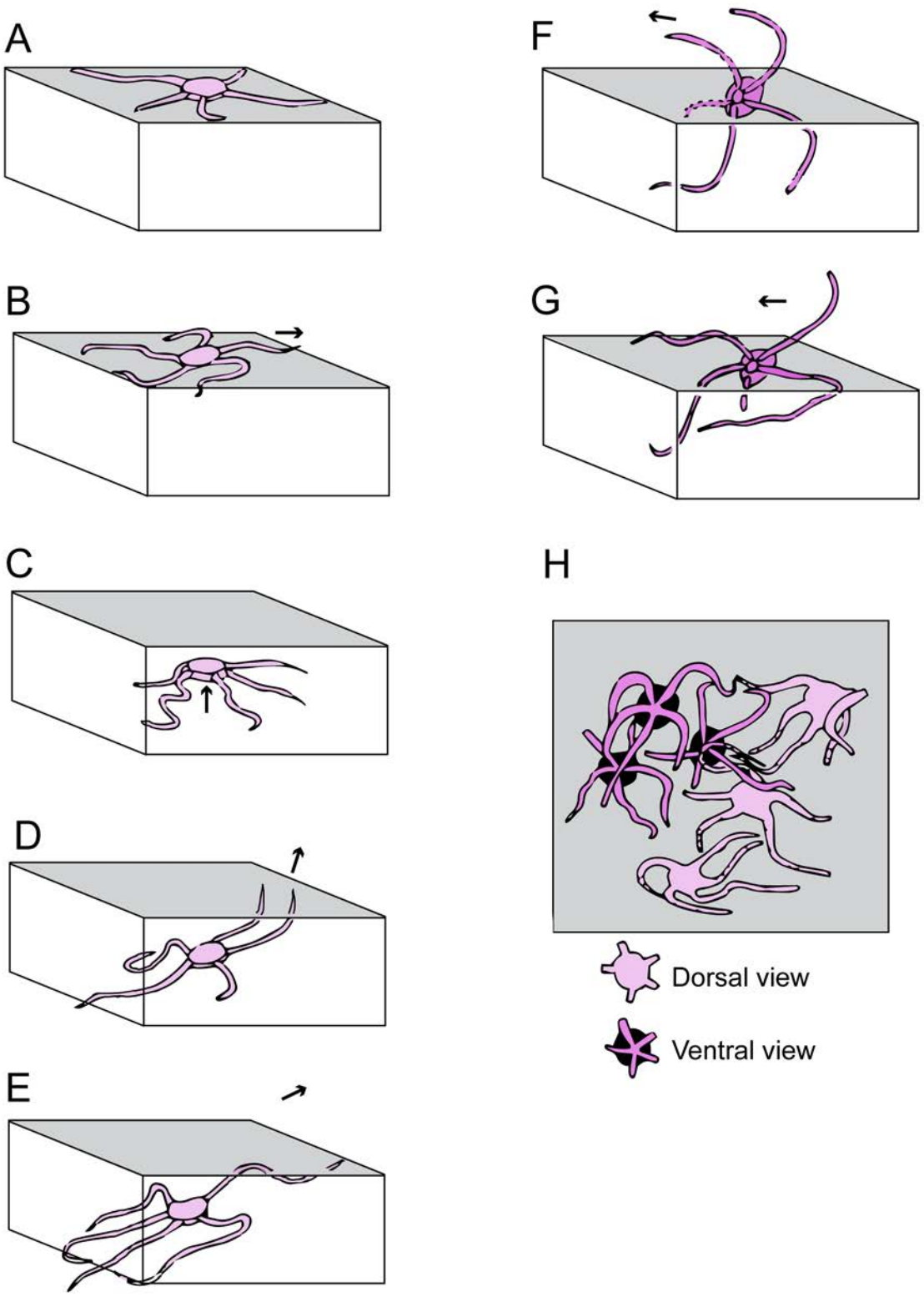

Figure 10. Postures of fossil *Ophiura sarsii sarsii*: (**A**) Resting posture; (**B**) walking posture; (**C**)-(**E**) escape posture oral side down (light pink); (**F**)-(**G**) escape posture oral side up (dark pink); (**H**) irregular posture (redrawn from Ishida and Fujita, 2001). Arrows refer to direction of the leading arm.

Stylophorans

Taphonomic measurements of fossil stylophorans include: specimen counts (number of preserved thecae); thecal length and width; level of occurrence in the fossiliferous bed (upper, lower or middle parts of the bed) as well as the position of the distal aulacophore (either preserved in a flexed or extended position). Very fine morphological features, such as the cover plates of the distal aulacophore or thecal surfaces and interplate sutures, were not observable using the 2D slices and 3D reconstructions because either the resolution of the scans is insufficient or the perseveration of the stylophorans is poor. Inverted and life position orientations can be identified in the *Placocystella* by the position of the brachial spikes (Lefebvre, 2003). Reflective of the fossil preservation quality, the two taphonomic groups for stylophorans that are used in this study are modified from the classification proposed by Martin *et al*. (2015) (Table 1).

Crinoids

Only crinoid ossicles and columnals fragments are observed in the deposit. Crinoids are described using Wright (1983) columnal morphotypes: circular, pentagonal, hexagonal, stellate or semi-circular articular facet. The length of the ossicles and lumen were measured, and abrasion levels were noted.

Table 1: Semi-quantitative taphonomic scale used for both ophiuroids and stylophorans, analogous to the decay stages used by Kerr and Twichett (2004).

Taphonomic groups	Ophiuroids	Stylophorans
Group 1	Fully articulated arms and only minor signs of disarticulation (i.e., lack of distal arm portions/tips).	Distal aulacophore (brachials, stylocone, cover plates and ossicles); proximal part of aulacophore preserved; complete to slightly disarticulated theca; digits preserved (the latter is only applicable to *Placocystella)*.
Group 2	Partially disarticulated, having only median portion of arms preserved. Also, included in this group are ophiuroids with only one or two arms at median portion with the rest of the arms fully articulated.	No distal aulacophore, complete or dissociated proximal aulacophore, complete to partially disarticulated theca
Group 3	Disarticulated with only isolated disk without arms or only proximal portions preserved.	Only isolated aulacophore fragments observed

2.4.2 Shells

The fossiliferous bed was described in the field and laboratory using sedimentological, taphonomical and palaeoecological methods outlined by Kidwell *et al.* (1986) and Kidwell and Holland (1991). Several quantitative indicators of physical environmental parameters were taken into account *sensu* Brett and Baird (1986). In the field, the thickness, lateral extent, contact surfaces and geometries of the fossil deposit were recorded along with taxonomic data from the bed. For the classification of shell bed types, Parsons *et al*. (1988) (a modification of Kidwell *et al*., 1986) is used (Table 2). Taphonomic features were only observed in fragments bigger than 2 mm, which are referred to as bioclasts (i.e., fragments of shells or other fossil remains forming grains in the sediment). Particles smaller than 2 mm are considered shell detritus/hash, and are not considered in this study.

The orientation of shells (i.e., convex-up or convex-down) and their size frequency (albeit not studied here due to the poor resolution of shells in the scans) can be inferred to indicate the magnitude of the current action, prior to or during burial (e.g., Brett and Baird, 1986). Disarticulation, which occurs very rapidly in bivalved shells can indicate the rate of burial (as previously discussed in the echinoderm section). The degree of fragmentation is not only a sensitive palaeo-hydrodynamic indicator, but also evidence for biological processes such as predation (Brett and Baird, 1986). Shell fragmentation was partially assessed by direct observation of bioclast concentrations in the rock samples as well as by estimations using the cross-sectional views of rock samples and CT scans. Due to the fragile nature of the bed, only partly exposed shells were measured directly, and therefore the true degree of fragmentation is not fully quantified. Encrustation was not observed on any shells, however bioeorsion in the form of commensal borings is found in many of the larger *Australospirifer* brachiopod valves.

Table 2: Proxies used in characterising bioclast-bearing fossiliferous beds (adapted from Kidwell and Holland, 1991).

Stratigraphy/Sedimentology	
Thickness	
Lateral extent (in metres)	
Nature of the bedding planes (sharp, gradational, erosional, etc.)	
Geometry of bed (lens, wedge, sheet, etc.)	
Internal structure	*Simple concentrations of fossils*
	Complex concentrations of fossils
Packing of shell material	*Dense (bioclast-supported)*
	Loose (matrix-supported with bioclasts closely associated)
	Disperse (matrix-supported with sparsely distributed bioclasts)
Size sorting	*Well-sorted (narrow range of bioclasts sizes)*
	Bimodal (few large bioclasts within finer bioclasts)
	Poorly sorted (wide range of bioclast sizes)
Taphonomy	
Orientation in plan view	*Unimodal*
	Bimodal
	Random
Orientation in cross-section	*Concordant (parallel to bedding)*
	Oblique
	Perpendicular (at right angles to bedding)
	Random
Convexity of individual shells	*Convex-up*
	Convex-down
Pedicle/brachial valve ratios	
Right/left valves ratios	
Degree of articulation	*Articulated shells contribute with two valves*
Degree of fragmentation	*Low (<10 % surface removed)*
	Moderate (10-50% of surface removed)
	High (> 50% of surface removed)
Surface abrasion, corrosion (loss of shell ornamentation)	
Bioeorsion	
Encrustation	
Palaeoecology	
Number of species	
Relative abundance of species	
Taxonomic composition	*Monotypic*
	Polytypic
Life habits	

Taphonomic characteristics are essential for determining the extent to which the bioclasts are transported from their original life position and therefore how closely this deposit represents original communities. Fossil assemblages as defined by Kidwell *et al.* (1986) consist of a) *autochthonous* remains, organisms that lived within the local community and may have been preserved in life position; b) *parautochthonous* remains, assemblages composed of autochthonous components that have been moved (disarticulated, reoriented, concentrated) from their original position by biogenic agents (bioturbators, predators, scavengers) or sedimentological (physical processes) but not transported out of the community; c) *allochthonous* remains, composed of specimens transported out of their life habit. It is important to keep in mind that factors such as bioturbation and/or physical reworking cause time-averaging (temporal mixing) of different communities, which may lead to increased pseudo-diversity in a given assemblage (Kidwell and Bosence, 1991).

Fossil preservation, an indicator of the burial rate, was also assessed because articulated multi-element skeletons and shells in life position indicate rapid deposition, in contrast to highly corroded, broken, or worn fossils, which suggest a long residence time on the sea floor (Parsons *et al.,* 1988).

All basic descriptive statistics were calculated using PAST software (Hammer *et al.,* 2001). Histograms (frequency distributions) were used for ophiuroid and stylophoran size distribution analysis. Normality of size-frequency distributions was checked using the Shapiro-Wilk test. Taphonomic groups are expressed as a semi-quantitative scale using average valves (in percentage) measured in each sample.

2.5 MORPHOLOGICAL DESCRIPTION

All fossil specimens in this study are preserved as natural moulds and therefore to facilitate their morphological description blackened silicone rubber moulds were made from selected specimens and whitened with ammonium chloride sublimate (see Appendix 1.3 for silicone casting method).

Over 700 ophiuroid specimens and over 150 stylophoran specimens, were excavated from the Karbonaatjies obrution bed, and they are housed in the Iziko Museum of South Africa (SAM). Of these individuals, 5 are designated type specimens.

CHAPTER 3 TAPHONOMY AND PALAEOENVIRONMENT

3.1 OBSERVATIONS

The Lower Devonian Karbonaatjies obrution bed is dominated by an echinoderm-rich assemblage of the proposed protasterid *Gamiroaster tempestatis* (see taxonomy chapter), the anomalocystid *Placocystella africana* (Reed, 1925), the mitrate *Paranacystis* cf. *petrii* Caster, 1954 and numerous unidentified crinoid ossicles (Fig. 11). Furthermore, brachiopods (mainly *Australospirifer* and *Australocoelia*), bivalves, trilobite thorax fragments, gastropod fragments, fish spine fragments and numerous unidentified shell fragments are also present, and have an abundance that is constant throughout the bed. The skeletal remains occur as external moulds without the original skeletal calcite.

The Karbonaatjies obrution bed occurs as a 5 cm thick-lens of medium-grained sandstone that pinches out laterally within 1.5 m (for more details on the bed, see Reid *et al*., 2015). This fossiliferous bed generally lacks any primary sedimentary structures, except for some very vague and locally developed horizontal laminations. The lower surface of the fossiliferous lens has an irregular erosional contact, while the upper surface is gradational with the overlying siltstone that terminates in interference ripple marks (Fig. 12).

The Karbonaatjies obrution bed displays differential preservation of shells (brachiopod, bivalve, gastropod, trilobite) and echinoderms (crinoid ossicles, ophiuroids and stylophorans) from bottom to top, with the proportion of disarticulation and fragmentation decreasing upward within the bed. The bed is located below a barren, fine-grained silty sandstone/mudstone with bidirectional ripple cross-laminations and above a very fine-grained siltstone with one large articulated specimen of the ophiuroid *Eophiura* Jaekel, 1903 and scattered disarticulated bivalves. The latter is 10 cm thick, and the preservation of shells and ophiuroid in it is better than in the Karbonaatjies obrution bed. The contact between these two beds is sharp.

Figure 11. Virtual reconstruction of the Karbonaatjies obrution bed shows over 700 articulated ophiuroids (light pink = ophiuroids oral side down; dark pink = ophiuroids oral side up); 145 *Paranacystis* cf. *petrii* Caster, 1954 (green); eight *Placocystella africana* (Reed, 1925) (red); numerous crinoid ossicles (blue); fragmented ophiuroid arms (pale orange) and large shell fragments (yellow). See Supplementary data set 1.1-1.4 for high quality image allowing the viewer to zoom into finer details, as well as a 3D movie (https://figshare.com/s/cefe3dd5fcc4cb8b46d4).

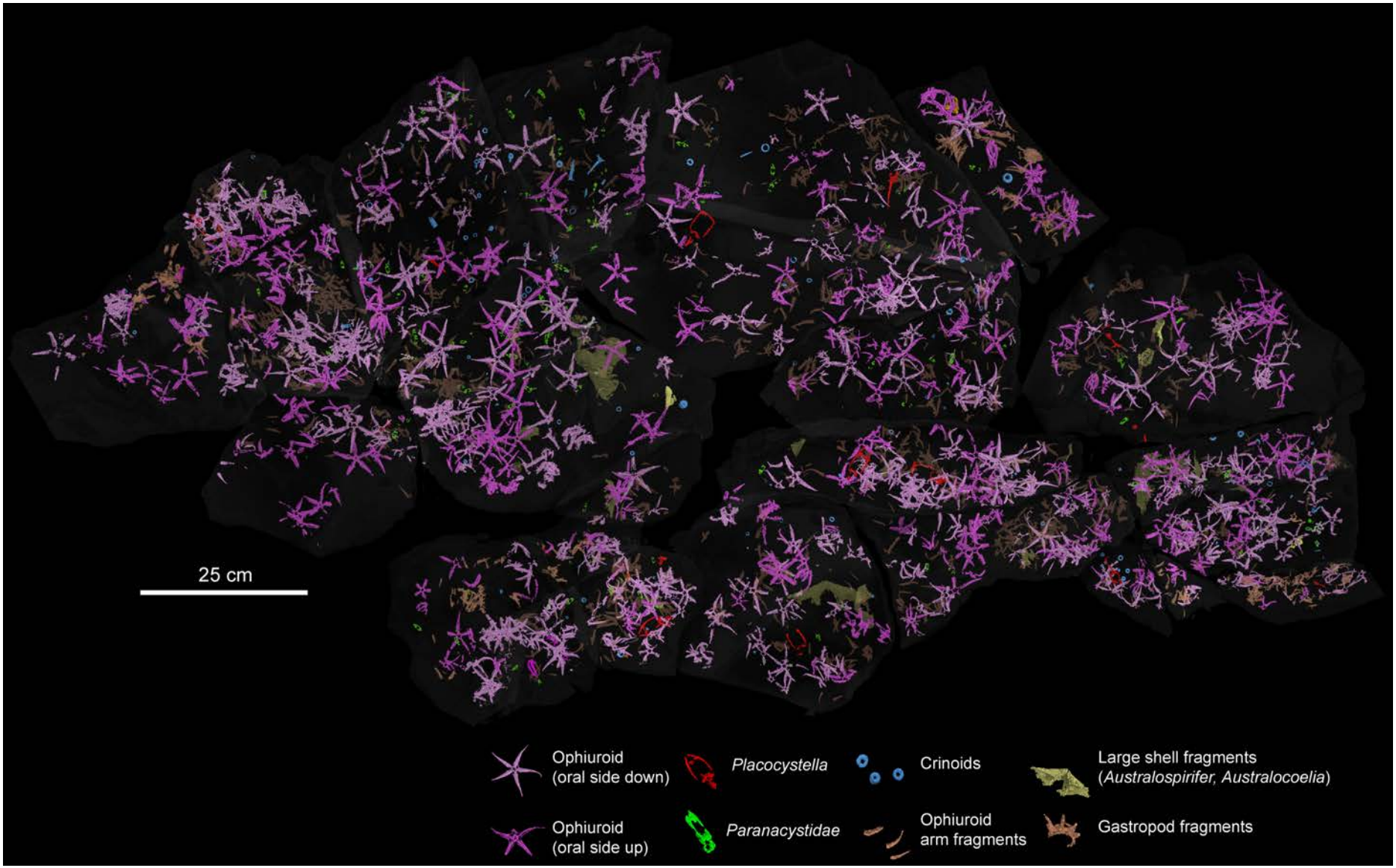
25 cm
Ophiuroid
(oral side down)
Ophiuroid
(oral side up)
Placocystella
Paranacystidae
Crinoids
Ophiuroid
arm fragments
Large shell fragments
(Australospirifer, Australocoelia)
Gastropod fragments

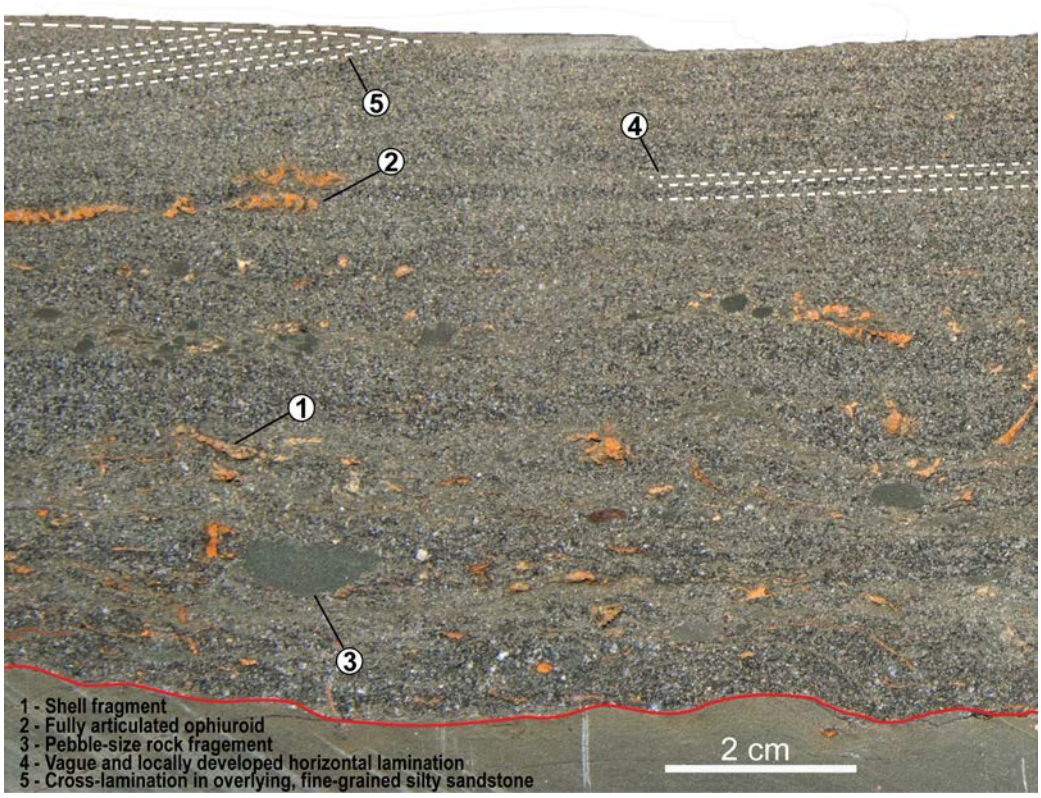

Figure 12. Key sedimentological features of the Karbonaatjies obrution bed, which is a 5 cm thick, ~1.5 m wide, medium-grained sandstone bed. This fossiliferous bed generally lacks any primary sedimentary structures, except for some very vague and locally developed horizontal laminations. The lower contact is sharp with minor erosional relief (red), which is overlain by closely packed fossil fragments with an upward decrease in abundance. The upper contact is gradational with the overlying, unfossiliferous siltstone, which terminates in interference ripple marks.

3.2 ECHINODERM TAPHONOMY RESULTS

Ophiuroids

The ophiuroid assemblage occurs as monospecific dense aggregations within roughly three separate horizons (Fig. 13). Using 2D image slices of the scans as well as 3D reconstructions of specimens, a total of 714 skeletons are recorded measured (Appendix 2 and 3). Ophiuroid specimens show no evidence of abrasion, regeneration of arms or bite mark traces. Approximately 634 disarticulated ophiuroid arms not attached to disks were counted from the 3D models, however it should be noted that arm fragments are difficult to recognize because of the high density of articulated ophiuroids and low resolution of some scans.

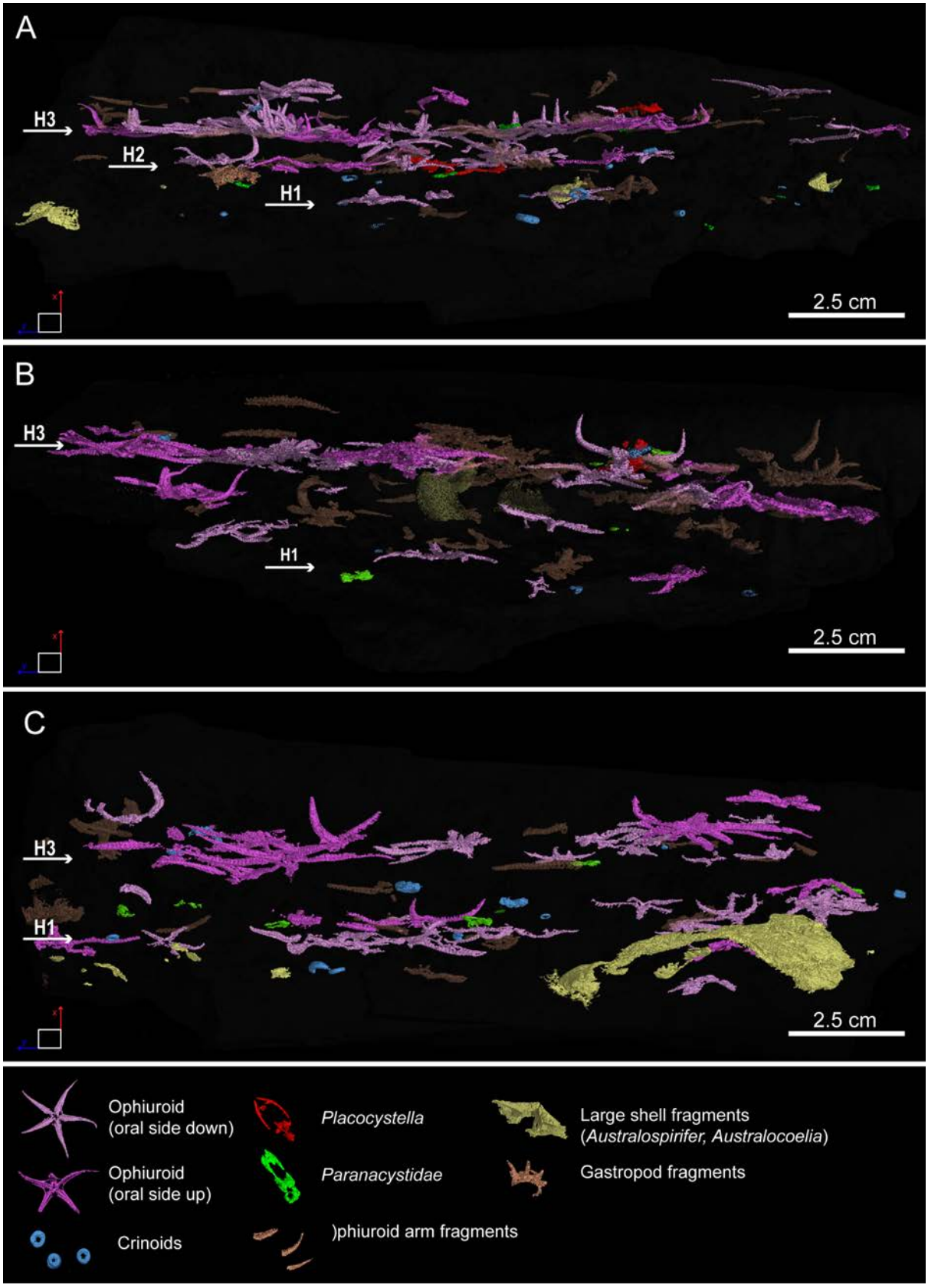
A
H3
H2
H1
2.5 cm
B
H3
H1
2.5 cm
C
H3
H1
2.5 cm
Ophiuroid
(oral side down)
Ophiuroid
(oral side up)
Crinoids
Placocystella
Paranacystidae
)phiuroid arm fragments
Large shell fragments
(Australospirifer, Australocoelia)
Gastropod fragments

Figure 13. Virtual reconstruction of selected ophiuroid-rich samples from the Karbonaatjies obrution bed. (**A**)-(**C**) Samples R, UU and SS (see Methods Chapter for location of samples within in the bed). Each sample shows three vaguely defined ophiuroid 'horizons' (H): H1: located ~1 cm above the erosional contact, consists of fully articulated ophiuroids (pink), shell fragments (yellow), crinoid ossicles (blue) and articulated paranacystids (green). H2: defined by the smallest (3 mm disk diameter) fully articulated ophiuroids, shows a marked decrease in shell fragments. H3: located ~3-5 cm above the erosional contact, consists of only fully articulated ophiuroids in a dense aggregate, as well as, articulated *Placocystella* (red) and rare trilobite thorax fragments. No other shell fragments are present at this level. Ophiuroid arm fragments persist throughout the bed (pale orange).

Ophiuroids within the obrution bed fall into three taphonomic groups based on the state of their overall preservation (Fig. 14 -see Table 1 in Methods): 1) well-preserved ophiuroids with fully articulated arms and only minor signs of disarticulation (i.e. lack of distal arm portions/tips); 2) partially disarticulated, having only median portion of arms preserved. Also, included in this group are ophiuroids with only one or two arms at median portion with the rest of the arms fully articulated; 3) disarticulated with only isolated disk without arms or only proximal portions preserved. Of the 714 ophiuroids counted only 670 specimens could be accurately placed into the taphonomic groups: 54% are well preserved with fully articulated arms (Group 1), some even retain their delicate tips, which are not wider than 0.30 mm (smallest disc dimeter: 1.45 mm), and only a very small portion (approximately 8%) of Group 1 show minor signs of disarticulation (lack distalmost part of arms); 41% of specimens are partially disarticulated (Group 2), a majority of these ophiuroids in this group consist of one, two or three of their arms at median portion with the remaining arms fully articulated to the tip and the remaining specimens with all five arms at median portion; finally, only a few ophiuroids (10%, Group 3) have disks with proximal portions of the arm or lack any arms (articulated stumps) (Fig. 15A). The remaining 44 specimens could not be placed into a taphonomic group due to scans being too faint and/or obscured by artefacts. All arms and jaw structures appear to have exceptional preservation with little abrasion observed. Amongst all of the complete skeletons are a labyrinth of fragmented/isolated arms. An estimated 634 disarticulated arms were counted. Arms are complete or near complete and distributed randomly throughout the bed and occasionally in dense aggregations (Fig. 16).

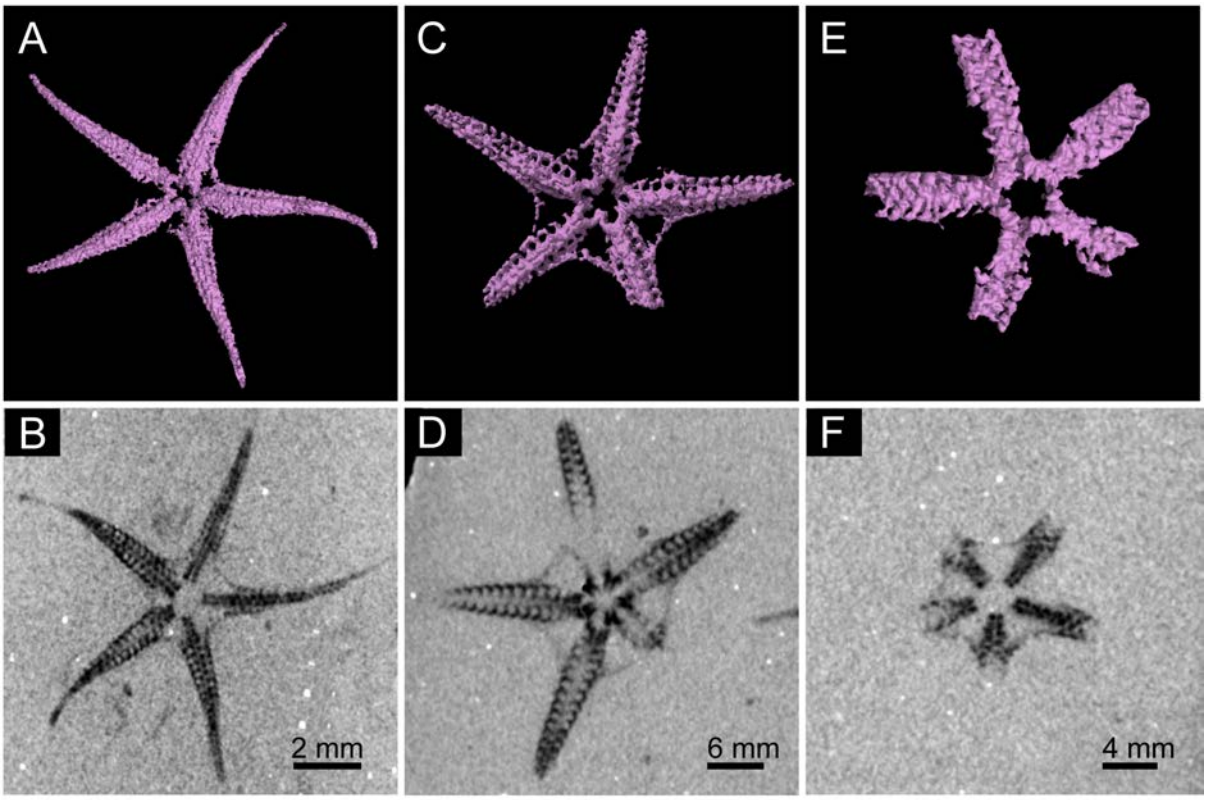

Figure 14. Ophiuroid taphonomic groups in the Karbonaatjies obrution bed. Group 1 (**A-B**): well-preserved ophiuroids with fully articulated arms, ophiuroid specimen (sample UU) preserved with delicate arm tips; Group 2 (**C-D**): partially disarticulated ophiuroids having only median portion of arms preserved (sample R); Group 3: (**E-F**) disarticulated with only isolated disk, ophiuroid specimen (sample R) with proximal arm stumps preserved. (A-E) 3D reconstructions of the ophiuroids seen in the 2D image scans (B-F).

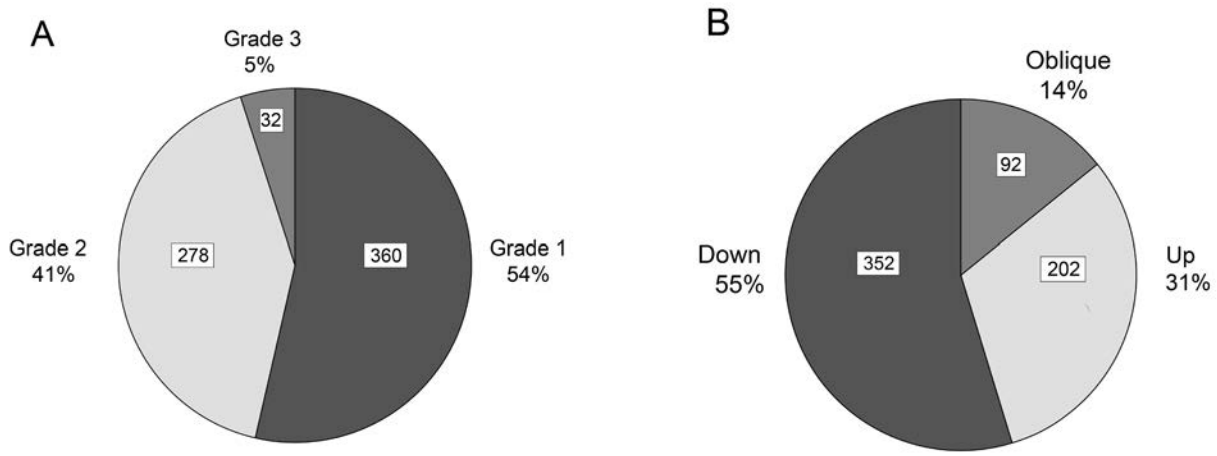

Figure 15. Frequency diagrams of taphonomic groups in the Karbonaatjies obrution bed. (**A**) Percentages of ophiuroids in each taphonomic group. (**B**) Distribution of ophiuroids with oral side down, oral side up and oblique to the bedding plane. Refer to Appendix 3.

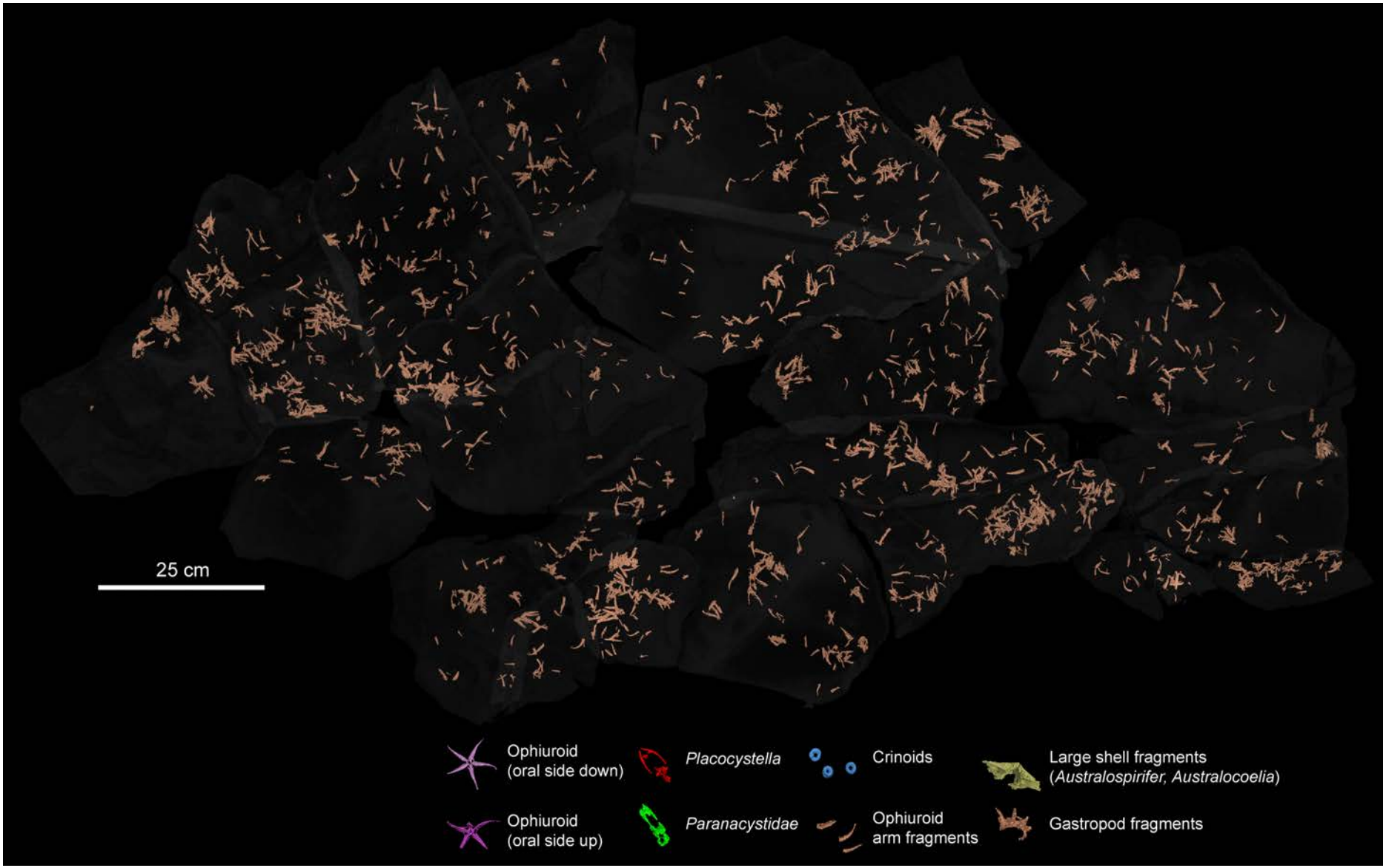
25 cm
Ophiuroid
(oral side down)
Ophiuroid
(oral side up)
Placocystella
Paranacystidae
Crinoids
Ophiuroid
arm fragments
Large shell fragments
(Australospirifer, Australocoelia)
Gastropod fragments

Figure 16. Virtual reconstruction of the Karbonaatjies obrution bed shows over 634 fragmented/ isolated arms that are complete or near complete. Arms are distributed randomly throughout the bed and occasionally in dense aggregations.

Specimens preserved oral side down (i.e., in normal position or life position) are more common (54%). Comparatively few are preserved oral side up (31%) and even fewer are preserved oblique to the bedding plane (14%) (Fig. 15B). A large proportion of the ophiuroids have equally spaced arms that extend straight out from the disc and occasionally with the tips of the arms slightly curved (Fig. 17A). Only a few of these ophiuroids have unequally-spaced arms asymmetrically arranged (Fig. 17B) and an even smaller percentage with all five arms bent in the same direction (however no preferred orientation is apparent) (Fig. 17C).

Approximately 15% (100 ophiuroids out of 670) were observed with one or more arms extended upward in to the sediment surface. Of the 100 specimens with extended arms, two types of positions are observed: 1) More than half of the 100 specimens are *oral side down* (*normal position*) (Fig. 18A and B) with equally spaced arms and discs in a bedding plane parallel position. The leading arms (1, 2 or 3) raised either from the proximal portion or the median portion of the arm, however in a few specimens only the tips are raised upwards. The trailing arms are extended backward, opposite to the leading arms. The lateral arms are curved backward with the tips bent in a "u" shape. Only a few ophiuroids have upward tilted disks at about 10° or less; 2) Less than half of the 100 specimens are in an *oral side up* (*inverted position*) (Fig. 18A-C): the same positions as the ophiuroids oral side down are observed if the disk is parallel to the bedding plane. However, many of the oral side up ophiuroids (with their arms up) have disks that are oblique to the bedding plane, at angles higher than 30°. This involves one leading arm raised vertically, lateral arms curved outward and trailing arms extended/curved slightly downward.

Figure 17. Ophiuroid arms arrangement in Karbonaatjies obrution bed. (**A**) Most ophiuroids in resting postures have equally-spaced arms that are extended more or less straight; (**B**) Few ophiuroids display irregular postures with equally-spaced arms (marked by an arrow) and (**C**) arranged in the same direction. (A-E) 3D reconstructions of the ophiuroids seen in the 2D image scans (B-F).

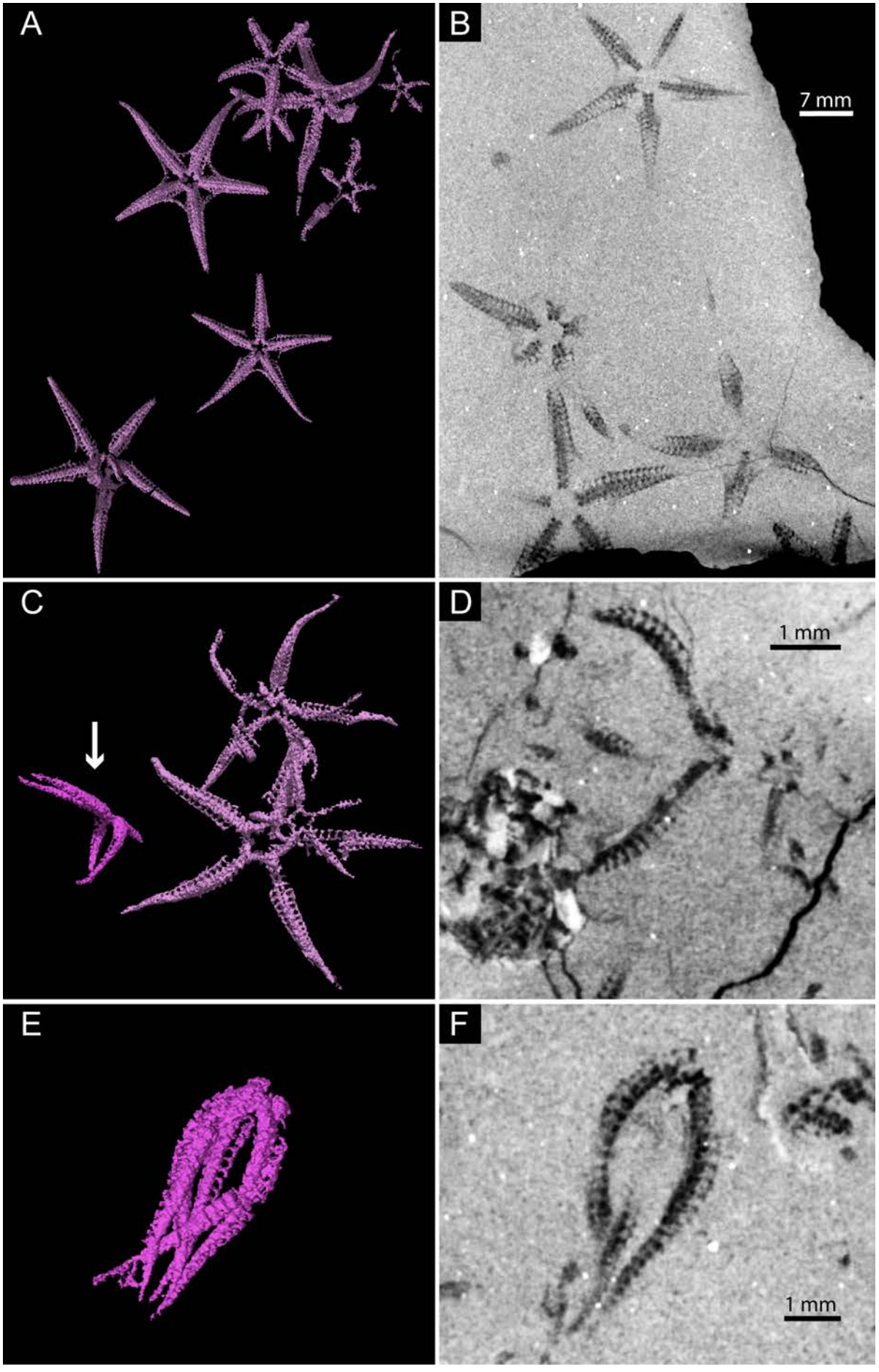
A
B
7 mm
C
D
1 mm
E
F
1 mm

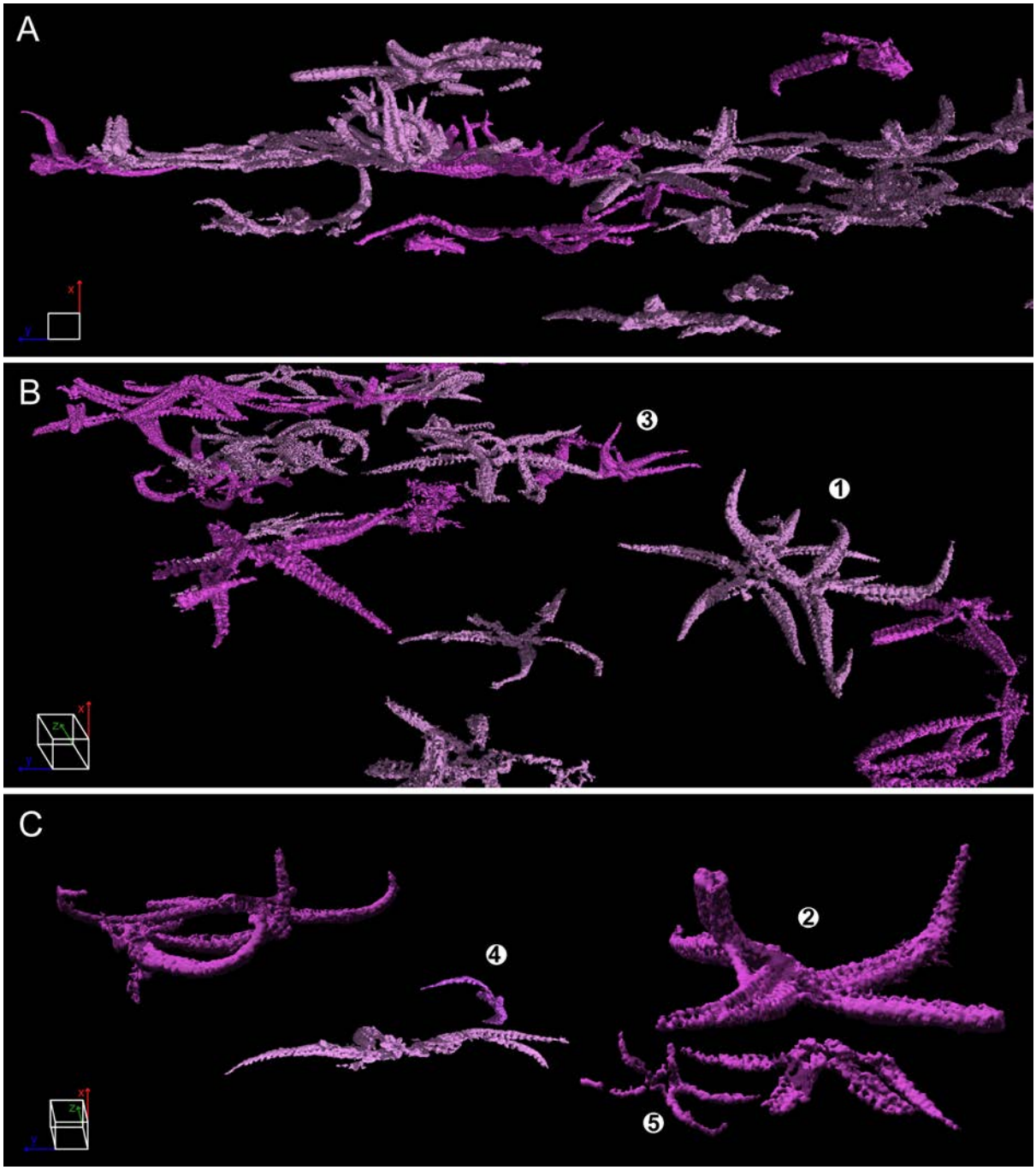

Figure 18. (**A**-**C**) Ophiuroids in oral side down (normal) position (light pink) and oral side up (inverted position) (dark pink) have arms extended upward within the obrution bed. These positions are interpreted as *escape postures*: (1) Ophiuroid with three arms raised up from the median portion; (2) inverted ophiuroid with one arm raised up (missing distal portion of the arm) and disk slightly raised; (3-5) ophiuroids with disks at angles tilted at >30°. 3D cube illustrates orientation of view.

Stylophorans

The Karbonaatjies obrution bed yielded eight *Placocystella africana* (Reed, 1925), as well as 145 specimens of *Paranacystis* cf. *petrii* Caster, 1954, which were recorded and measured using 2D images of the scans as well as 3D reconstructions of specimens (Appendix 2, 4 and 5).

Stylophorans are placed into two taphonomic groups based on the state of their overall preservation (Fig. 19 - see Table 1 in Methods), in all cases, only the outline of theca is preserved, and the various plates making up the two thecal surfaces are apparently absent: Group 1: distal and proximal part of aulacophore preserved (stylocone, brachials and ossicles), complete to slightly disarticulated theca, digits preserved (only applicable to *Placocystella*); and Group 2: no distal aulacophore, complete or dissociated proximal aulacophore, complete to partially disarticulated theca. The *Placocystella* individuals exhibit various states of disarticulation from fully articulated to almost completely disarticulated. Approximately 50% of all stylophorans are preserved with both proximal and almost all of the distal aulacophore, theca and digits intact (Group 1). Specimens with the aulacophore in an extended position (Fig. 19A) and flexed over the theca (Fig. 19B) are very rare, but present. The remaining specimens do not preserve digits and distal aulacophore (Group 2). One specimen without its distal aulacophore is preserved with the proximal aulacophore angled upwards relative to the horizontal plane of the theca (Fig. 19C). Aulacophore fragments are also found throughout the lower part of the bed.

Almost all paranacystid*s* specimens are fully articulated (Group 1) and include the distal aulacophore, which is preserved either flexed over or under the theca (19%) or curved to the side of theca (20%) (Fig. 19E-G). However, in more than half of the specimens the aulacophore is too indistinct to be analysed due to problems previously discussed in Appendix 1.2. The paranacystids are only found within the shell hash in the lowermost 1-2 cm of the obrution bed (Fig. 13). Individuals do not exhibit any preferential alignment to each other.

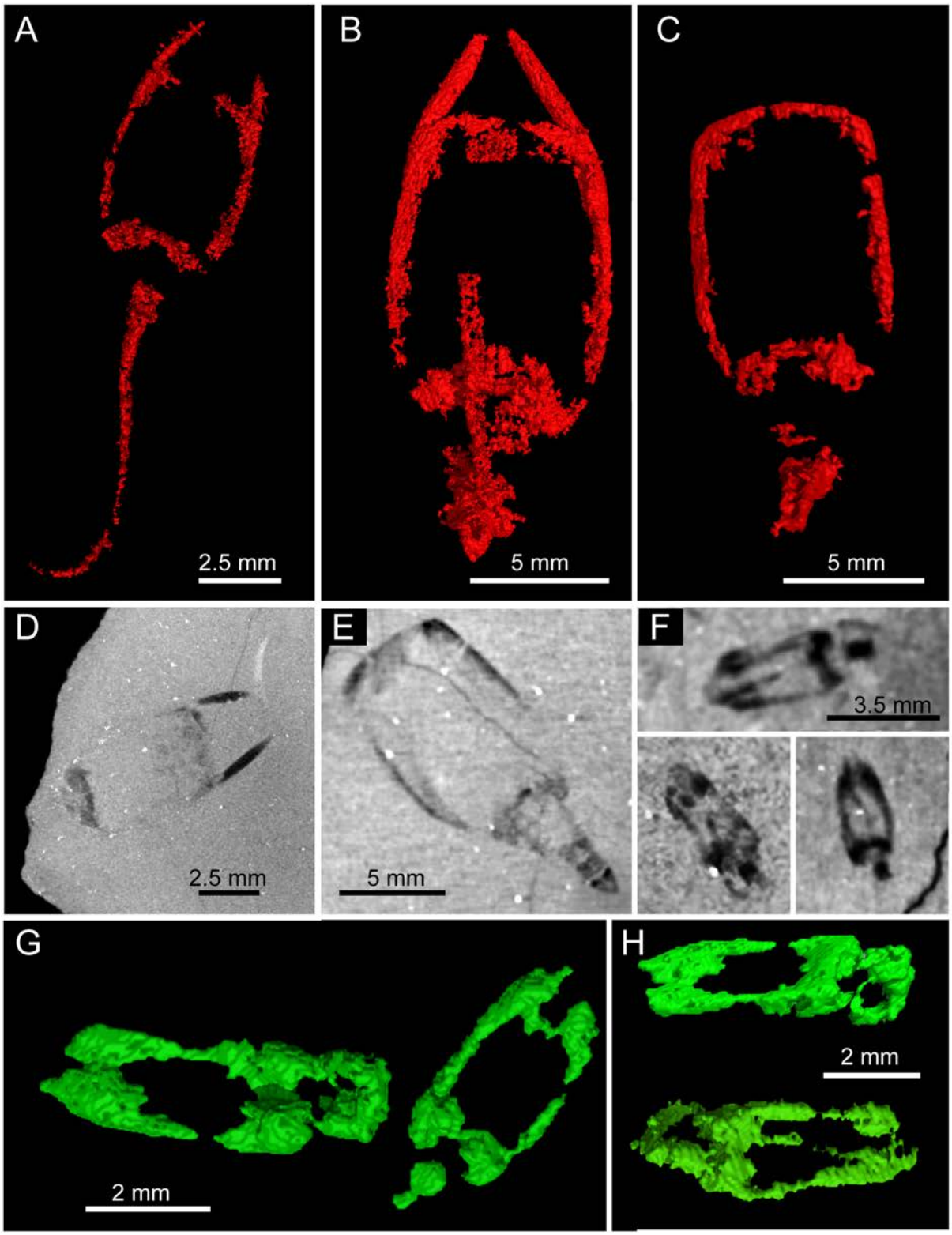

Figure 19. Stylophoran taphonomic groups in the Karbonaatjies obrution bed. Group 1 (**A,B,F,G,H**): distal and proximal part of aulacophore preserved, complete to slightly disarticulated theca, digits preserved (only applicable to *Placocystella*), (A) specimen with stretched out aulacophore (sample UU2), (B) aulacophore flexed over the theca (sample VV2), (F, G, H) articulated paranacystids showing different orientations, aulacophore seen curved under the theca or to the side; Group 2 (**C**): No distal aulacophore, complete or dissociated proximal aulacophore, complete to partially disarticulated theca. (**D-E**) 2D images of various states of preservation.

The life orientations of the stylophorans and especially the paranacystids, cannot be ascertained with confidence, because the CT scans (and possibly lack of preservation) do not display the thin lower and upper surfaces of the theca. It is generally interpreted that life position for stylophorans is indicated by a flat lower surface, on which it rested in life, and a convex upper surface (e.g. Lefebvre and Vizcaïno, 1999; Ruta, 1999; Lefebvre, 2003); if this is the case for *Placocystella* then the orientation of the brachial spines with respect to the bedding can infer life positions. Consequently, Group 1 includes two *Placocystella* preserved in life position i.e. with their brachial spines directed downwards. Only half of the specimen's brachial spines were confidently recorded (Appendix 5).

Crinoids

No complete crinoids occur within the obrution bed, however isolated crinoid ossicles (approximately 80) were found scattered throughout the shell debris in the lowermost few centimetres of the obrution bed (Fig. 20). These have been identified as stem fragments that are moderately to highly abraded (see Donovan *et al*. 2010 for more examples of 3D reconstructed crinoid ossicles). Ossicles range in diameter from 1 mm to 7 mm, averaging at approximately 3 mm. All ossicles have a circular or stellate lumen and vary from broad to relatively narrow. Some ossicles with a stellate lumen have a raised lumen rim. Crinoids are distributed randomly throughout the bed (Fig. 21)

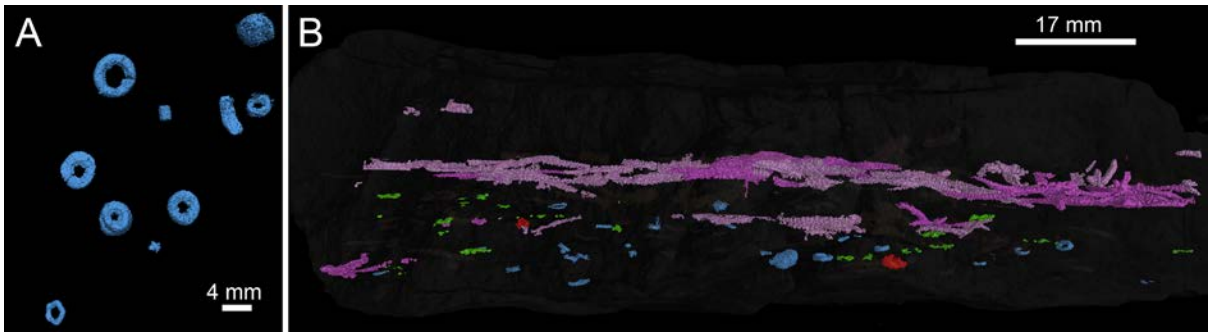

Figure 20. Virtual reconstruction of selected crinoid ossicles (blue) in the Karbonaatjies obrution bed (**A, B**) Note that crinoid ossicles only occur within the lower 1-2 cm of the bed (Sample D).

Figure 21. Virtual reconstruction of the Karbonaatjies obrution bed showing random distribution of crinoid ossicles.

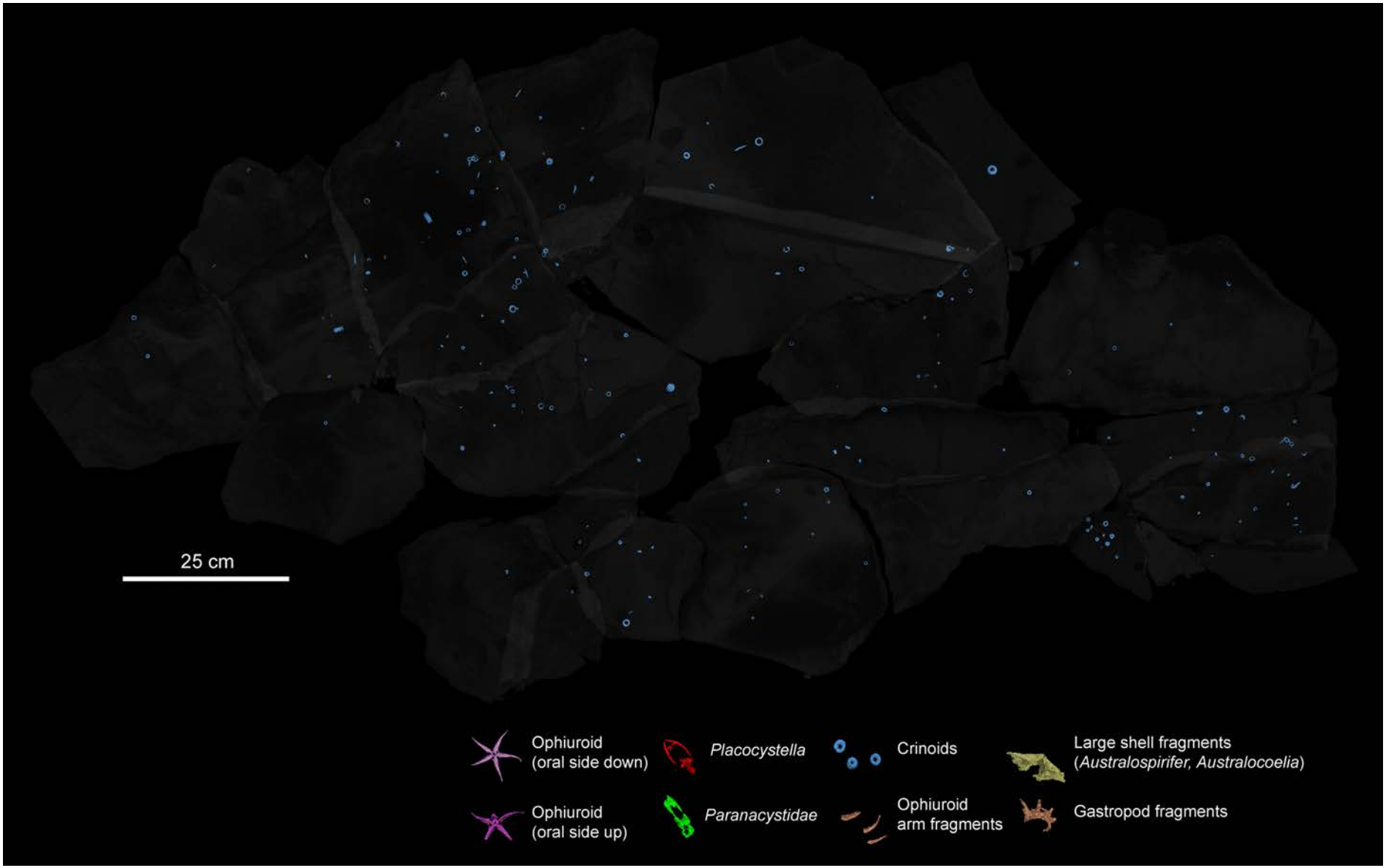
25 cm
Ophiuroid
(oral side down)
Ophiuroid
(oral side up)
Placocystella
Paranacystidae
Crinoids
Ophiuroid
arm fragments
Large shell fragments
(Australospirifer, Australocoelia)
Gastropod fragments

3.3 POPULATION STRUCTURE AND DYNAMICS

3.3.1 Density

Ophiuroids

The number of ophiuroids counted (Appendix 3) over a combined surface area of 3375 cm^2 of 26 representative samples (rock samples) was used to calculate the ophiuroid population density (individuals/m^2) in the Karbonaatjies obrution bed. Although the aggregation of specimens per sample varies (Appendix 2), on average, the result show that the obrution bed contains 2000 individuals per square meter.

Inter-individual distances vary from individuals in contact with each other and even overlap one another to those separated at length (Fig. 11). The ophiuroids in the lower half of the obrution bed are however all separated. The overall distribution is distinguished by the random ophiuroid clusters within the obrution bed, which shows a notable lateral decrease in ophiuroid density.

Stylophorans

The same method of population density estimation was applied to the *Paranacystis* stylophorans. Although the aggregation of specimens per sample varies (Appendix 2), on average, the Karbonaatjies obrution bed contains approximately 400 stylophorans per square meter. *Paranacystis* are found only within the shelly layer and are randomly spaced in relation to one another (Fig. 22). *Placocystella* do not form aggregations and are found spread randomly within upper parts of the obrution bed (Fig. 22).

Figure 22. Virtual reconstruction of the Karbonaatjies obrution bed shows over 145 articulated *Paranacystis* cf. *petrii* Caster, 1954 (green) and eight *Placocystella africana* (Reed, 1925) (red).

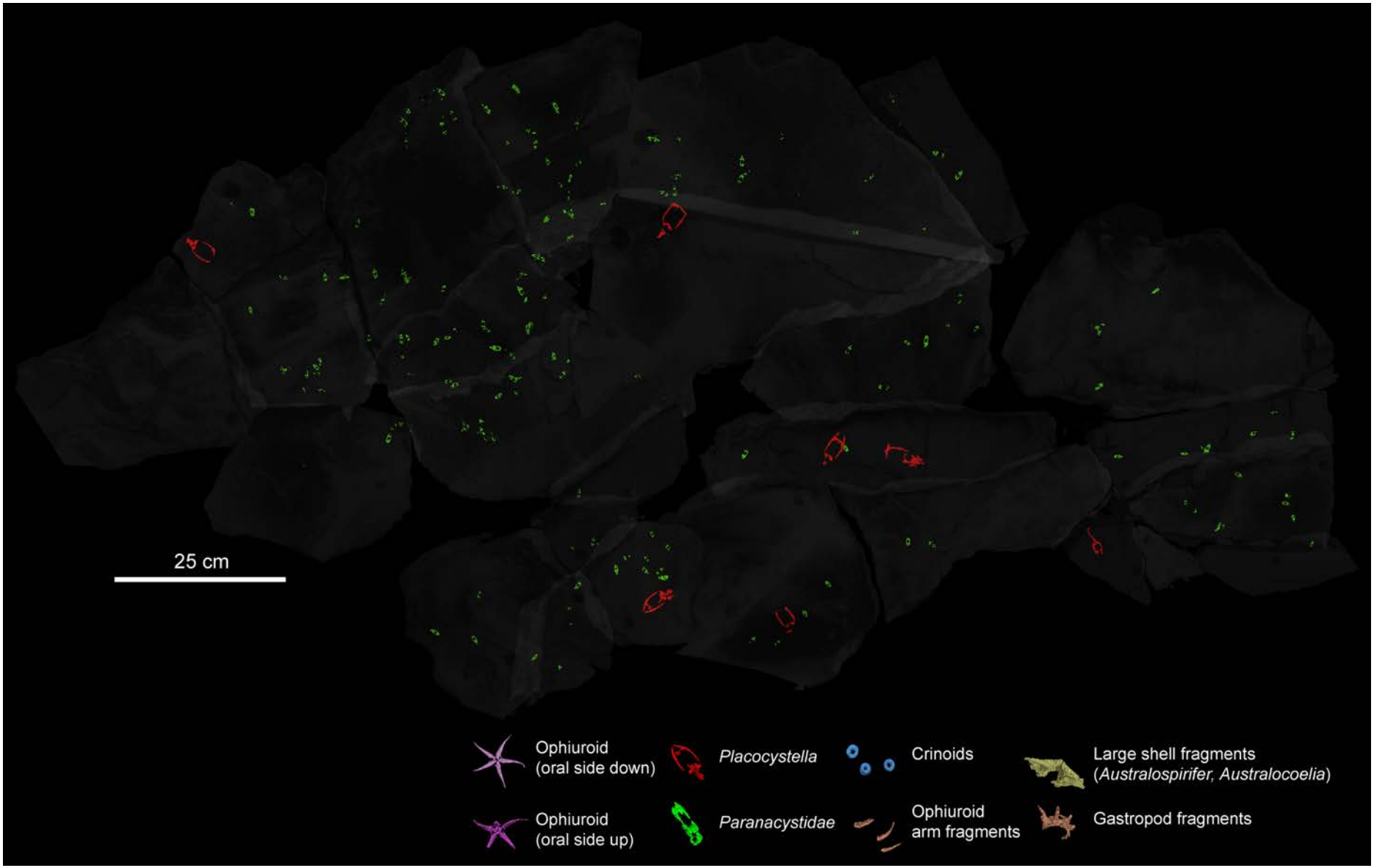
25 cm
Ophiuroid
(oral side down)
Ophiuroid
(oral side up)
Placocystella
Paranacystidae
Crinoids
Ophiuroid
arm fragments
Large shell fragments
(Australospirifer, Australocoelia)
Gastropod fragments

3.3.2 Size distribution

There are only a few size frequency distribution studies on fossil ophiuroids (Kesling and Le Vasseur, 1971; Twitchett *et al*., 2005; Zatoń *et al*., 2008; Martínez *et al*., 2010) and to-date, none were identified on stylophorans. Basic statistics of the size distribution (e.g., Shapiro-Wilk test) are shown in the Appendix 6 and in the corresponding histogram (Fig. 23). The ophiuroid histogram shows a possible bimodal distribution of the different size classes, while the *Paranacystis* histogram shows a normal distribution. It is noteworthy that ophiuroids and *Paranacystis* specimens smaller than ~2 mm as well as *Placocystella* with thecae smaller than 6 mm in length are not represented.

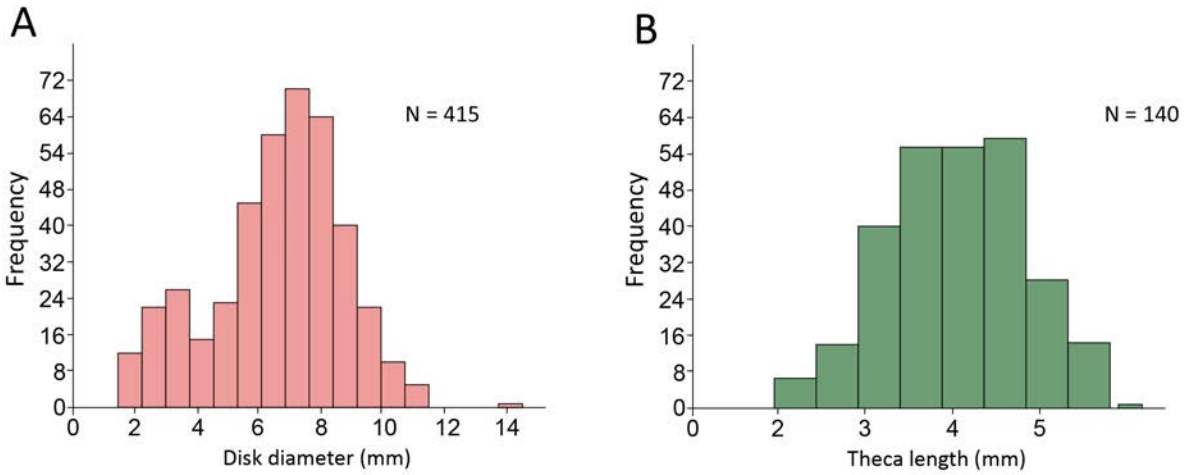

Figure 23. Frequency distribution of (**A**) ophiuroids showing a bimodal distribution pattern (**B**) paranacystids with a normal distribution pattern.

3.4. INTERPRETATION OF ECHINODERM TAPHONOMY

3.4.1 Obrution by storm deposition

Reid *et al*. (2015) demonstrated that the Lower Devonian succession that contains the Karbonaatjies obrution bed was deposited within a storm-influenced, proximal part of an offshore transition zone in a shallow marine environment (see Fig. 6 in Introduction). Obrution events (*sensu* Seilacher *et al*. 1985) or rapid burial events occur within a few hours to days and are commonly caused by raging storms (tempests) that may trigger a range of depositional events (i.e., sediment slides, slumps, debris flows, turbidity currents, etc.) and lead to the formation of tempestites, turbidites and other mass movement deposits (Brett, 1990; Reid *et al*., 2015). Fossil preservation under these episodic sedimentation events is very different to preservation during calm intervals of background sedimentation, when preservation of fossils

occurs over long periods of time with the organism exposed at the water-sediment interface to biochemical degradation that promotes the disarticulation of echinoderms (Brett and Baired, 1986; Brett *et al*., 1997).

Because the multielement skeletons of echinoderms, composed of calcareous endoskeleton parts that are connected by soft tissue, are very sensitive to post-mortem depositional processes, echinoderms are rarely observed as fully articulated specimens in the fossil record (Brett *et al*., 1997). Confirming this, experimental taphonomy has shown that ophiuroid disarticulation occurs within ~15 hours of death, complete disarticulation into endoskeleton components takes place within one to two weeks (e.g., Meyer, 1971; Schäfer, 1972; Lewis, 1986, 1987; Kidwell and Baumiller, 1990; Kerr and Twitchett, 2004). Lefebvre (2007) compared stylophoran preservation and paleoecology to that of ophiuroids and showed that because stylophorans are also composed of multiple delicate skeletal elements (e.g., theca, aulacophore), the two taxa may have similar taphonomic trends.

Based on their preservation, both ophiuroids and stylophorans in the Karbonaatjies obrution bed can be classified as Type 1 echinoderms according to the taphonomic grade classification of Brett *et al*. (1997). Type 1 echinoderms in this classification are characterised by a skeleton of very weakly articulated plates (ossicles), which can only preserve if buried very rapidly by a sufficiently thick sediment mass that inhibits biochemical degradation, mechanical disarticulation as well as biogenic disturbances such as burrowing by scavengers (Brett and Baird, 1986; Speyer and Brett, 1991; Brett *et al*., 1997). The majority of ophiuroids and stylophorans in the Karbonaatjies obrution bed display an overall high level of articulation and lack any signs of abrasion, suggesting that preservation resulted from a sudden burial. Additionally, the majority of stylophorans are preserved with the most fragile portion of the aulacophore fully intact and rarely in an extended position (life position/feeding posture), further confirming this sudden burial (Lefebvre, 2007). However, many *Placocystella africana* are incomplete with spines and the distal aulacophore missing. This is presumably due to the post-mortem detachment of these flexible, loosely articulated structures (Rahman *et al.,* 2009).

The ophiuroids in the Karbonaatjies obrution bed display almost equal oral side down (presumed life position) and oral side up (inverted position, this includes oblique positions) orientation. It is common in extant ophiuroid communities to have a small percentage of ophiuroids temporary overturned due to a change in body posture (Fujita and Ohta, 1989; Shroat-Lewis, 2007), though it is more likely that such a bimodal orientation of specimens

indicates the displaced nature of individuals that were likely transported by storm induced currents prior to deposition (Zatoń *et al.,* 2008).

The ophiuroids in the Karbonaatjies bed consist mainly of articulated specimens (Group 1) and partially disarticulated specimens (Group 2) with a small amount of completely disarticulated specimens (Group 3). This mixture of disarticulation stages indicates some specimens underwent different periods of decay prior to transport and final burial, a time averaged community, however the fully-articulated nature of more than half of the delicate ophiuroids and stylophorans indicates that transport may have happened while the animals were alive or soon after their death and the transport had to be followed by immediate burial (e.g. Rousseau and Nakrem, 2012). However, it was noted in the experiment by Kerr and Twitchett (2004) that the degree of disarticulation in fossil ophiuroids is not directly related to the nature and distance of transport, even if substantial transport did occur, full articulation is still possible when ophiuroids are alive or recently dead (within a couple of hours). Consequently, the ophiuroids and stylophorans may be allochthonous or para-autchthonous (somewhat transported before burial) as opposed to autochthonous (*in situ* burial). The completeness of the echinoderms in the Karbonaatjies obrution bed suggests that if there was transport before burial, it was somewhat limited in both strength and distance. This transportation could also be the cause of the breakage of many ophiuroid arms throughout the deposit and my account for the large number of Group 2 specimens (this concept is further discussed below). It is also likely that the current brought in fragmentary remains from elsewhere and potentially incorporating into its sediment load time averaged material that decayed/accumulated on the seafloor over longer periods represent the reworking of previously buried carcasses during the storm.

3.4.2 Autecology of ophiuroids and stylophorans

Gregarious behaviour of ophiuroids and stylophorans

Dense ophiuroid populations in modern environments are relatively common. These extensive and dense populations, on the order of hundreds to thousands of individuals per square meter, are generally dominated by one species of epifaunal and infaunal, suspension feeding ophiuroids (Fujita and Ohta, 1989, 1990; Aronson and Blake, 1997). Such densities of epifaunal ophiuroids are more commonly observed in marine bathyal (water depths: 200-3000 m) and abyssal habitats (e.g., Fujita and Ohta, 1989,1990; Shin and Koh, 1993; Metaxas and Giffin, 2004 recorded 1700 individuals/m^2 at water depths > 250 m) and less common in water

depths shallower than 100 m (e.g., northern Europe Warner, 1971; British Isles Aronson, 1989; a predation free salt water lake Aronson and Harms, 1985). Dense beds of ophiuroids have been recorded in the fossil record since the late Middle Ordovician (Fujita and Ohta, 1989, 1990; Hunter *et al*., 2007). Dense epifaunal ophiuroids are found in other Palaeozoic (e.g. Kesling, 1969; Kesling and Le Vasseur, 1971 recorded 4500 individuals/m^2 of *Strataster Ohioensis*) and Mesozoic (Wright, 1863,1880; Chatwin, 1948) deposits as well. From the Ordovician to the Jurassic, dense epifaunal populations are commonly found in more shallow water settings, however this changed during the Cretaceous onward possibly due to the shallow marine environment dramatic evolutionary radiation of decapod crustaceans and teleostean fish that probably increased the predation pressure on echinoderms in shallow water environments (Aronson and Sues, 1987; Aronson, 1989, 1992; Fujita, 1992; Aronson and Blake, 1997). This interpretation suggests that, in Palaeozoic times, dense assemblages of epibenthic ophiuroids and stylophorans were probably restricted to palaeo-environments where predators were rare or absent (Lefebvre, 2006).

As mentioned above, most of the modern dense ophiuroid populations are monospecific or dominated by one species (e.g., *Ophiura sarsii* in north-eastern Japan - Fujita and Ohta, 1989). This trend is also observed in many dense ophiuroid fossil assemblages (as mentioned above) as well as in the Karbonaatjies obrution bed, which contain approximately 2000 individuals/m^2 consisting of a single Lower Devonian ophiuroid taxon (see Taxonomy Chapter). This number compares well with many previously calculated modern ophiuroid communities from the British Isles (Aronson, 1992), Antarctica (Aronson and Blake, 2001), a Bahamian saltwater lake (Aronson and Harms, 1985), as well as fossil communities from the Eocene (Antarctic Peninsula-Blake and Aronson, 1998) and Triassic (Poland-Radwanski, 2002; Zatoń *et al*., 2008). This is also similar to Palaeozoic studies such as Kesling and Le Vasseur (1971) which describe a Mississippian shallow water, epifaunal, suspension feeding ophiuroid population of 4500 individuals/m^2. Regardless of signs of transport (as discussed above), it is highly probable that the clustering of the ophiuroids in the Karbonaatjies obrution bed is largely due to gregarious behaviour rather than only being passively transported and agglomerated by currents. Furthermore, a pulsating, storm-induced current may have repeatedly washed over the in situ ophiuroid aggregation, dislodging and then transporting them over some distance (but not out of their life habit). This may explain the dense aggregations of individuals arranged in successive horizons (see Fig. 13).

Conditions that facilitate such dense aggregations are: 1) low predation pressure (frequency of predatory attacks measured by the percentage of regeneration of one or more arms) and 2) low predator density resulting in decreased mortality and therefore increased population density of epifaunal suspension feeding ophiuroids (Aronson, 1987, 1989; Aronson and Heck, 1995; Aronson and Blake, 1997). There is a positive correlation between the frequencies of sublethal arm damage with rates of lethal predation. For example, the dense aggregations of ophiuroids from Aronson's (1989) study on *Ophiothrix fargilis* and *Ophiocomina nigra* showed low frequencies of arm damage due to sublethal predation, which occurs when ingesting the arm of an ophiuroid by a predator that does not result in death. It is important to note that infaunal ophiuroids that occur at the same high densities as epifaunal ophiuroids have showed very high rates of sublethal arm damage, this however can be attributed to some epifaunal Ophiuroidea having toxicity (repellent mucus) or possessing long arm spines like *O. nigra* (Sköld and Rosenberg, 1996; Aronson and Blake, 1997). Warner (1971, 1979) and Warner and Woodley (1975) proposed that the formation of dense ophiuroid aggregations increased individual feeding success by slowing down and/or stabilising the currents and thus increasing the deposition of food particles and protection from high current flows. Additionally, many studies have showed that dense populations are a great advantage for reproductive success owing to the external fertilisation of not just ophiuroids but many other echinoderms (Lawrence, 1987; Emson, 1998). Arm regrowth, evidence for sublethal arm predation in the specimens from the Karbonaatjies obrution bed is missing and this may suggest either the predator attacks were successful in capturing full ophiuroids or that predation pressure was low in this Lower Devonian ophiuroid population (and in line with other Palaeozoic communities globally). Alternatively, it is possible that the high density of ophiuroids lowered the effectiveness of predators by offering protection for individuals at the centre of the accumulation (Metaxas and Giffin, 2004).

Relatively dense assemblages of stylophorans are common in the fossil record. For example: 100 fully articulated cornutes, rapidly buried alive, were described from the deep outer shelf deposits of the Middle Cambrian Wheeler Formation in Utah (Ubaghs and Robison, 1988); a dense population of primitive stylophoran were found in the proximal shelf, storm-dominated environments of the Middle Cambrian Jince Formation in Bohemia (Parsley and Prokop, 2001), it is suggested that some animals were tumbled in a rigorous current and subsequently buried in a jumble orientation; 300 cornutes were observed from the Lower Ordovician Anti-Atlas in Morocco (Martin *et al*., 2015) were accumulation of the cornutes were a result of distal

storm scour and re-deposition of a para-autochthonous monospecific community. It is therefore likely that the stylophorans could have shared the same gregarious behaviour as the ophiuroids from the study as their mode of life is comparable to that of ophiuroids (Lefebvre, 2003,2007). The occurrence of over 100 paranacystids, fully articulated, possibly autochthonous individuals is suggestive of a gregarious mode of life. A gregarious mode of life seems to be a characteristic feature for many extinct and extant echinoderms, and such a mode of life for stylophorans likely provided the same benefits as for gregarious ophiuroids (Lefebvre, 2007).

The co-occurrence of such abundant ophiuroids and stylophorans has been reported from older deposits of the Middle Ordovician (Hunter *et al*., 2007), Upper Ordovician (e.g., Spencer 1950; Donovan *et al*., 1996; Jefferies *et al*., 1996; Lefebvre, 2006) to Lower Devonian (e.g., Dehm, 1932; Caster, 1954; Ruta and Bartels, 1998; Glass 2005). With the addition of the Karbonaatjies obrution bed, this demonstrates that a mixed ophiuroid-stylophoran assemblage is a relatively common occurrence in the late Ordovician to early Devonian time.

Loss of arms by autotomy vs. in storms

The ophiuroids in the Karbonaatjies obrution bed can be assigned to either Decay Stage 1 or Decay Stage 2 of Kerr and Twitchett's (2004) study that was conducted on modern ophiuroids. Here Stage 1 indicates loss of ventral plates, oral shields, tooth papillae and jaws, and fully articulated arms, and Stage 2 shows arms beginning to break off at/near the disc, at least one arm remaining attached and disarticulated arms beginning to fragment.

However, Stage 2 is not easily applied to fossil examples, because modern ophiuroids are known to regularly lose their arms under a number of circumstances. Therefore, the ophiuroids without arms and the large presence of arm fragments in the Karbonaatjies obrution bed could mean both burial before decay or loss during the storm event. The nature of fragmented arms is further complicated by the fact that most Palaeozoic ophiuroid arms have a different internal anatomy to modern ophiuroids. *Gamiroaster* belongs to an extinct group of ophiuroids, which show plesiomorphic (ancestral trait) characters not found in extant ophiuroids, such as unfused ambulacral plates within the arms as opposed to firmly fused vertebrae in living ophiuroids (Stöhr *et al.,* 2012). In extant ophiuroids, loss of arms is a result of: 1) post-mortem damage of skeletons by hydrodynamic disturbances (e.g., rocks shifting during storms); 2) arm autotomy, which is self-mutilation achieved by an intrinsic mechanism and is nervously mediated, predominantly caused by partial or sublethal predation (as a self defence mechanism) (Emson and Wilkie, 1980; Aronson, 1991; Oji and Okamoto, 1994; Lawrence and Vasquez, 1996;

Wilkie, 2001; Lawrence, 2012); and 3) exposure to extreme or harsh weather conditions, as found by Woodley *et al*. (1981) who showed an increase in damaged arms after Hurricane Allen, and Makra and Keegan (1999) who suggested that the frequent winter storms caused wave/tide induced currents resulting in increased arm loss. Storms and hurricanes causing arm loss was also observed in crinoids (Ameziane and Roux, 1997). However, it is very difficult to distinguish between self-defensive induced autotomy and physical stress induced arm loss in fossil examples.

As previously mentioned, there is no evidence in either the partially broken specimens or the isolated arms for repair and regrowth (which provide evidence for predation pressure), and therefore, it can be tentatively assumed that arm loss was not result of predation pressure but rather mechanical fracturing of the arms either when the ophiuroids tried to escape from the sediment influx caused by the storm or when they tumbled a short distance in the currents. In such events, the arms could remain intact as the ligaments are strong enough to hold the individual arms together for a short while before being entombed in the sediment (Donovan, 1991; Kerr and Twitchett, 2004). A number of specimens showed a broken arm proximal to the disc (Fig. 24), which could possibly be post-depositional breakage caused by burrowing organisms (e.g. Salamon *et al*., 2012; Jaselli, 2014) or fracturing due to localized, passive movement of the obrution sediment during compaction (early diagenesis). Interestingly, a 'clean break' between a fragmented arm and modern ophiuroid specimen is strongly associated with autotomy in ophiuroids (Lawrence *et al*., 1986; Wilkie, 2001). However, it is possible that the 'clean cut' arms next to the disks are simply random associations due to transport.

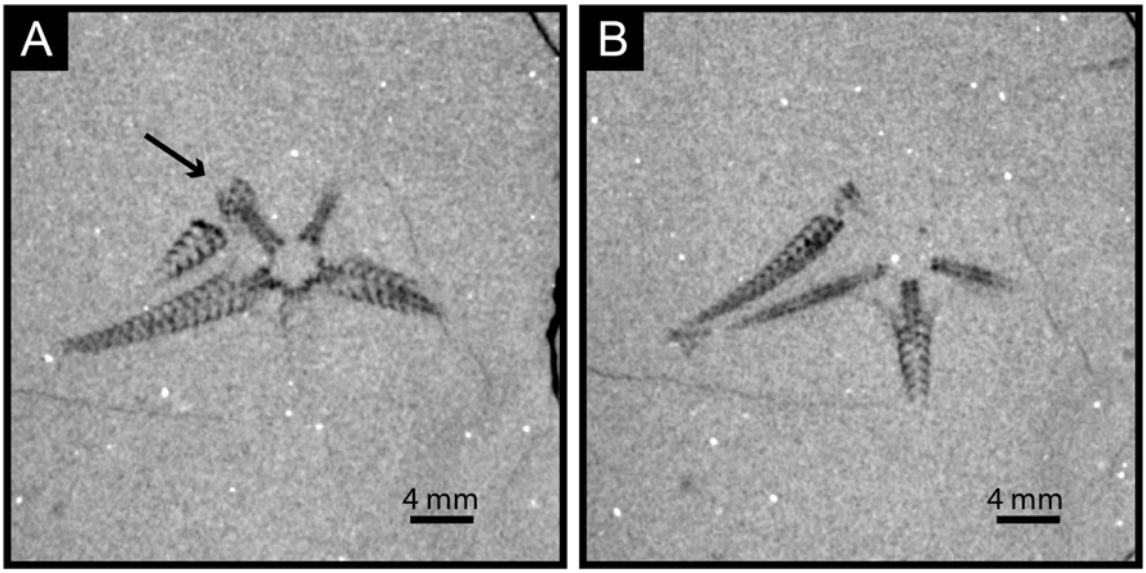

Figure 24. (**A**-**B**) Ophiuroid with broken arm next to disk. The arrow points to a clean break.

Escaping ophiuroids and distressed stylophorans

The ophiuroids within the obrution bed exhibit postures similar to those found within Ishida and Fujita (2001) study (Fig. 10 in Methods). The majority of the individuals (~ 80%) display *resting postures* similar to living ophiuroids, where the arms are equally-spaced and extended straight. A very small percentage of ophiuroids display *irregular postures*, the arms are unequally-spaced (asymmetrically arranged) and in some cases the arms are aligned in the same direction. This position is generally observed in ophiuroids that experience a rapid influx of sediments, a good example being the ophiuroids preserved in the Lower Devonian Hunsrück Slate in Germany (Bartels *et al*., 1998). The alignment of the specimens' arms reflects the current flow direction that embedded them, however these individuals are not aligned but rather randomly orientated throughout the bed. One of the most striking feature of the obrution bed are the ophiuroids observed with one or more arms extended upward into the overlying sediment. This has been identified as an *escape posture*. Ishida and Fujita (2001) observed that ophiuroids buried under 1-3 cm of sediment raised one to three arms towards the surface, eventually emerging and regaining radial symmetry. The similar sequence of events was observed for ophiuroids in an inverted position. Extant, actively crawling or burrowing ophiuroids can often escape rapid burial, however it is common for echinoderms to die when smothered because their ambulacral/water-vascular systems may become clogged by sedimentary particles (Rosenkranz 1971; Schäfer 1972). It is found that more than 5 cm of sediment is sufficient to immobilise and kill ophiuroids (Donovan, 1991; Ishida and Fujita, 2001). Consequently, for the majority of fossil ophiuroids in the bed, the sudden burial event (storm deposit) probably lead to death by suffocation, entombing them in the resting position with arms stretched out, while a few may have briefly survived the limited transport and attempted escape by moving their arms after burial, even if in an inverted position. It is also probable that some of the ophiuroids had died and suffered from decay before the catastrophic event which may explain specimens totally lacking in arms. According to the study by Kerr and Twitchett (2004) it took approximately 3 days for the ophiuroids to reach disarticulation stage 3, a complete loss of arms from the disk. The observed stylophorans, with most specimens fully articulated, suggest that they were probably instantly smothered without any attempt to escape (e.g., Sutcliffe *et al*., 2000, Rahman, *et al.,* 2009).

Reports on fossil ophiuroids exhibiting escape behaviour are rare. Brett (1983) and Taylor and Brett (1996) reported on a single Silurian *Protaster* embedded at an oblique angle in the Rochester Shale with "contorted" arms, and suggested that this indicated a failed escape. Furthermore, Jagt (2000) described a single Upper Cretaceous ophiuroid in escape posture, two leading arms bent in an attempt to escape with the disk orientated at 90° to the bedding plane. Salamon *et al*. (2012) alluded to the possibility that overturned Triassic ophiuroids are evidence for escape behaviour. Additionally, vertical and horizontal ichnotaxa *Asteriacites lumbricalis* von Schlotheim, 1820 from the Upper Carboniferous have been interpreted as either escape or feeding structures made by epifaunal ophiuroids (Bromley, 1996; Mángano *et al*., 1999).

Many of the *Paranacystis* stylophorans are preserved with the aulacophore flexed over or under the theca or curved to the side. This posture of the aulacophore is now commonly interpreted as a result of post-mortem contraction of tendons/muscles and not a feeding position (Jefferies 1984; Parsley 1988, 1991; Ruta and Bartels 1998; Lefebvre 2003). The latter is because in this position the elevated aulacophore is hydrodynamically unstable. Other interpretations suggest that this is a distressed posture due to turbulent currents (Parsley, 1991; Lefebvre, 2003, 2007; Parsley *et al*., 2000). One *Placocystella* individual is preserved with its aulacophore extended, which suggests life position, because apparently these stylophoran would extend their aulacophore over the seafloor to feed (cf. Parsley *et al.,* 2000; Lefebvre, 2003). Additionally, most *Placocystella* have the brachial spines orientated downwards, in which also suggests life position, because the brachials may have been used as anchorage in the sediment (cf. Lefebvre, 2003). Interestingly, another *Placocystella* individual has its proximal aulacophore angled upwards, taking up a position that is very similar to interpreted feeding posture of the ankyroid *Vizcainocarpus naimae* Parsley and Gutierrez-Marco, 2005, where the distal ends are draped over a sand wave (i.e., not positioned into the water column but rather arched over the sediment) (Parsley and Gutiérrez-Marco, 2005).

Mode of life

Extant ophiuroids exhibit a wide array of feeding types such as epifaunal and infaunal suspension feeding, deposit feeding (microphagous), scavenging and predation (macrophagous). Reid *et al*. (2015) suggested that the ophiuroids possibly fall into the epifaunal category due to having short arms in relation to disk diameter (e.g. Twitchett *et al*., 2005). This ratio is useful for determining extant ophiuroid modes of life but becomes difficult to apply to Palaeozoic ophiuroids with a different arm anatomy. Ophiuroids are known to inhabit many

different sedimentary environments at all depths, however the majority prefer low-energy waters with a low sedimentation rate (Roman, 1994). In general, ophiuroids that are predatory have short tube feet and short arm spines, whereas suspension and detrital feeders have long tube feet and long spines (Warner, 1983). However, there are certain ophiuroid species that inhabit high energy environments that have relatively short and blunt arms, an example that modern ophiuroids are not mutually exclusive to one feeding habit (Hess and Meyer, 2008).

Shackleton (2005) and Glass and Blake (2004) provide comprehensive overviews of the possible life modes in Palaeozoic ophiuroids, and more specifically, Spencer and Wright (1966) suggest that Palaeozoic ophiuroids were more likely sedentary infaunal deposit and suspension feeders. Shackleton (2005) states that there is no evidence of ciliary or suspension feeding in Ordovician ophiuroids and that deposit feeding was a facultative strategy in derived ophiuroids. However, the arms of most derived Ordovician ophiuroids were mobile enough to lift their arm up into the water column and use tube feet to collected suspended food particles (Shackleton, 2005). Many protasterid ophiuroids have short spines (none are actually seen preserved in *Gamiroaster*) and generally exhibit relatively flexible arms (as seen in the escaping specimens). This may allude to macrophagous feeding habits, however *Gamiroaster* has no whip-like arm tips, which would be flexible enough to wrap around prey. It is more likely that *Gamiroaster* was deposit feeding, however evidence other than the short arms is lacking to determine whether *Gamiroaster* preferred an infaunal or epifaunal mode of life. Although it is possible that Palaeozoic ophiuroids could also have been suspension feeders, adapted to occasional scavenging, however their arms are not as flexible as modern forms that have a more advanced filter-feeding habit (Shackleton, 2005). Interestingly, if *Gamiroaster* was adapted to a deposit feeding lifestyle, this would suggest their inferred gregarious behaviour may have been an adaptation in aid of reproduction and/or to reduce predation rather than for feeding.

Stylophoran life position and mode of life has been subject to much controversy over the years due to lack of agreement on aspects of anatomy but more specifically on the interpretation of their appendage (aulacophore). The appendage in all stylophorans consists of: 1) a highly flexible proximal part made up of imbricated rings; a 2) median part made of a single skeletal element (stylocone or styloid); and 3) a delicate part made of a series of ossicles (brachials and cover plates). It is seen as a muscular stalk (e.g. Philip, 1979; Kolata and Jollie, 1982), a chordate tail (e.g. Jefferies, 1967; Cripps and Daley, 1994), a muscular locomotory organ (Clausen and Smith, 2005) or a feeding arm (e.g. Ubaghs, 1961; Parsley, 1988; David *et al*.,

2000). The most widely accepted theory is that they are believed to be benthic organisms, which feed with their arm (aulacophore) extended over the substrate and facing the current (Parsley, 1991; Lefebvre and Vizcaïno, 1999; Lefebvre, 2007; Parsley *et al*., 2000). According to Lefebvre (2007) anomalocystitids such as *Placocystella* found in this bed, have ratchet sculptures (burrowing sculptures) which are associated with a semi-infaunal mode of life and that the two large transverse blades on the lower surface of the stylocone are used as anchorage into the substrate (Fig. 25). Paranacystids and *Placocystella* have been referred to as being sessile organisms (Caster, 1954; Lefebvre, 2007), however there is good evidence that mitrates like *Rhenocystis* were capable of extensive locomotion (Sutcliffe *et al*., 2000; Rahman *et al*., 2009). *Rhenocystis* is very similar in morphology to *Placocystella* and is therefore likely that the stylophorans found in this bed were capable of facultative mobility.

Mitrates (and cornutes) are sometimes found associated with populations of ophiuroids of which they form dense, low diversity assemblages (Lefebvre, 2007). Such associations have been documented in several deposits from the Middle Ordovician to the Middle Devonian. The oldest evidence for a gregarious mode of life for ophiuroids and mixed ophiuroid-stylophoran associations was found in the Llandeilian (Middle Ordovician) of Western France (Hunter *et al*., 2007). There are many more examples of such associations, for example the Upper Ordovician Lady Burn Starfish Bed of Scotland (Spencer, 1950; Donovan *et al*., 1996) and the Emsian Hunsrück Slate in Germany (Bartels *et al*., 1998). It is therefore plausible that the two groups of echinoderms in the Karbonaatjies obrution bed shared an analogous mode of life, as Lefebvre (2007, p. 168) suggested both ophiuroids and stylophorans were "small, flattened, free living, unattached, gregarious, epibenthic or infaunal echinoderms, which were using their highly flexible arms for feeding, anchoring to the substrate and/or for limited mobility".

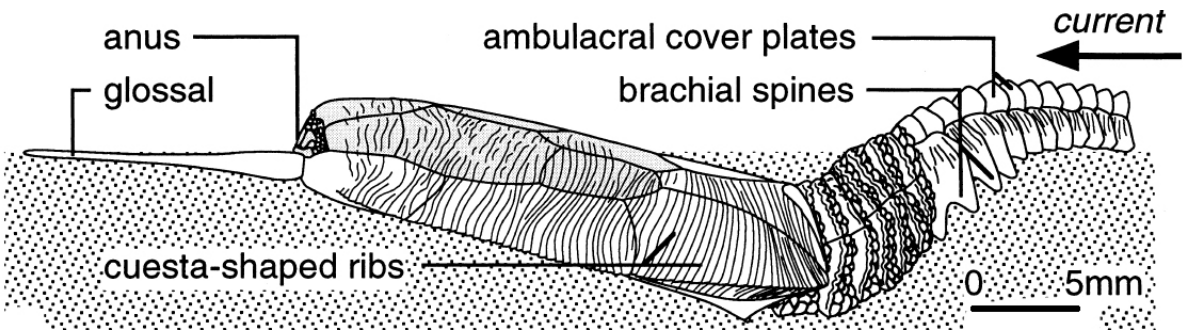

Figure 25. An example of interpreted life position of the Mitrocystitida *Placocystites forbesianus* de Koninck, 1869 (taken from Lefebvre, 2003).

Population structure

The apparent lack of juveniles is a common problem in many fossil populations and not just in the present study. This can be due to hydrodynamic sorting by currents, mechanical destruction, predation, migration, growth and mortality rates or different habitat of juveniles to adults (Hallam, 1972; Dodd *et al*., 1985). The latter is common in modern ophiuroids where the young move away from the adult population, however this is not always the case for ophiuroids like *Ophiothrix fragilis,* where the young are found closely associated with the adults (Morgan and Jangoux, 2004). Generally, collecting bias can be a cause (collecting the larger and better looking specimens), however due to the non-destructive and unbiased nature of CT scanning this error was minimized in this study. Mechanical destruction eliminated a potential reason for the different age classes as ambulacra ossicles smaller than 0.3 mm (much smaller than the missing discs and theca) at the tip of the arms are preserved. Regardless of the transport mechanism (discussed below) and probable hydrodynamic sorting, it is likely that the ophiuroids and stylophorans formed multi-individual assemblages characterised by a normal distribution. The possible bimodal distribution seen in the ophiuroids is more indicative of recruitment periods (production and release of gametes was likely seasonal), which at the time, consisted of a population dominated by large/older individuals (e.g. Fujita and Ohta, 1990). In contrast, the absence of multiple size modes in the stylophorans, which show a broad range in sizes, could indicate the reproduction was not seasonal, with the assemblage representing the continual accumulation of individuals of different ages.

3.5 SHELL TAPHONOMY RESULTS

All shell specimens in the Karbonaatijies obrution bed are preserved as moulds (internal moulds predominate). The obrution bed is dominated by shell fragments ~2 mm or larger in size, which includes unidentified brachiopods, bivalves, trilobite thoracic segments, gastropod fragments, crinoid ossicle and stem fragments, and fin spine fragments (Fig. 26). Only a total of 40 spiriferid brachiopods were large enough (30-60 mm in length) to be identified as *Australospirifer* and three as *Australocoelia* (Fig. 26A-D). In addition, a total of eight bivalves were identified as possibly *Nucliites* or *Palaeoneilo*. Amongst all of the shell fragments are fully articulated ophiuroids, ophiuroid arm fragments, articulated paranacystids and *Placocystella* aulacophore fragments (but no articulated specimens).

The obrution bed is a medium-grained quartz-rich siltstone. Quartz grains are well-sorted, sub-angular and set in a fine-grained clayey-silty matrix. (Fig. 27). Fragments smaller than 2 mm in diameter are considered shell debris (hash), whereas those that are 2 mm and larger in diameter make up 15–20 % of the bioclasts (with the rest of the bioclasts being intact ophiuroids and stylophorans). The bioclasts (shell fragments and intact echinoderms) are generally loosely packed (i.e. matrix-supported), and a few may be in direct contact with one another. The shell fragments are well- to moderately sorted with a bimodal size distribution where the larger identifiable brachiopods and bivalves (30-60 mm in length) are dispersed among much finer shell fragments (2-3 mm). Of the larger and relatively more intact brachiopod and bivalve shells, 48 were measured and counted (Appendix 7 and 8). All 40 brachiopods and 8 bivalves are disarticulated, and ~60% are in convex-up and, 40% in convex-down position (none are oblique). Brachiopod valve lengths vary from 3 to 6.5 cm and bivalves vary from 2.5 to 4.5 cm in length. Pedicle valves dominate (84% of valves), and for bivalves, left valves appear to be more common, however it is difficult to quantify as most of the umbos are absent or eroded and ventral margins are broken. The orientation of specimens is horizontal and concordant (parallel to the bedding plane), with the exception of one vertical brachiopod valve. The larger brachiopods and bivalves measured have a varying degree of fragmentation from low too high for both valves. However, the fragmentation index for the whole obrution bed (not including the ophiuroids and stylophorans) is moderately high to very high. All measurable brachiopods and bivalves are only slightly corroded, micro-ornamentation is lost but costae (ribbing) and growth lines are intact.

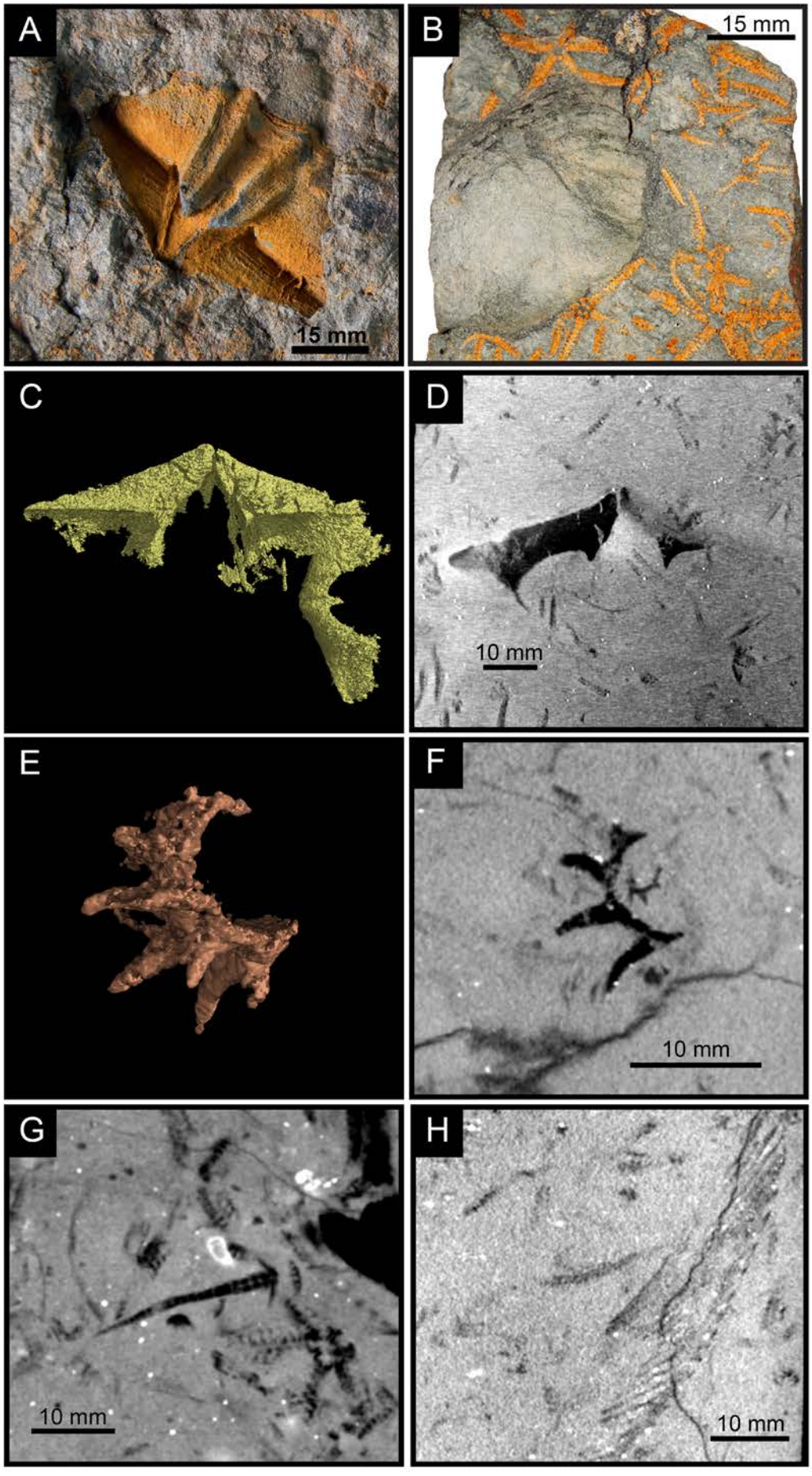
A
15 mm
B
15 mm
C
D
10 mm
E
F
10 mm
G
10 mm
H
10 mm

Figure 26. Shell specimens in the lower part of Karbonaatjies obrution bed. (**A**) Pedicle valve of brachiopod *Australospirifer* sp. (**B**) Unidentified bivalve possibly *Palaeoneilo*. Note the articulated ophiuroids surrounding the valve. (**C-D**) Convex up and convex down pedicle valves of *Australospirifer* found within the first horizon of ophiuroids. Note that the larger shells are surrounded by ophiuroids and smaller unrecognisable shelly fragments. (**E-F**) Unidentified gastropod shell fragment with double ridged spines that are similar to *Platyceras dumonsum* from the Lower Devonian of New York. (**G**) Fragment of an aulacophore (stylocone, brachial spines and arm ossicles preserved) of probably *Placocystella* sp. Note the articulated ophiuroid and paranacystid amongst the shell fragments (shadowy marks). (**H**) Fin spine showing unique comb-like pattern, possibly from a Palaeozoic shark ?*Ctenacanthus*.

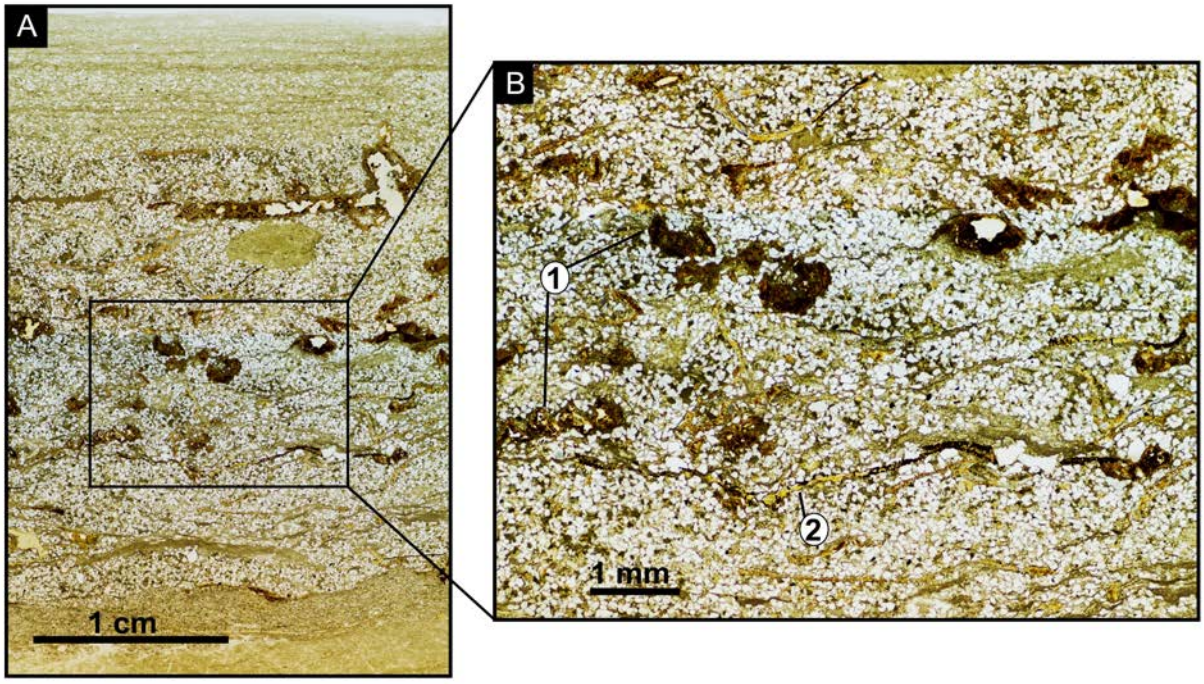

Figure 27. (**A**) Photographed thin section of the Karbonaatjies obrution bed, fossils are dark brown. (**B**) Magnified image of ophiuroid fossils (1) and shell debris (2).

Clionoides Fenton and Fenton, 1932 (synonymy for *Vermiforichnus* Cameron, 1969) borings are found in 10% of the visible brachiopod valves (Fig. 28), with each bored (mainly pedicle) valve containing more than 10 individual borings.

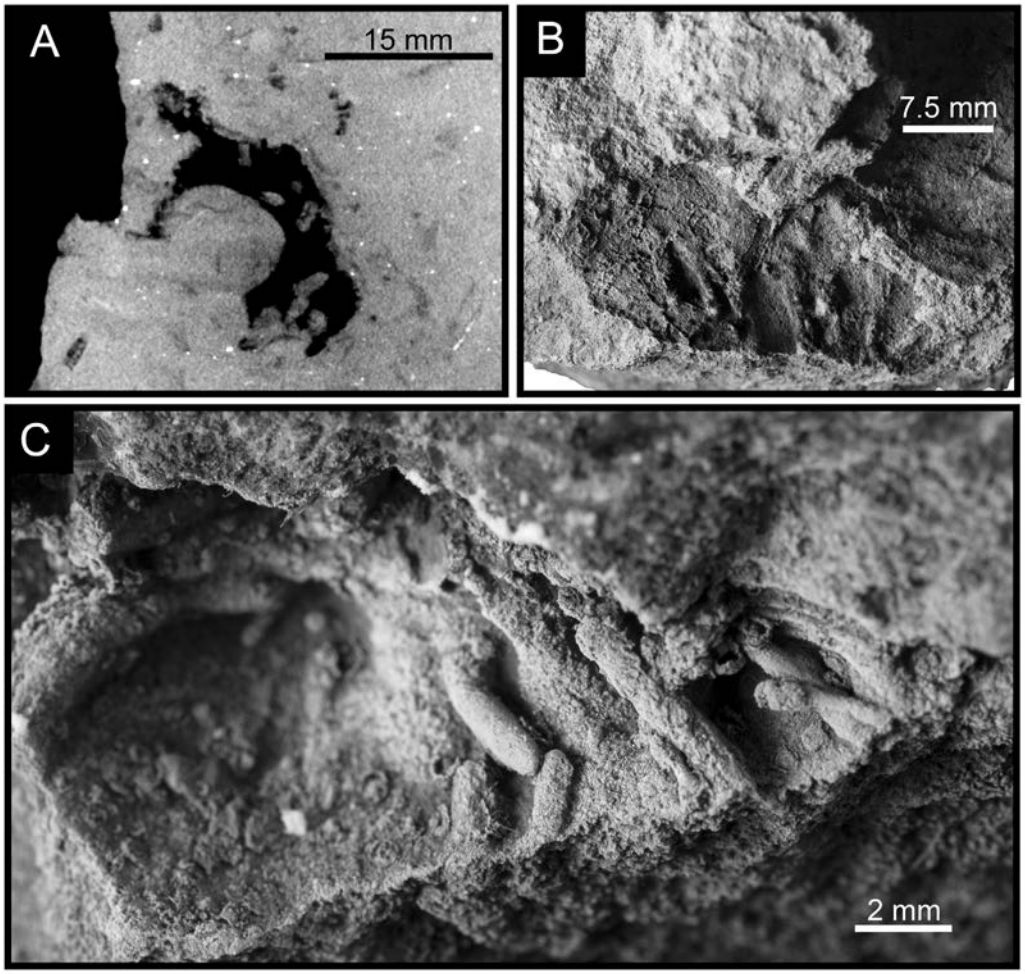

Figure 28. (**A-C**) *Clionoides clarkei* (Cameron, 1969) found within 10% of brachiopod valves, mainly the pedicle valves of *Australospirifer* sp. (**A**) 2D image scan showing a cross sectional view of sediment filled tunnels in the pedicle valve. (**C**) Tunnels approximately 1 mm diameter.

3.6 INTERPRETATION OF SHELL TAPHONOMY

Disarticulation and fragmentation

The high fragmentation and total disintegration of the shells in the Karbonaatjies obrution bed can be attributed to physical reworking by mainly energetic, storm-induced currents and/or bioturbation as well as long residence time on the seafloor. With the exception of the brachiopod pedicle valves, most of the brachiopods and bivalves were subject to rapid fragmentation. The destruction of shells is generally not attributed to storms (Davies *et al*. 1989), however winnowing and mixing of the shells caused by storm induced currents can cause mechanical abrasion and breakage.

Skewed pedicle/brachial proportions of brachiopod fossil assemblages have been assumed as a result of differential destruction and transport of valves, environmental energy and residence time of the seafloor (Brett and Baird, 1986). The preferential valve destruction is due to differences in valve thickness; as the brachial valve is more susceptible to mechanical breakage or *in situ* disintegration into unrecognisable fragments (Holland 1988; Velbel and Brandt, 1989). In case of bivalves, the right valve is generally thinner and more fragile than the left valve, which is therefore more likely to contribute to the fragmented remains. The higher number of *Australospirifer* pedicle valves in the Karbonaatjies obrution bed is explained by the above processes. However, the well-preserved fragile echinoderms found intact within the shell hash and among the more robust, larger shell fragments complicates the simple explanation by mechanical breakage and transport, and strongly suggest that the transport medium as a dense current, was no longer in traction with the seafloor where the moving fragments rubbed against one another but *en masse* (Reid et al. 2015). Therefore, those echinoderms that were picked up in the final stages of the currents evolution could remain better to fully-articulated, because they were moved in isolation (i.e., without abrasion) in these sediment laden currents (Reid *et al*., 2015). It is also plausible that, at least some of the poorly sorted debris of trilobite thorax fragments, crinoid ossicles, gastropod fragments, fish spine fragments and even the *Placocystella* aulacophore was not solely brought in by high energy currents, but was part of a shell pavement indicative of a time averaged deposit, this concept is discussed further below (Reid *et al*., 2015).

Reorientation convex-up or down valves

The dominance of articulated and convex-down orientation has previously been reported as a result of burial without the influence of storms, because storm-induced currents can overturn

the hydrodynamically unstable convex-down orientated shells (Speyer and Brett, 1986; Brett and Baird, 1986). However, this bed does show a general lack of preferred orientation, with only 10% more of the valves being in convex-up position. This could imply that currents lead to convex-up orientations, and that the convex-down valves settled out from suspension (Clifton, 1971; Futterer, 1982; Fürsich and Oschmann, 1993; Kidwell and Bosence, 1991; Chen *et al*., 2010).

3.7 DEFERENTIAL PRESERVATION OF TAXA

Differential preservation of the fossils in the Karbonaatjies obrution bed points to a complex burial history. The mixture of fully articulated ophiuroids and stylophorans amongst shell fragments indicate possible mingling of different generations of bioclasts, either by bioturbation or, more likely in this case, transport of fragments from nearby environments (Reid *et al*., 2015).

The obrution bed has been identified as what Parsons *et al.* (1988, p. 113) defines as a "simple shell bed" (which does not imply a simple origin for the concentration or taphonomic history, nor a single event), with the following features: the 2-5 cm thick bed consists of an irregularly erosive base, overlain by mostly shell and crinoid debris that makes up the lower third of the bed. This shell material consists of mostly unrecognisable shell fragments on the order of 1-7 mm in size, amongst the shell debris are articulated ophiuroids and stylophorans. The middle third of the bed contains larger recognisable fragments of brachiopods and bivalves as well as fully articulated ophiuroids and stylophorans. The upper third of the bed only contains much larger (in size and frequency) fully articulated ophiuroids and stylophorans with only rare shell fragments (mainly trilobite thorax fragments). Simple shell beds display differential preservation of fossils from bottom to top, with the highest degree of disarticulation, fragmentation and post-mortem destruction in the lower part and decreasing upward. It is noteworthy that all shells remain fragmented throughout and that the frequency decreases at upper portions, however the ophiuroids and stylophorans remain fully articulated from the lower third to the top of the bed.

The occurrence of preserved delicate ophiuroid and stylophorans within the upper portions of the shell bed requires rapid burial and with little transport. However, the presence of the sharp erosional base, rip-up clasts and a significant amount of shell and crinoid fragments within a matrix-supported fabric (as opposed to mud-supported) indicate high energy depositional conditions and possible transport and winnowing of material (this includes shells that may have

been exhumed from the lithified underlying substrate). Additionally, the rippling of the bed top and convex up brachiopods and bivalves suggest current action affected the skeletal accumulation prior to burial. It is event that the obrution bed represents a storm event characterised by winnowing and rapid burial and is plausible that this bed does not record a single event of reworking but rather a time averaged scenario, where the shell fragments records long term reworking and winnowing while the articulated echinoderms indicate rapid entrapment. The disarticulated and moderately abraded crinoid ossicles as well as the *Clionoides* borings within the *Australospirifer* fragments are further evidence that some specimens spent a large amount of time decaying on the seafloor and more likely form part of the substrate that the ophiuroids were inhabiting. Consequently, this co-occurrence is a result of mechanical mixing created by the storm induced current. Successive generations of shells and other detritus mixed during this time. Sporadic storm induced currents may have resuspended and concentrated the shells further, entrapping live or recently dead echinoderms from nearby or even living on the shelly substrate.

The dense aggregations of individual fully articulated ophiuroids arranged into successive horizons (or vague laminations- Fig. 13) within the highly-fragmented shells might explain the evolution of this transport medium. The initial highly abrasive current that incorporated sediment, winnowed shell fragments and dead or alive echinoderms into itself, could have evolved into a higher sediment concentration current (Fig. 29). The mode of transportation of the (organic and inorganic) fragments in the dense current was no longer in traction (where the moving fragments rubbed against one another and the sea floor), but ‘‘en masse’’ (Reid *et al*., 2015) (Fig. 29B). This may have resulted in the echinoderms being picked up in the final stages of the current’s evolution and thus could remain fully-articulated because they were moved in isolation within the sediment laden currents (Fig. 29B). As previously mentioned it is plausible that the shell debris and other fragments were not only brought in by the high-energy currents but was part of a shell pavement.

As mentioned earlier, the Voorstehoek seawater was relatively cold during the Malvinokaffric time thus favouring the articulation of echinoderm skeletons by slowing down the rate of decay of soft tissue (Kidwell and Baumiller, 1990).

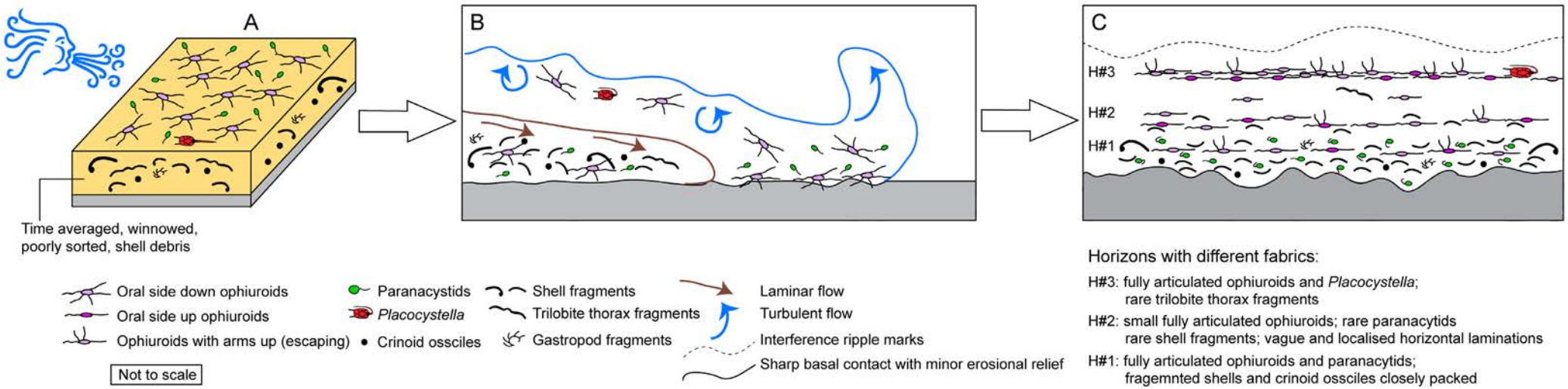

Figure 29. Schematic flow chart showing interpreted sequence of events responsible for generating the Karbonaatjies obrution bed. (**A**) Potentially gregarious ophiuroid and stylophoran community living on a substrate of time averaged shell debris. (**B**) Concentrated density flow (brown arrows), with entrained shell debris and echinoderms, diluted enough to allow for the upper part of the flow to be turbulent (blue arrows). (**C**) The deposit characterised by an erosional base overlain by vaguely Laminated ophiuroid horizons.

There is no doubt that this obrution bed illustrates a complex history of admixture of shells and echinoderms in different states of preservation, creating a time-averaged accumulation. Time-averaging was first defined by Walker and Bambach (1971) as fossil assemblages that accumulate from the local community over long periods of time and that these assemblages do not reflect the local community/ecological structure. However, in rare cases such as during the formation of the Karbonaatjies obrution, sudden burial may entomb a living community of ophiuroids (and potentially stylophorans) that reflect little or no time-averaging within a clearly time averaged shelly debris that depicts a depositional history previous to the obrution event responsible for the sudden smothering of echinoderms (Kidwell and Bosence, 1991). This story is further complicated by the fact that the echinoderms have been buried along with the shelly remains of probably earlier colonists of the site, mixed in with other subsequently introduced shelly material.

Other fossiliferous beds found within the vicinity

A single fully articulated specimen of a relatively large and rare proto-ophiuroid *Eophiura* sp. Jaekel, 1903 was found half a centimetre bellow the erosional base of the obrution bed within a silty mudstone (Fig. 30A) (see Taxonomy Chapter for diagnosis and Fig. 3 for location in relation to the Karbonaatjies obrution bed). Amongst the ophiuroid are internal moulds of disarticulated small, deep-burring, deposit feeding bivalves probably *Palaeoneilo*, all convex up, with little to no fragmentation (Fig. 30B). It is likely that this deposit represents previous rapid *in situ* burial during a storm. Half a meter above the obrution bed another single, large unidentified ophiuroid was preserved adjacent to a single articulated crinoid stem (Fig. 30C and D). Multiple individuals of the ophiuroid *Haughtonaster reedi* Rilett, 1971 were found one meter above the obrution bed within a trilobite moult assemblage consisting of the single taxon *Bainella africana* (Salter, 1856) (Fig. 30E and F) (see Taxonomy Chapter for diagnosis of the ophiuroid). These sporadic occurrences of well-articulated, active, free-living ophiuroids amongst somewhat barren silty sandstones and mudstones suggest that periodic storm disturbances, which resulted in event beds, were common during the deposition in the Voorstehoek Formation.

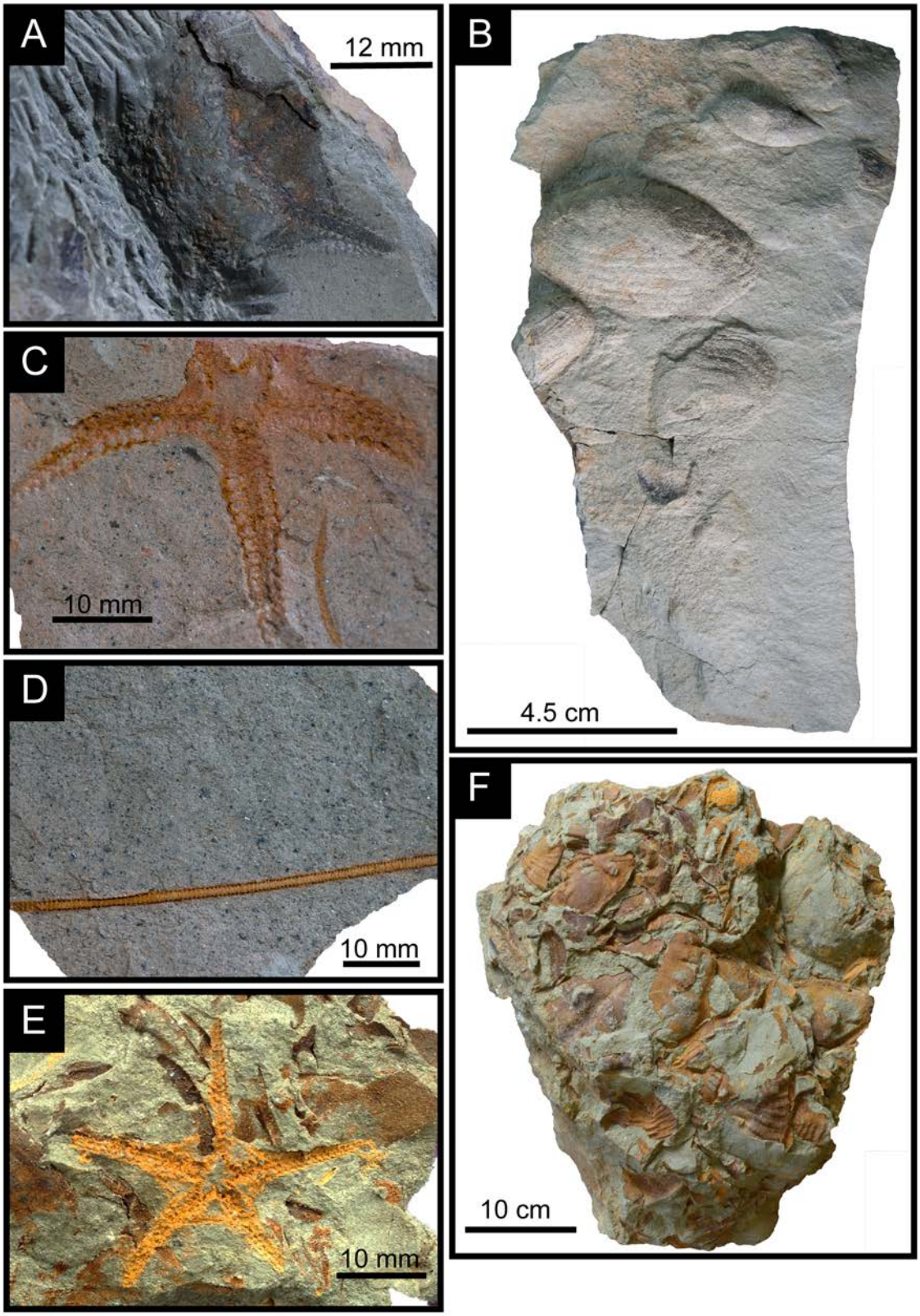

Figure 30. (**A**) One partially complete *Eophiura* sp. (SAM-PB-022505A), (**B**) Convex up left valves of ?*Palaeoneilo* and a single *Nuclulites* sp. (**C**) Unidentified ophiuroid preserved with a single crinoid stem (**D**), and (**E**) *Haughtonaster reedi* (SAM-PB-022507) preserved within a trilobite moult assemblage of *Bainella africana* (**F**).

CHAPTER 4 SYSTEMATIC PALAEONTOLOGY

"Unnamed forms become forgotten merely through the lack of a name with which to record them" - Savage 1970

The most diverse Lower Devonian echinoderm assemblage in the world is in the extensively documented Hunsrück Slate (Rhineland-Palatinate) in Germany and consequently the best source of data for Early Devonian ophiuroids (e.g., Glass and Blake, 2002; Blake, 2003, 2009; Glass, 2004, 2008; Glass and Poschmann, 2006). The Malvinokaffric fauna of the Bokkeveld Group is in third place globally in terms of the Early Devonian asterozoan diversity, along with the slightly more diverse Talacasto Formation (Precordillera) of Argentina (Haude, 1995, 2004, 2010) (Table 3). The first asterozoan and mitrate in the Bokkeveld Group were recorded by Reed (1925), whereas ophiuroids were mentioned by Rossouw (1933), Spencer (1930, 1950a) and Rilett (1971). The first extensive revision of South African ophiuroids including crinoids, blastoids and asteroids was by Jell and Theron (1999), who also described the collections in the South African Museum (now Iziko Museum) and the Geological Survey of South Africa (now Council for Geoscience).

Table 3. Ophiuroid occurrences across the Malvinokaffric faunal province. (modified from Hunter *et al*., 2016). * Denotes ophiuroids revised and discussed in this study.

Argentine Precordillera (Haude, 2004)		**South African Bokkeveld** (Jell and Theron, 1999**)**	**Falkland Islands** (Hunter *et al*., 2016)
Eophiuridae	*Haughtonaster* sp.	**Haughtonaster reedi*	
		**Eophiura* sp.	
Cheiropterasteridae	*Hexuraster* sp.	**Hexuraster weitzi*	
Encrinasteridae	*Magura yach*	*Ecrinaster tischbeinianus*	
	Magura sp.	*Marginura hilleri*	
Protasteridae	*Eugasterella* sp.	*Eugasterella africana*	*Darwinaster coleenbiggsae*
		Startaster ohoiensis	
		Startaster stuckenbergi	
		**Gamiroaster* sp. nov.	
Ophiurinidae	*Argentinaster bod.*		
	Argentinaster sp.	*Argentinaster* sp.	
Furcasteridae	*Furcaster separatus*		
Eospondylidae	*Eospondylus* sp.		

Aligning with recent approaches in asterozoan palaeontology (e.g., Shackleton, 2005; Blake *et al.* 2015), this study aims to: 1) systematically describe a new addition to the Malvinokaffric asterozoan faunas; 2) revise some of the genera previously described by Jell and Theron (1999); and 3) identifying the mitrate stylophorans, which in South Africa, are poorly studied and in need of revision.

Terminology. From Spencer and Wright (1966), Glass and Blake (2004), Shackleton (2005), Glass (2006), Blake (2013).

Class STENUROIDEA Spencer, 1951

Order STENURIDA Spencer, 1951

Family EOPHIURIDAE Schöndorf, 1910

Diagnosis. Taken from Shackleton (2005): Ambulacral transverse bar bearing lateral ridges; adambulacrals with vertical spine-bearing ridge; calcified stone canal; aboral plates straight-sided polygons; dorsal epispire gaps extend sub-ambitally; oral area with buccal slits; mouth angle plate crossed by single deep proximal groove.

Remarks. The order Stenurida Spencer, 1951, was recently recognised by Blake (2013) at the class level as Stenuroidea. To which he included *Eophiura bohemica* Jaekel, 1903 on the bases of having an extra set of ossicles between the ambulacra and the adambulacral. Whereas, Shackleton (2005) assigned Eophiuridae to the class Ophiuroidea Gray, 1840 which is defined by the appearance of apomorphies such as an interradial disk with separated arms and the reduction of adambulacral size approaching the jaw. There is much discussion in the literature, I use the classic, most readily available treatment, that of Spencer and Wright (1966) and Blake (2013).

Genus *Eophiura* Jaekel, 1903

Type species. *Eophiura bohemica* Jaekel, 1903 [*nomen nudum*] by subsequent monotypy of Schuchert, 1914.

Diagnosis. Taken from Shackleton (2005): Inferomarginal ossicles alternate between small and large size; additional spine-bearing ossicle in jaw causing mouth angle plate to be L-shaped.

Eophiura sp.

Figure 31

Material. Specimen SAM-PB-022505A,B, preservation is good but only ventral ambulacrals, adambulacrals and a single series of apparent marginals adjacent to the adambulacrals are exposed. No other disk or jaw elements are discernible.

Occurrence. Lower Devonian Voorstehoek Formation, Bokkeveld Group, Karbonaatjies Farm, ~10 km from Hex River Pass, Western Cape, South Africa (see Chapter 1-Fig. 3 for stratigraphic detail).

Description. Ventral portion of the disk and arms only preserved (Fig. 31A). Portion of disk preserved sub-pentagonoal; strong marginal ridge between interradii; blocky marginal ossicles, disk appears to have patches of sub-polygonal granules. Disk spines are not apparent. Short elongated, rapidly tapering arms, pointed at distal end (Fig. 31B-C). Lateral arm plates are not covering distal arm tips. Madreporite not seen (i.e., unclear whether it is not preserved, obscured or too small to recognise). Mouth frame ossicles not preserved. Only oral surface of the arm preserved and bears ambulacral, embedded virgal and laterals. Ambulacral ossicles alternate over the mid-line, periradial suture narrow and straight (Fig. 31B and C). Each ambulacrum has a prominent periradial ridge and transverse bar separating the podial basins, giving a T-shape to the oral surface of the ossicle. Laterals are stout, blocky and slightly asymmetric. Associated spines short and evenly spaced (Fig. 31B). Smaller rounded articulation sites for groove spines are visible along the ventral edge of the lateral; a number of spines are visible on the mouldic original (Fig. 31A). Only one groove spine preserved on each lateral. Embedded virgal are complex and difficult to intercept due to poor preservation; however, they appear to alternate with respect to each ambulacrum, and are positioned in indentations between the ambulacral proximal and distal surfaces.

Remarks. Description based on a single incompletely preserved specimen, with an overall form that places it within the Family Eophiuridae. This specimen possesses the typical T-shaped ambulacrals caused by a prominent periradial ridge and transverse bar that separates the podial basins, that forms a biseral alternate row (Shackleton, 2005). Whereas in Protasteridae Miller, 1889 and Encrinasteridae Schucherts, 1914 the podial basin lies entirely on the distal abradial margin of an ossicle. Assignment to *Eophiura* is based on presence of blocky asymmetric outer

plates or laterals, a series of virgals and a concave interradial disk. *Eophiura* closely resembles *Pradesura* Spencer, 1951, but has blockier laterals. The laterals of *Pradesura* have a blocky nose and head projecting distally. These sickle-shaped outer plates are similar in appearance to *Palaeura* Jaekel, 1903 and in Protasteridae. *Palaeura* Jaekel, 1903 differs from *Eophiura* and *Pradesura* through its lack of a sub-lateral series.

No species assignment is made because of the lack of data on the mouth frame of the present specimen. However, this specimen does have some differences in the arm morphology compared to *E. bohemica*: the sub-laterals are much stouter than elongated and the laterals do not appear to alternate between small and large in size.

In South Africa, Rilett (1971) originally assigned a new genus *Haughtonaster* Rilett, 1971 from the Gydo Formation, to the family Eophiuridae. However, *Haughtonaster* shares no affinity with Eophiuridae, discussed in detail below, and will not be compared to the specimen here-in. This specimen is the only known Eophiuridae described in from South Africa.

Associated fauna

This specimen was found half a centimetre bellow the erosional base of the Karbonaatjies obrution bed within a silty mudstone (Fig. 3E). A number of well-preserved bivalves are found within the same level including several internal moulds of *Palaeoneilo* sp. Hall and Whitfield, 1869 and one taxon identified as *Nuculites* sp. Conrad, 1841, were found. Both bivalves are common in the Voorstehoek Formation in close proximity to the study site (see Oosthuizen, 1984; Almond, 2011).

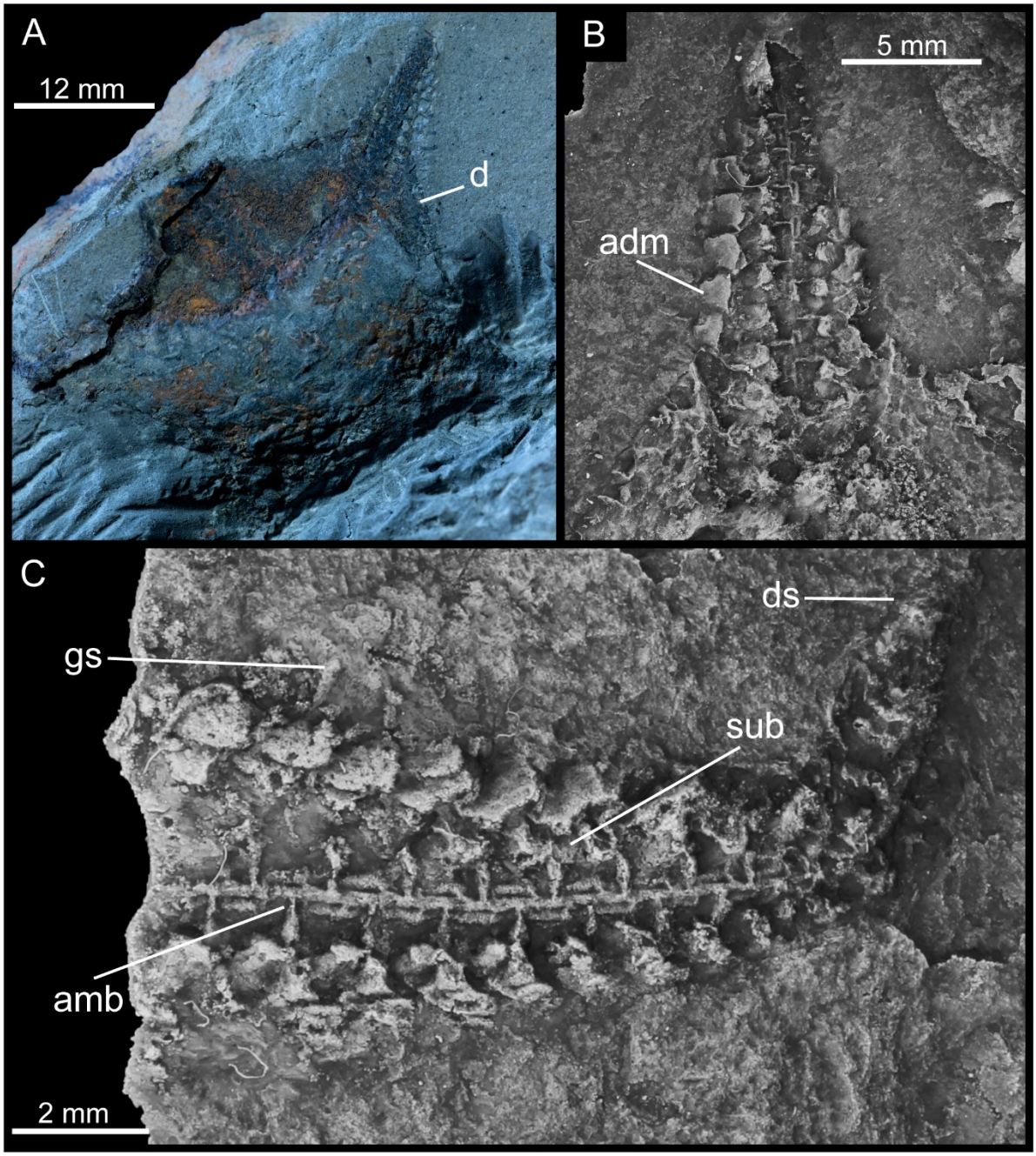

Figure 31. *Eophiura* sp. Jaekel, 1903 from the Lower Devonian Voorstehoek Formation, Western Cape, South Africa. (**A**) Specimen SAM-PB-022505A, original natural specimen. (**B**) Specimen SAM-PB-022505A and (**C**) specimen SAM-PB-022505B, oral surface of the arm. Abbreviations: adm = adambulacrals or laterals; amb = ambulacrals; sub = sublaterals; gs = groove spines; d = disk; ds = distal arm. Photographs taken of silicone moulds (B and C) that were whitened with ammonium chloride.

Class OPHIUROIDEA Gray, 1840

Order OEGOPHIUROIDEA Matsumoto, 1915

Suborder LYSOPHIURINA Gregory, 1897

Family ENCRINASTERIDAE Schuchert, 1914

Subfamily ENCRINASTERINAE Schuchert, 1914

Diagnosis. Taken from Harper and Morris (1978, p. 156). "Small- to large-sized ophiuroids; ambulacral ossicles alternating, commonly with boot-shaped oral surfaces; adambulacral ossicles subventral, composed of heavy plates continuous in a radial direction, with broad oral surfaces, often bearing rows of pustules, and commonly with curved sutures producing rope-like twists; disk large, with well-developed interrays, commonly bounded by stout frame of marginal ossicles; podial basins supported by ambulacrals and adambulacrals, tending toward size reduction laterally"

Remarks. Rilett (1971) assigned *Haughtonaster* to the Family Eophiuridae to which Jell and Theron (1999) also assigned mature specimens (fig. 36, p. 158 in Jell and Theron, 1999) there is however insufficient information on why these specimens were firstly assigned the "adult form" of *Haughtonaster reedi* Rilett,1971 and why these "mature" specimens are placed in the family Eophiuridae. According to Rilett (1971, p. 32), *Haughtonaster* is "placed in the Family Eophiuridae because it shares with *Eophiura bohemica* Jaekel, 1903 the alternating ambulacrals and blunt extremities of the arms, regarded as typical by Spencer and Wright (1966: U82)". Rilett (1971, p. 32) stated: "This species cannot be referred to the Encrinasteridae because its arms differ considerably from those of species classified in this family." Eophiuridae is distinct from Encrinasteridae in essentially having T-shaped ambulacrals, consisting of a periradial and transverse bar, meaning that the podial basins are shared equally by adjacent ambulacrals. In Encrinasteridae, each podial basin lies on the distal abradial margin, giving the boot-shaped appearance of the ambulacrals. Another distinctive feature of Eophiuridae is that the mouth angle ossicles are at 90 degrees, as well as, circumorals separated to form V-shaped extensions to the buccal cavity (fig. 12, p. 54 in Shackleton, 2005). *Eophiura bohemica* is even more distinctive in having mouth angle plates that are L-shaped due to an extra adambulacral ossicle, as well as, possessing a series of sub-laterals, of which none of the Encrinasteridae possess. It is for these reasons that the "adult form" of *Haughtonaster* referred to in Jell and Theron (1999) shares no affinity with Eophiuridae and should be assigned to Shackleton's (2005) plesion 7 (Family Encrinasteridae).This designation is based on the

following gross morphological features: the arms are petaloid and rapidly tapering; the alternating ambulacrals possess a roughly boot-shaped oral surfaces; mouth frame composed of relatively stout ossicles; and a well-defined disk bound by a frame of marginal ossicles. Although *Haughtonaster* is somewhat similar in the arm and jaw structure to members of the Protasteridae, it also lacks key diagnostic features of protasterids, such as vertical spines on the adambulacrals and a disk lacking marginalia. For the purpose of this study, comparisons will only concern the "adult" specimens of *Haughtonaster* and not the "juvenile" holotype (SAM 3881) and paratype (SAM 3375). Further revision is needed to determine whether these specimens represent an early ontogenetic stage that would change to show more typical features of *Haughtonaster* during life.

In a recent review of encrinasterid ophiuroids, Blake *et al.* (2015) followed two subfamilies: Armathyrasterinae Harper and Morris, 1978 and Encrinasterinae Schuchert, 1914. The latter incorporates the following genera: *Encrinaster* Haeckel, 1866, *Euzonosoma* Spencer, 1930, *Urosoma* Spencer, 1930, *Crepidosoma* Spencer, 1930, *Marginura* Haude, 1999 and *Ophiocantabria* Blake, Zamora and García-Alcalde, 2015. *Cheiropteraster* Stürtz, 1890 and *Loriolaster* Stürtz, 1886, which are suggested to be separated based on the disk and ambulacral ossicles (Blake *et al*., 2015).

Haughtonaster departs from the diagnosis of Harper and Morris (1978) quoted above in that the adambulacrals are devoid of any pustules and lacking spines on the arms, but is still placed into the Subfamily Encrinasterinae for all of the above and below mentioned reasons.

Haughtonaster Rilett, 1971

Type species. Haughtonaster reedi Rilett, 1971

Diagnosis. Revised from Jell and Theron (1999). Encrinasterid ophiuroid with concave disk margins, bound by marginalia. Disk spines absent. Arms weakly petaloid; podial basins deep, adambulacrals robust; pointed transverse nose region articulating over ambulacrals. 1st ambulacral or circumolar strong curved ridge forming very distinctive elliptical basins interradially.

Remarks. *Haughtonaster* bears a strong resemblance to the genus *Encrinaster* Haekel 1866 and *Encrinaster tischbeinianus* (Roemer, 1863) both found in the Lower Devonian Voorstehoek Formation (fig. 40-43 p. 165 in Jell and Theron, 1999). The morphological similarities include: rapidly tapering arms, interradial disk outline convex and bound by large, flat overlapping marginalia; boot-shaped ambulacrals that alternate about the periradius, in oral view stout and sub-quadrate; a periradial suture slightly zigzag aborally and straight ventrally; adambulacrals are stout with pointed transverse nose region and a blocky head region; adambulacrals enclose the ambulacral groove distally; two enlarged circumoral ossicles and mouth angle plates that are crossed by two grooves. However, *Haughtonaster* differs from all other genera in the encrinasterids in three important ways. Firstly, adambulacrals are more robust, with a larger, and longer, pointed transverse nose region articulating over the ambulacrals to the periradial suture. Secondly, *Haughtonaster* has a distinct petaloid-shaped mouth angle ossicles, that form a deep interraidial hollow in ventral view. Thirdly, it lacks any spines and spine bases on the adambulacrals and marginalia. In summary, *Haughtonaster* has too many distinctive characters to be placed within any of the seven genera assigned to the family by Spencer and Wright (1966, p. 86). Blake *et al*. (2015) followed Spencer and Wright (1966) in that disk configurations provide differences amongst encrinasterid genera and so will be used in comparison: *Cheiropteraster*, *Loriolaster* and *Mastigactis* lack marginal ossicles whereas *Haughtonaster* disk is clearly bound by large, flat overlapping ossicles similar in appearance to those of *Encrinaster*; the marginals in *Euzonosoma* are much more rounded and blocky in appearance, similar to *Ophiocantabria* (Shackleton, 2005, Blake *et al*., 2015). *Ophiocantabria* and *Marginura* are also distinct in having concave disk margins rather than convex as seen in *Haughtonaster*, *Encrinaster*, *Euzonasoma* and *Crepidosoma*.

Haughtonaster reedi Rilett, 1971

Figure 32

1925 *Echinasterella* sp. F.R.C Reed *Ann. S. Afr. Mus.,* p. 22, figs. 32-33.
1971 *Haughtonaster reedi* Rilett *Ann. Na. Mus*., p. 21, figs. 30-32.
1999 *Haughtonaster reedi* Rilett ; *Jell and Theron*, p. 157, figs. 36,37.

Type material. Holotype SAM3881 (*juvenile*); Paratype SAM3375 (*juvenile*); *"adult"* specimens from *Jell and Theron* RO122, RO804, ROC50, B4567, SAM13472, SAM13470.

Occurrence. Holotype from the Lower Devonian (Emsian) Gydo Formation, Bokkeveld Group,Ceres, South Africa.

Material examined in this study: SAM-PB-022506 and SAM-PB-022507.

Occurrence. Collected from the Lower Devonian Voorstehoek Formation, Bokkeveld Group, Karbonaatjies Farm, ~10 km Hex River Pass, Western Cape, South Africa (see Chapter 1- Fig. 3 for stratigraphic detail).

Diagnosis. Same as for genus by monotypy.

Description. Small to medium sized. Disk pentagonal and convex with diameter of 1.2 cm. Disk bound by flat, overlapping marginalia between interradii, weakly polygonal plates in interradius (Fig. 32A and B). Disk spines appear to be absent. Arms of medium length (2 cm), weakly bowed in proximal half and rapidly tapering distally; pointed and enclosed at the distal end. Madreporite not seen (i.e., unclear whether it is not preserved, obscured or too small to recognise). Ventrally, mouth angle ossicles (mao) are bowed and slender, adjacent ossicles abut to form a distinctive petaloid-shape that form a deep interradial hollow between them (Fig. 32B). Adambulacrals articulated to the interradial lateral surface of the mao. Aboral view of the jaw frame show enlarged sub-trapezoidal "circumoral" ossicles (1st ambulacral) that articulate with the mouth angle plates, and bear two transverse grooves. Distal groove is broad and continuous, running across the circumoral ossicles and bears a single deep pore on each ossicle, while proximal groove is deeper, wider and parallel to the first (Fig. 32A) Ambulacral ossicles alternate over mid-line, narrow periradial suture slightly zigzag aborally, straight orally (Fig. 32B). In aboral view ambulacrals are quadrate with prominent proximal and distal ridges mark the aboral surface (ridge-bound indentations). Oral ambulacral surface with prominent boot-shaped (Fig. 32B). Groove crosses distal surfaces from podial region to periradius, circular heel depression on ambulacrals. Podial basins circular, deep and large (Fig. 32B). Adambulacral (lateral) ossicles are slightly sickle-shaped in oral view. Laterals are very stout with a distinct elongated, pointed nose region articulating to the ambulacral region and a blocky head region, bearing no visible spines (Fig. 32C). Towards the arm tips, adambulacrals close

over the ambulacral groove orally (Fig. 32D). The aboral surface of each adambulacral ossicle is broad and sub-quadrate, as well as oblique with respect to the head. The proximal edges of opposing adambulacrals are closest together and heads diverge distally, each slightly abutting/overlapping the adjacent adambulacral. No evidence of articulation sites or grooves spines. Vertical spines are not preserved.

Remarks. As for genus.

Associated fauna

Multiple individuals of the ophiuroid *Haughtonaster* were found one meter above the Karbonaatjies obrution bed within a trilobite moult assemblage consisting of the single taxon *Bainella africana* (Salter, 1856) (Fig. 3A).

Figure 32. *Haughtonaster reedi* Rilett, 1971 from the Lower Devonian, Voorstehoek Formation, Western Cape, South Africa. (A) Specimen SAM-PB-022506, aboral surface showing detail of central disk. (B)-(C) Specimens SAM-PB-022507, SAM-PB-022506, oral surface showing details of mouth angle ossicles and proximal arms. (D) Specimen SAM-PB-022506, distal portion of arm. Abbreviations: adm = adambulacrals or laterals; amb = ambulacrals; sub = sublaterals; mao = mouth angle ossicles; dist. g. = distal groove; co = circumoral ossicles; p = pore; pb = podial basin; m = marginalia; ps = periradial suture. Photographs taken of silicone moulds that were whitened with ammonium chloride.

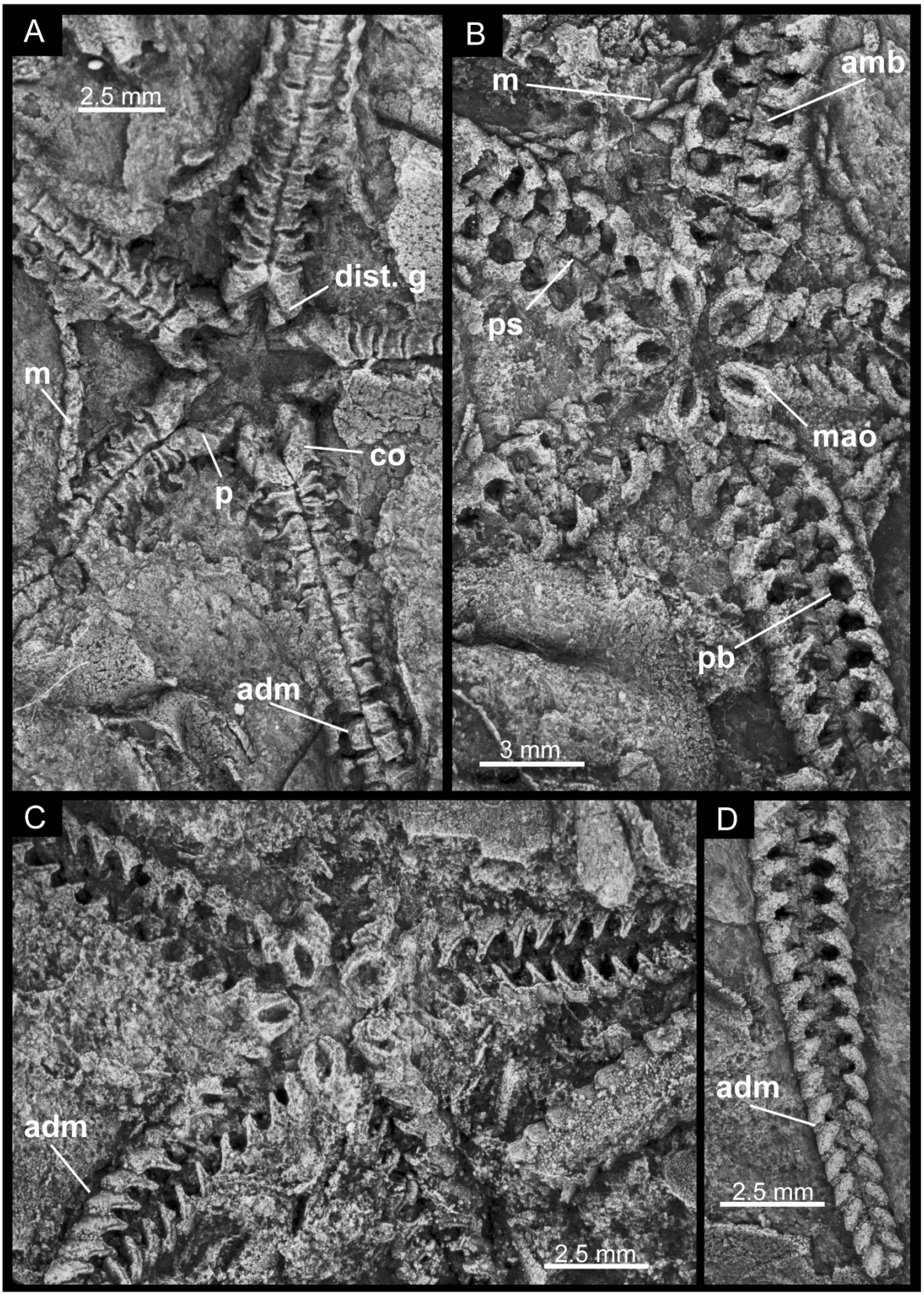
A
2.5 mm
dist. g
m
co
p
adm
B
m
amb
ps
mao
pb
3 mm
C
adm
2.5 mm
D
adm
2.5 mm

Family PROTASTERIDAE Miller, 1889

Diagnosis. Hunter *et al.* (2016) revised the diagnosis as follows: Ambulacral ossicles not fused across the mid-line; periradial suture distinct, either straight or zigzag; opposing or alternating ambulacrals; adambulacral groove spines broadened towards the tip (i.e., paddle-shaped); longitudinal ridge for groove spines raised and curved; adambulacral vertical spines of greater length than adambulacrals.

Remarks. This diagnosis follows that of Shackleton (2005) emended by Hunter *et al*. (2016) which emphasises characteristics of the periradial suture (straight or zigzag/sinuous) and paired or offset ambulacrals.

Subfamily PROTASTERINAE Hunter, Rushton and Stone, 2016

Diagnosis. "Ambulacrals alternating by up to half an ossicle length; periradial suture distinct, either straight or zigzag. Ambulacrals boot-shaped. Adambulacrals elongated with a bulbous nose or sickle-shaped. Mouth angle plates stout, crossed by oblique ridge in lateral section." (Hunter *et al.*, 2016, p. 6).

Remarks. This new subfamily was recently proposed by Hunter *et al.* (2016) to accommodate for genera that possess alternating ambulacrals (as opposed to paired ambulacrals e.g. *Furcaster* Stürtz, 1886, *Hypohiura* Jaekel, 1923 and *Lapworthura* Gregory, 1897) and places emphasis on the variation in boot-shaped ambulacra as a morphological classification between Protasteridae (Glass and Blake, 2004)

Gamiroaster gen. nov.

Etymology. "Gamiro" derived from the Khoikhoi word for star, was chosen to honour the "first peoples" of the Western Cape, South Africa.

Type species. Gamiroaster tempestatis sp. nov., by original designation.

Diagnosis. Protasterid ophiuroid with periradial suture tight, narrow and zigzag, both aborally and orally. Oral ambulacral boots: Width of foot (W_F) is equal to the length of the leg (L_L); width of distal fitting (W_{DF}) greater than length of the foot (L_F) and equal in width of the central leg (W_{CL}). Distal end of W_{DF} is slightly concave, abradial edges curved. Toe (W_T) is shorter than width of distal fitting (W_{DF}). The abradial edge of the toe is straight to convex. Width of toe (W_T) is approximately half the width of foot (W_F). Podial basins large, sub-rounded and deep.

Remarks. The comparison here serves to differentiate *Gamiroaster* from other protasterids, with emphasis on the described protasterids by Jell and Theron (1999) of the Lower Devonian Bokkeveld Group in South Africa. Variations in boot-shaped ambulacral will be used here to differentiate between the various protasterid genera, as used in Glass and Blake (2004), Glass (2006) and Hunter *et al*. (2016) (Fig. 33).

Spencer (1950a) originally described several specimens from the Lower Devonian Bokkeveld Group as a new species *Hexura weitzi* assigned to the Family Euzonosomatidae Spencer, 1930. This material was subsequently restudied by Jell and Theron (1999) who assigned these specimens to three different taxa: 1) Spencer's holotype specimen SAM11055 (figs. 1, 2, p. 301, unknown formation) was reassigned to *Hexuraster weitzi* (Spencer, 1950a) (figs. 38, 39 in Jell and Theron, 1999, p. 162-163) but placed into the family Cheiropterasteridae Spencer, 1934; 2) Spencer's specimens which he illustrates in figured 4 and 5, were re-identified as *Encrinaster tischbeinianus* (Roemer, 1863) (figs. 40-43 in Jell and Theron, 1999, p. 165-170); and 3) Spencer's specimen shown in figure 3 (p. 301) as the new species *Eugasterella africana* Jell and Theron, 1999 (figs. 46-48, p. 174-178).

Spencer (1934, p. 439) erected the family Cheiropterasteridae for ophiuroids with alternating cylindrical ambulacrals, adambulacrals lacking vertical spines, and an extremely swollen disk, subsequently Spencer and Wright (1966) synonymized Cheiropterasteridae and Euzonosomatidae with Encrinasteridae. However, Jell (1997, p. 162) maintained the family on the basis of a very unique feature: "an unplated skin to the dorsal disk and extent of the disk to, or very close to the tips of the arms." This unique feature is apparent in Jell and Therons's (1999) figure 38 of *Hexuraster weitzi* (lectotype SAM11055), however, this is not the case for the specimen R045 (fig. 39, p. 163 in Jell and Theron, 1999, Gydo Formation) of the same taxa, nor are the cylindrical ambulacrals, T-shaped adambulacrals and lateral spines apparent.

Whether Cheiropterasteridae should be re-erected as a family or synonymized with Encrinasteridae is beyond the scope of this paper. The discussion here serves to point out that the only specimen R045 (fig. 39; p. 163 in Jell and Theron, 1999) resembles *Gamiroaster tempestatis* and not the lectotype specimen (SAM11055 – fig. 38, p. 162 in Jell and Theron, 1999). On the basis of having a small thin web like disk; arms are slightly petaloid; the mouth frame ossicles are similar in appearance; the ambulacrals are boot-shaped; and disk, groove or lateral spines are absent. However, *Gamiroaster* is distinctive from *Hexuraster* (R045 fig. 39; p. 163 in Jell and Theron, 1999) in that the boot-shaped ambulacral has a much wider (L_F) and shorter (W_F) foot and distal fitting (W_{DF}). The adambulacrals in *H. weitzi* (R045 fig. 39) also differ in that the adradial nose is narrow, short and rectangular and the abradial head is large and flat (large distal facet?) that along with the nose region give a more L-shaped appearance rather than a sickle or crescent shape seen in *Gamiroaster.* Finally, due to the shape and size of the ambulacrals and adambulacrals in *H. weitzi* the podial basins are wide and sub-circular compared to narrow and circular basin in *Gamiroaster*. It is possible then that specimen R045 (fig. 39; p. 163 in Jell and Theron, 1999) belongs to the family Protasteridae, but further revision to assess this is needed.

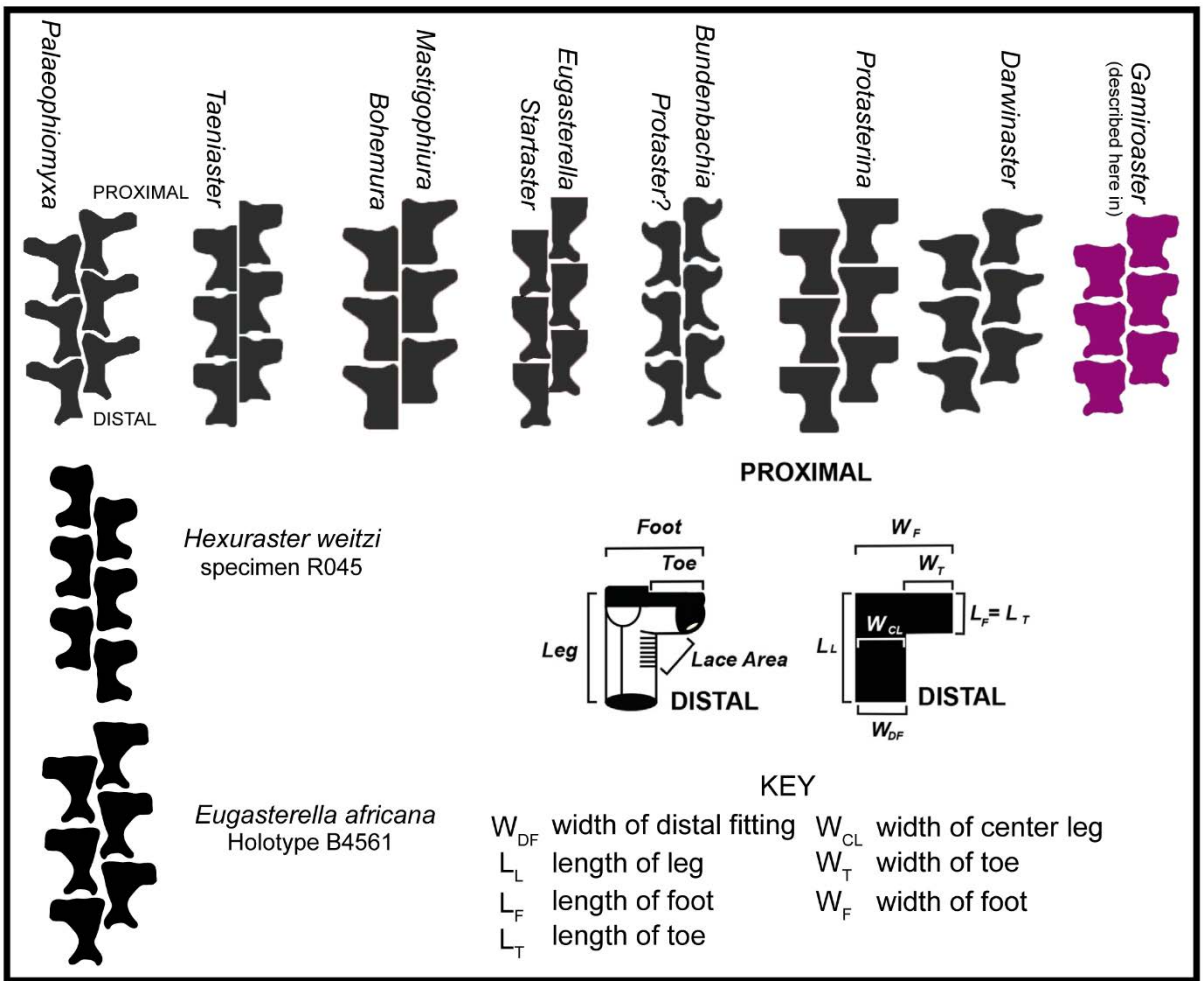

Figure 33. Ventral outlines of protasterid ophiuroid ambulacrals, common terminology used when describing the boot-shaped ambulacrals (modified from Glass and Blake, 2004 and Hunter *et al.,* 2016).

The blocky appearance of the ambulacra in *Gamiroaster* bears some resemblance to those of *Eugasterella africana* Jell and Theron, 1999 (Holotype B4561, Voorstehoek Formation, fig. 46, p. 175) and *Strataster stuckenbergi* (Rilett, 1971) (Holotype NM 831, Gydo or Voorstehoek Formation, fig. 54-56, p. 183) in that the width of the foot (W_F) and length of the leg (L_L) are roughly equal, the length of the toe (L_T) is relatively wide with a straight to convex abradial edge, the width of the foot (W_T) is relatively short and a slightly sinuous ambulacral groove (Fig. 33). This is not the same for the type species *Eugasterella logani* (Hall, 1868) and *S. ohioensis* Kesling and Le Vasseur, 1971, where the width of the toe (W_T) and consequently the width of the foot, is much shorter and only slightly wider than the central leg (see Harper, 1985 for a comprehensive review of *E. logani*). However, *Gamiroaster* has a notably wider width of the centre leg than the above-mentioned genera. The ambulacrals of *Gamiroaster* differ greatly from the overall sinuous shape seen in *Palaeophiomyxa* (Stürtz, 1886) and *Bundenbachia* Stürtz, 1886, in particular the prominent curvature of the toes, sinuously concave distal and

proximal settings and the relatively narrow width of the central leg (Glass and Blake, 2004) (Fig. 33). *Gamiroaster* shares a wide centre of the leg and blocky appearance (foot is as wide (W_F) as the length of the foot (L_L)) with *Darwinaster* Hunter, Rushton and Stone, 2016, *Mastigophiura* Lehmann, 1957 and *Bohemura* Jaekel, 1903, although *Gamiroaster* differs in that the distal position of the toe is almost at right angles to the adradial edge of the leg (i.e. lace area) making the toe wide and blocky as opposed to tapering to a narrow tip (see comparison in Glass and Blake, 2004; Glass, 2006; Hunter *et al*. 2016). This is also evident in *Taeniaster* Billings, 1858 and *Protasterina* (Glass and Blake, 2004) in that the length of the toe (L_T) is relatively wide with a straight to convex abradial edge, however *Taeniaster* however has a characteristically straight periradial suture and *Protasterina* has straight distal and proximal settings and a unique hour glass-shaped leg (Glass, 2006; Hunter *et al*., 2007) (Fig. 33). Although *Gamiroaster* does not have a highly distinctive ventral shape to the ambulacrals, the differences compared above set it apart from other protasterid genera. Lastly, *Gamiroaster* has very distinct heart-shaped mouth angle ossicles (mao) (Fig. 34C).

Tempestatis sp. nov.

Figure 34

Type material. Holotype by monotypy SAM-PB-022501, due to general poor preservation a number of paratype material was selected: SAM-PB-022502, SAM-PB-022503, SAM-PB-022504.

Etymology. Named after the storm (tempest) that consequently smothered the ophiuroids.

Occurrence. Lower Devonian Voorstehoek Formation, Bokkeveld Group, Cape Supergroup, Karbonaatjies Farm, near the Hex River Pass, Western Cape, South Africa (see Introduction Chapter- Fig. 3 for stratigraphic detail).

Diagnosis. Disk web-like; no apparent marginal ridge between interradii; thin skin stretched over disk. Disk spines absent. Medium length, gradually tapering arms; pointed and enclosed at the distal end. Aboral surface of the arm smooth with quadrate plates. Ambulacral ossicles alternate over mid-line, periradial suture tight, narrow and zigzag, both aborally and orally. Oral ambulacral surface with prominent boot-shape ambulacral plates. Groove crosses distal

surfaces from podial region to periradius. Oral ambulacral boots have blocky ambulacrals with concave distal and proximal fittings. Width of foot (W_F) is equal to the length of the leg (L_L); width of distal fitting (W_{DF}) greater than length of the foot (L_F) and equal in width of the central leg (W_{CL}). Toe (W_T) is shorter than width of distal fitting (W_{DF}). The abradial edge of the toe is straight to convex.

Description. Small sized protasterid with diameter of 8 mm. Disk web-like or slightly concave, extending to the 4th ambulacral (Fig. 34A and B). Both aboral and oral disk are preserved, however this is not wholly apparent from the silicone moulds; thin skin stretched over disk and proximal arms is however apparent in CT scans (Fig. 35); disk appears naked with no patches of granules and lacks marginal ossicles. Disk spines appear to be absent. Arms 18 mm from the mouth angle plates; slightly bowed from mouth frame to about the margin of the disk and gradually tapering; pointed and enclosed at distal end (possibly due to post-mortem contraction) (Fig. 35). Madreporite not seen (i.e., unclear whether it is not preserved, obscured or too small to recognise). Ventral oral surface consists of visible mouth angle ossicles (mao). Abradially the circumoral ossicle surface curved and bears a distal facet, which adjoins first arm ambulacral and a proximal facet that articulates to the corresponding facet on the mouth angle plate. Mao are distinctive in that they are curved inwards towards the buccal region abutting with the opposite mao creating a triangular heart shape with the accompanying circumoral ossicles (Fig. 34C). In aboral view the mouth frame ossicles are slender and slightly bowed to form a petaloid or heart-shape. There appears to be no apparent buccal slit. The furrow is open to the end portion of the arms; this is seen in the CT scans and derived 3D models (Fig. 35). The distal-most ends of the arms are either missing or poorly preserved in the silicone moulds, however clearly visible in the CT scans; arms remain flattened in form, becoming slightly enclosed towards the tip where the adambulacrals close over the furrow (Fig. 35). The aboral surface of the arm smooth with quadrate plates (Fig 34B and E). Ambulacral ossicles alternate over the mid-line, periradial suture tight and slightly sinuous along oral surface and more strongly zigzag along aboral surface of the arm. Number of ambulacrals in disk varies between four and five on oral surface (Fig. 34A). Aboral ambulacral sub-cylindrical, with slight ridge bound indentations. Ventral surface of ambulacral boot-shape is blocky; width of foot (W_F) is as wide as the length of the leg (L_L). Width of the distal fitting (W_{DF}) is larger than the length of the foot (L_F) and equal in width to the central leg (W_{CL}). Distal end of W_{DF} is slightly concave to straight, abradial edge slightly curved. Toe (W_T) is shorter than width of distal fitting (W_{DF}). Abradial edge of toe straight to slightly convex. Width

of toe (W_T) is approximately half the width of foot (W_F). Proximal end of foot is straight to concave with a slight bulbous heel. Lace area is weakly concave. Podial basins large, sub-rounded and deep (Fig. 34D). Oral view of adambulacrals in CT scans shows adradial nose that thins to a point and abradial distal square head, ventral outline sickle-shaped (Fig. 35C). Laterals abutting laterals begin to overlap distally over the ambulacrals. No evidence of articulation sites or grooves spines. Vertical spines not preserved.

Remarks. Despite having 500 specimens within the Karbonaatjies obrution bed to observe, preservation is generally very poor. However, with the use of a 3D model made from one of the specimens within the bed, a rather unique perspective of the adambulacra or laterals can be seen.

Figure 34. *Gamiroaster tempestatis* from the Lower Devonian Voorstehoek Formation , Western Cape, South Africa. (**A**) Holotype SAM-PB-022501, general view of a nearly complete specimen in ventral view. (**B**) Paratype SAM-PB-022502, general view of a nearly complete specimen in aboral (dorsal) view. (**C**) Paratype SAM-PB-022504, detail of mouth angle ossicles. (**D**) Paratype SAM-PB-022503, arm in ventral view showing boot-shaped ambulacrals and lsightly zig-zag periradial suture. (**E**) Paratype SAM-PB-022503, arm in aboral (dorsal) view showing qudrate adambuacrlas. Abbreviations adm = adambulacrals or laterals; amb = ambulacrals; mao = mouth angle ossicles; pb = podial basin; ps = periradial suture. Photographs taken of silicone moulds that were whitened with ammonium chloride.

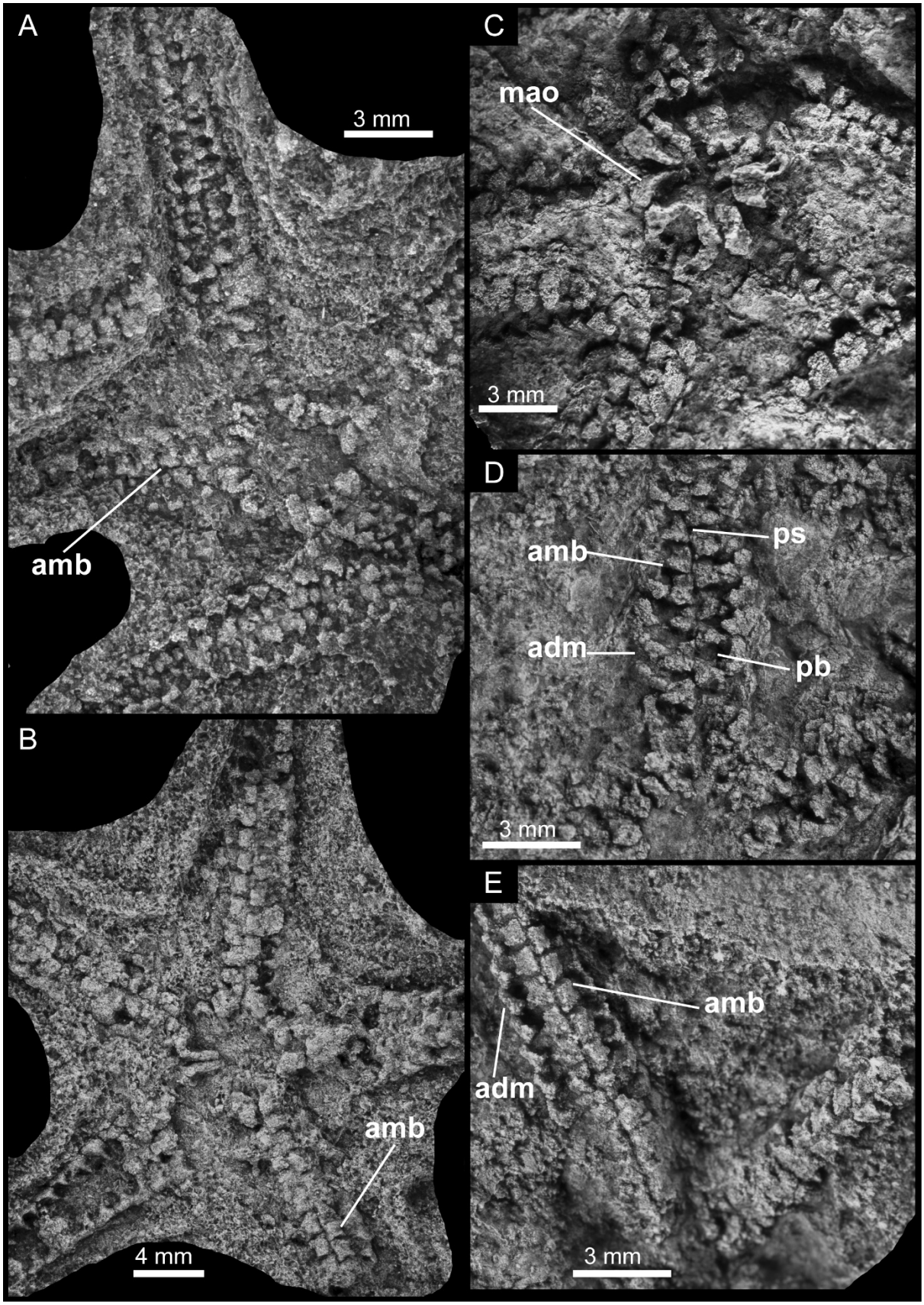
A
3 mm
amb
B
amb
4 mm
C
mao
3 mm
D
amb
ps
adm
pb
3 mm
E
amb
adm
3 mm

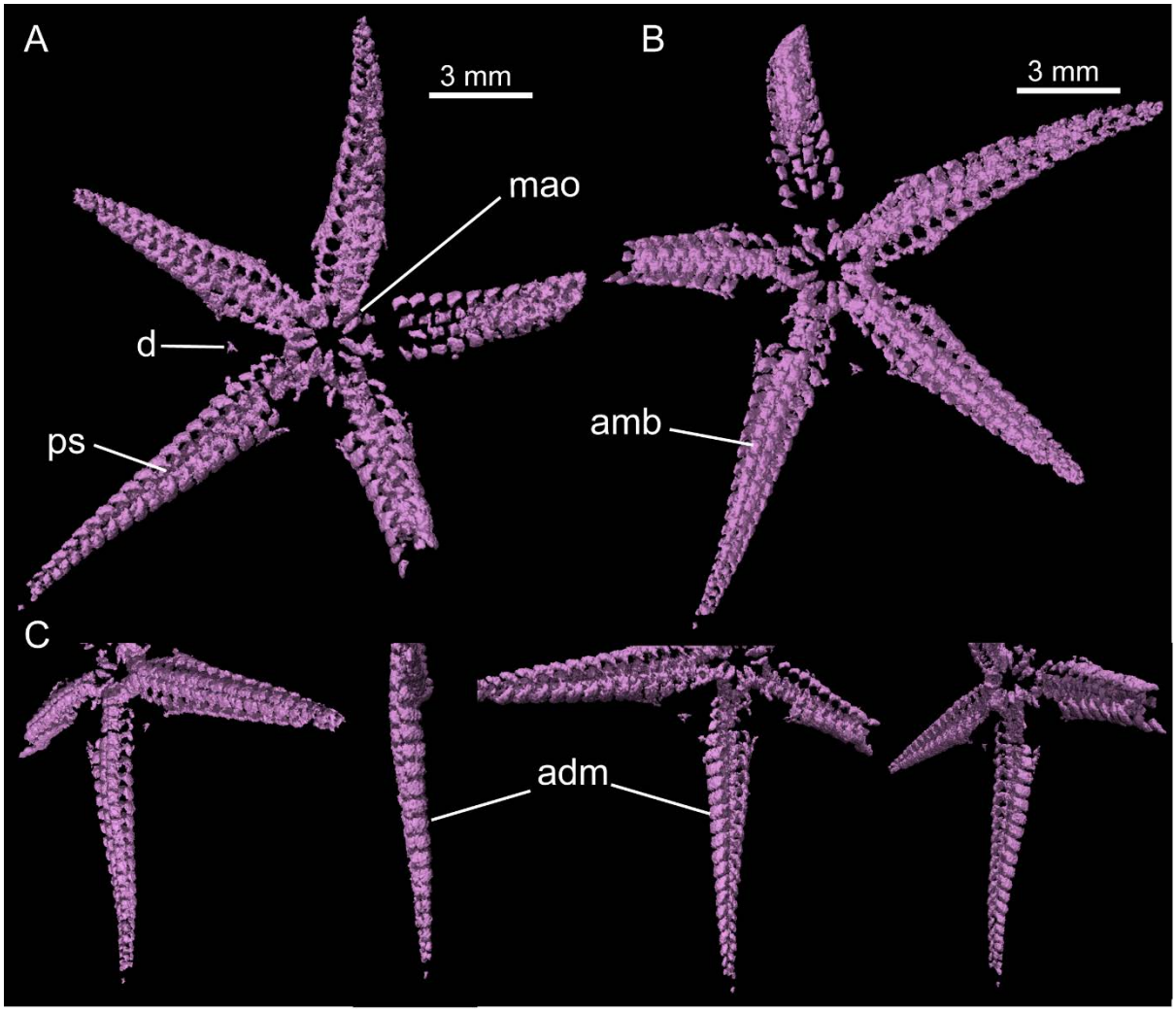

Figure 35. 3D reconstruction of *Gamiroaster tempestatis* specimen selected from sample UU2 (**A**) Oral view of specimen. (**B**) Aboral view of specimen. (**C**) 360° rotation of the arm, showing shape of adambulacrals. Abbreviations adm = adambulacrals or laterals; amb = ambulacrals; mao = mouth angle ossicles; ps = periradial suture; d = disk.

Class STYLOPHORA Gill and Caster, 1960

Order MITRATA Jaekel, 1918

Suborder ANOMALOCYSTITIDA Caster, 1952

Family ALLANICYTIDIIDAE Caster and Gill, 1967

Placocystella Rennie, 1936

1954 *Australocystis* Caster, p. 140.
1967 *Allanicytidium* Caster and Gill, p. 564.
1983 *Tasmanicytidium* Caster, p. 334.
non 2001 *Notocarpos* Philip; Lefebvre, p. 609.

Type species. Placocystella capensis Rennie, 1936 (= *Placocystella africana* Reed, 1925); from the Upper Emsian to Lower Eifelian Gydo and Voorstehoek Formations, Bokkeveld Group, Cape Supergroup, Western Cape, South Africa by original designation.

Diagnosis. See Ruta and Theron (1997) and for revised diagnosis Jell (2013).

Remarks. Stylophorans are considered herein as "normal" echinoderms, with feeding appendage (aulacophore), following interpretation originally proposed by Ubaghs (1961, 1968). Due to the poorly preserved nature of all stylophorans within the Karbonaatjies obrution bed, the studied specimen (and all larger stylophorans) is tentatively identified as *Placocystella*. Additionally, there are no clear plate boundaries or other definitive characters to better identified the stylophorans in the hand sample and the CT scan images. The general morphology (B. Lefebvre, personal communications, 2016) indicates that the specimens definitely belong to the Anomalocystitidae, and more precisely, to the Allanicytidiinae (e.g. the typical articulated posterior spines - Caster 1952; Ubaghs 1968; Ruta 1997). Therefore, it is likely that the specimens in this study are poorly reserved *P. africana*, because their morphology is compatible with that taxon, which were described from the same parts of the Voorstehoek Formation (Fig. 36).

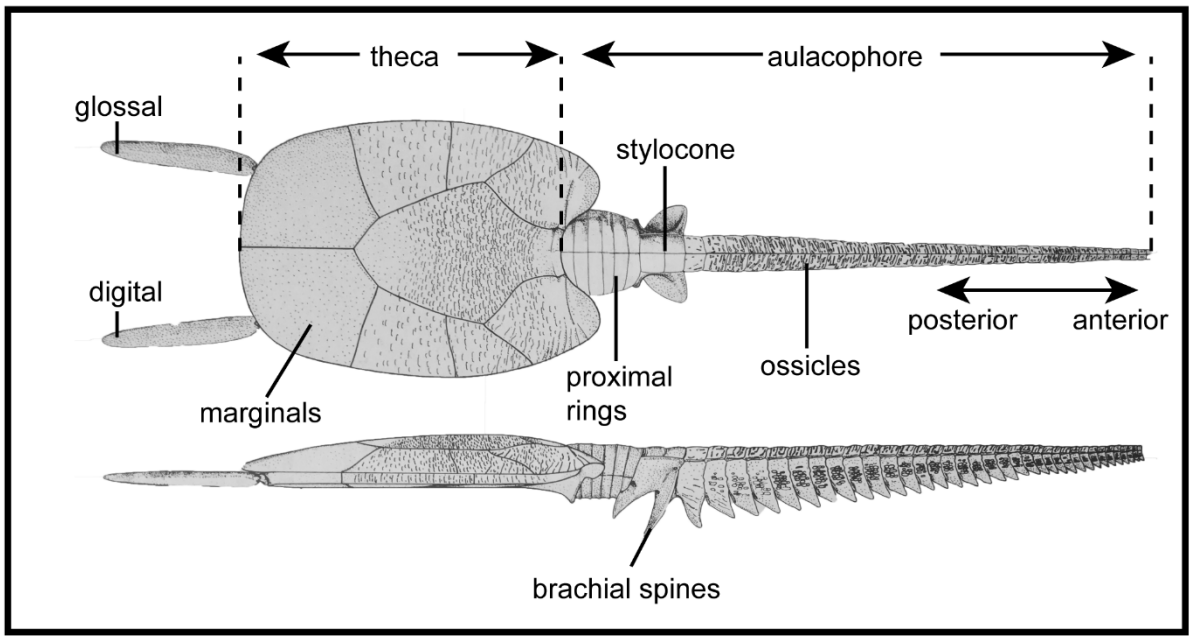

Figure 36. Reconstruction of *Placocystella africana* (Reed, 1925) (redrawn from Ruta and Theron, 1997).

Placocystella africana (Reed, 1925)

Figure 38

1925 *Placocystis africanus* Reed, p. 30, pl. 4, fig. 1.
1932 *Placocystites africanus* (Reed); Dehm, p. 65.
1936 *Placocystis africanus* Reed; Rennie, p. 273, pl. 31, fig. 1.
1936 *Placocystella capensis* Rennie, p. 269, pl. 31, fig. 1.
1941 *Placocystis africanus* Reed; Chauvel, p. 217.
1941 *Placocystella capensis* Rennie ; Chauvel, p 217.
1952 *Placocystis africanus* Reed; Caster, p. 19.
1952 *Placocystella capensis* Rennie ; Caster, p.19.
1954 '*Placocystis*' *africanus* Reed; Caster, p. 145, fig. 3a-c, 4; pl. 8, figs 5-8.
1954 *Placocystella capensis* Rennie ; Caster, p.145, fig. 3d-f.
1967 *Placocystella capensis* Rennie ; Ubaghs, p. 561, fig. 3d-f.
1979 '*Placocystis africanus*' Reed ; Derstler, p. 102.
1979 *Placocystella capensis* Rennie ; Derstler, p.102.
1983 *Placocystella* sp. Rennie ; Caster, p. 328.
1984 *Placocystella capensis* Rennie, pars ; Oosthuizen, p. 139.
1989 *Placocystella* sp. Rennie; Clarke and Jefferies, p. 95
1990 *Placocystella capensis* Rennie ; Cripps, p. 59.
1991 *Placocystis africanus* Reed; Parsley, p. 16.
1991 *Placocystella capensis* Rennie; Parsley, p.16.
1994 *Placocystella capensis* Rennie; Cripps and Daley, p. 125.
1997 *Placocystella africana* Rennie; Ruta and Theron, p. 208.

Type Material. Holotype SM A.3044; see Ruta and Theron (1997, Pl. 1-8, figs. 3-5;7-21) for list of additional South African material and Jell (2013) for specimens from Australia.

Material examined in this study: SAM-PB-022508A,B specimen missing distal aulacophore.

Occurrence. Holotype from the Lower Devonian Gydo Formation, Bokkeveld Group, Hex River Pass, South Africa; *Material examined in this study* collected from the Lower Devonian Voorstehoek Formation, Bokkeveld Group, Karbonaatjies obrution bed, ~10 km to Hex River Pass, Western Cape, South Africa (see chapter 1 for stratigraphic detail).

Description. Thecal length 11 mm, width 9 mm. No marginal plates, adorals or interplate sutures can be identified with certainty, other than the posterior margin of the upper thecal surface. Posterior spines prominent and tapering gently giving a "cigar-like" shape (Fig. 37A). Proximal aulacophore showing inferolaterals (Fig. 37B). Two large transverse brachial spines fan-shaped, distal spine is much stronger, directed rearwards and easily recognised in the CT scans.

Remarks. As for genus.

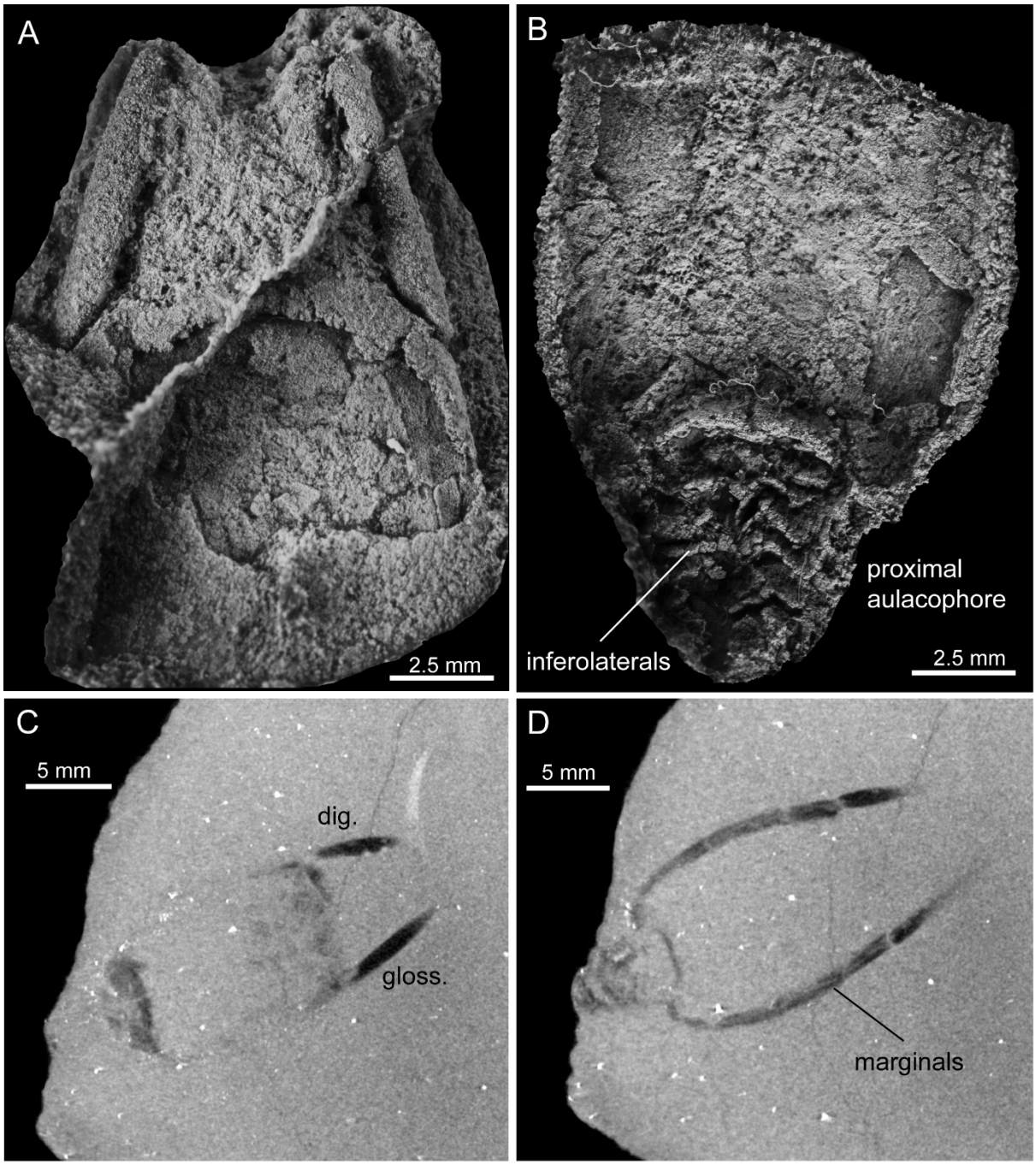

Figure 37. *Placocystella africana* (Reed, 1925), Lower Devonian Voorstehoek Formation, Western Cape, South Africa. (**A**) Specimen SAM-PB-022508A Disarticulated upper thecal surface showing typical "cigar-like" posterior spines. (**B**) Counterpart SAM-PB-022508B, showing proximal aulacophore. Photographs taken from silicone moulds there were whitened with ammonium chloride. (**C**)-(**D**) CT scan images of the same specimen. Abbreviations: dig. = digital; gloss. = glossal.

Suborder PARANACYSTIDA Caster, 1954

Family PARANACYSTIDAE Caster, 1954

Genus *Paranacystis* Caster, 1954

Type species. Paranacystis petrii Caster, 1954 from the Lower Devonian Ponta Grossa Shale, Paraná, Brazil.

Diagnosis. See Caster (1954) for a very comprehensive diagnosis and discussion.

Paranacystis cf. *petrii* Caster, 1954

Figure 39

Remarks. While CT scanning of the Karbonaatjies obrution bed revealed over 145 individual specimens tentatively assigned to paranacystids, attempts to carefully split the samples to reveal the specimens were unsuccessful, about three specimens were identified but only one preserved sufficiently to be studied and photographed albeit still very poorly preserved. Paranacystids are a small group of poorly known mitrates originally recorded form the Lower Devonian of the Paraná basin. They are characterized by the enlargement (widening) of one posterior marginal and the torsion of the anal opening (instead of being perpendicular to the main body axis, it is strongly oblique to it, and directed towards the left); another apomorphy of paranacystids consists in the posterior extension of both left and right adorals on the upper thecal surface (Caster, 1954; Ruta and Bartels, 1998; Ruta, 1999). Unfortunately, very few of these details can be observed in the photographs and the CT scan images of the current Voorstehoek specimens. Nevertheless, their general aspect, with the typical pointed posterior margin, suggests very probable paranacystid affinities.

Based on the general morphology (B. Lefebvre, personal communication, 2016), the strongly convex posterior aspect of the theca, with a single, large, protruding plate and lack of paired posterior spines is clearly more parancystid-like and not compatible with anomalocystitids or any of the other mitrate suborders (Caster 1952; Ubaghs 1968; see Ruta, 1997 for list for revised classifications).

In South Africa, Ruta (1997) described a new species *Paranacystis simoneae* from the Waboomberg Formation (Bokkeveld Group), which represents the first record of this genus from South Africa. Unfortunately, this description is based on the lower thecal surface of a single, posteriorly incomplete specimen and no affinities with the specimens in this study can be made. In support of placement within the Paranacystidea, undescribed paranacystids were collected and identified from a similar horizon within the Voorstehoek Formation (B. Lefebvre, personal communication, 2016). Therefore, it is possible the specimens within this study belong to the same species of paranacystid, and are thus close to or conspecific to *P. petrii* that was originally described from the Ponta Grossa Formation in Brazil (Fig. 38).

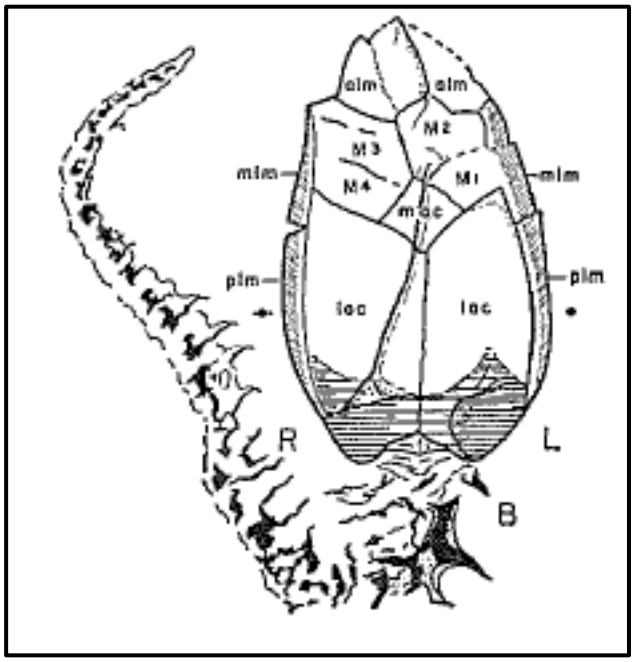

Figure 38. Reconstruction of *Paranacystis petrii* Caster, 1954. For details on nomenclature used see Caster (1954).

Material examined in this study. Specimen SAM-PB-022509*,* of all 140 mitrates identified within the Karbonaatjies obrution bed, only one specimen has fair preservation (albeit still highly weathered) to be studied in depth, however even this is missing its proximal end of the theca.

Description. Thecal length 3.5 mm, width 2.3 mm. Thecal outline lancet-shaped to ovate. Zygal bar? prominent, gently curving and can be seen in the CT images. Prominent aulacophore or stylocone can be seen. Strong relatively narrow lateral marginal plates can only be seen in this specimen. Whole aulacophore is preserved, flexed to the side of theca (Fig. 39).

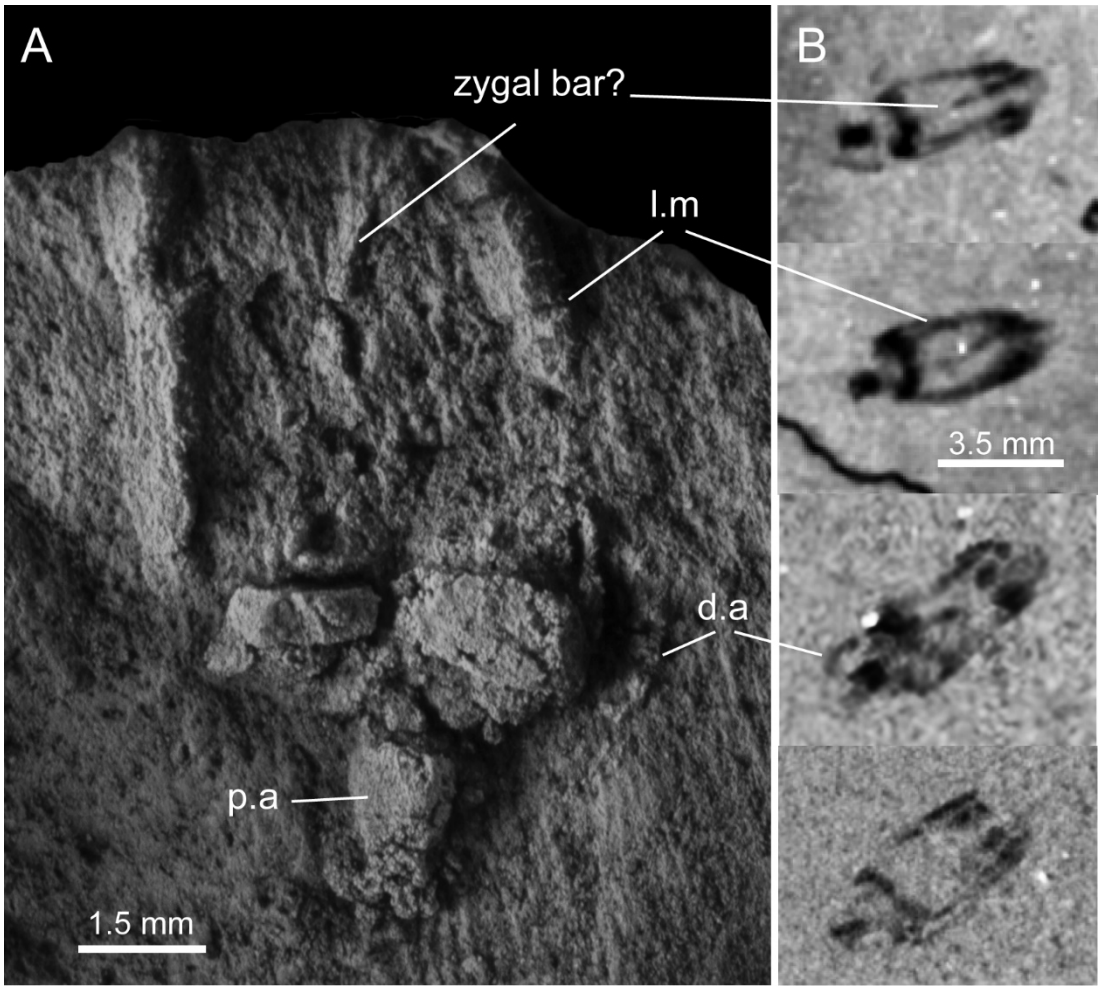

Figure 39. (**A**) *Paranacystis* cf. *petrii* Caster, 1954 from the Lower Devonian Voorstehoek Formation, Western Cape, South Africa specimen SAM-PB-022509 (**B**) A series of CT images of various specimens found throughout the Karbonaatjies obrution bed. Abbreviations: l.m = lateral marginals; d.a = distal aulacophore; p.a = proximal aulacophore.

Associated fauna

Almost all of the shelly fossils within the bed are too fragmented to be fully described, and only the larger, diagnostic and common brachiopod, including undetermined species, like *Australocoelia* sp. indet. Boucot and Gill, 1956 and *Australospirifer* sp. Caster, 1939 could be identified even in fragmented form (cf. Oosthuizen, 1984; Hiller and Theron, 1988; Almond, 2011). Trilobites and crinoids also occur but are too fragmented to place beyond class level. A number of gastropod fragments with double ridged spines are very similar to *Platyceras. dumosum* Conrad, 1840 from the Lower Devonian of New York, USA. Also occurring is the problematic conical-shelled *tentaculites* sp. von Schlotheim, 1820, a common taxon in Bokkeveld Group, were often identified throughout the Karbonaatjies obrution bed.

CHAPTER 5 CONCLUSIONS

The fossil ophiuroid population in the Emsian Karbonaatjies obrution bed is dominated by the proposed new genus and species, *Gamiroaster tempestatis,* which is part of the basal ophiuroid Family Protasteridae, a subject of ongoing taxonomic revisions. This proposed new ophiuroid and other associated invertebrates recovered from the obrution bed form part of the cold-water Malvinokaffric Realm Biota that characterized SW Gondwana.

During the Emsian, in the Clanwilliam sub-basin, the small ophiuroid *Gamiroaster tempestatis* formed multi-individual, dense populations. Possibly living amongst these ophiuroids was a relatively dense population of the small stylophoran *Paranacystis cf. petrii* and the larger mitrate *Placocystella africana.* The co-occurrence of abundant ophiuroids and stylophorans within the Karbonaatjies obrution bed is palaeoecologically significant, as it allows for the reconstruction of such ancient palaeo-communities and demonstrates that this occurrence is not uncommon in the fossil record. Furthermore, this is the first association of its kind to be formally described from South Africa.

Taphonomic evidence shows that the Karbonaatjies obrution bed preserved para-autochthonous (transported but not out of life habit) ophiuroid and stylophoran specimens. The majority of the fossil ophiuroids and stylophorans are fully articulated (Group 1) and in life position (i.e., intact arms and extended aulacophores), suggesting that the smothering occurred in a storm event that suddenly suffocated the echinoderm population. Only a few specimens may have briefly survived the mostly *en masse* transportation, and attempted escape by moving their arms up, through the sediment after burial, even if in an inverted position. It also possible that some of the ophiuroids had died before the obrution event, which may explain those specimens that are lacking arms (Group 3). The large amount of articulated arm fragments is attributed to mechanical fracturing when the ophiuroids tried to escape the storm-induced sediment influx or when they tumbled a short distance in the currents.

The Karbonaatjies obrution bed illustrates a complex history because it contains an admixture of shells and echinoderms in different states of preservation which is a hallmark of time-averaged accumulations. The community of intact ophiuroids and stylophorans reflects little or no time-averaging in contrast to the time-averaged shelly debris at the base of the bed that records a depositional history prior to the obrution event. It is likely that several earlier, high energy storm-generated currents transported and mixed successive generations of shells and

other detritus downslope, close to the offshore transition setting that was inhabited by the gregarious ophiuroids and stylophorans. At least some of the poorly-sorted debris of trilobite moults, gastropod shells and crinoid ossicles, which show no signs of abrasion, was not exclusively brought in by earlier high energy currents, but possibly accumulated *in situ* near or on the sea floor that was inhabited by the gregarious echinoderm community.

Finally, this study illustrates that micro-CT scanning is an invaluable taphonomic tool for analysing delicate fossils and accounting for all specimens irrespective of their preservation stages without damaging them. Furthermore, the method allows for a better quantification of the degree of fossil articulation, orientation, and population dynamics than traditional fossil assessment methods. In case of the Karbonaatjies obrution bed, this non-destructive technique allowed not only the visualisation of internal aspects of the fossil-rich layer, but also the discovery of extremely small paranacystids, which probably would have been missed or destroyed using traditional, mechanical fossil preparation techniques.

REFERENCES

Abel, R.L., Laurini, C.R. and Richter, M., 2012. A palaeobiologist's guide to 'virtual' micro-CT preparation. Palaeontologia Electronica 15, 17p.

Almond, J.E., 2011. Proposed Touwsrivier Solar Energy Facility, Farms Hartebeeskraal 36 and Ratelbosch 149, near Touwsrivier, Breede Valley Local Municipality, Western Cape Province. Palaeontological Impact Assessment: Combined Desktop Study and Field Assessment. Natura Viva cc, 33 pp.

Almond, J.E., Theron, J.N., Roberts, D.K., and Avery, G. 1996. Fossils sites in the southwestern Cape. Excursion guide, 9th Biennial Conference of the Palaeontological Society of South Africa, 26-27 September, Stellenbosch, 47 pp.

Ameziane, N. and Roux, M., 1997. Biodiversity and historical biogeography of stalked crinoids (Echinodermata) in the deep sea. Biodiversity and Conservation 6, 1557-1570.

Aronson, R.B., 1987. Predation of Fossil and Recent Ophiuroids. Paleobiology 13, 187–192.

Aronson, R.B., 1989. Brittlestar beds: low-predation Anachronisms in the British Isles. Ecology 70, 856–865.

Aronson RB., 1991. Predation, physical disturbance, and sublethal arm damage in ophiuroids: A Jurassic-Recent comparison. Mar Ecol Prog Ser 74:91–7.

Aronson, R.B., 1992. Biology of a scale-independent predator– prey interaction. Marine Ecology Progress Series 89, 1–13.

Aronson, R.B. and Harms, C.A., 1985. Ophiuroids in a Bahamian Saltwater Lake: The Ecology of a Paleozoic-like Community. Ecology 66, 1472-1483.

Aronson, R.B. and Sues, H.D., 1987. The paleoecological significance of an anachronistic ophiuroid community. Predation: direct and indirect impacts on aquatic communities, pp.355-66.

Aronson, R.B. and Heck Jr, K.L., 1995. Tethering experiments and hypothesis testing in ecology. Marine ecology progress series. Oldendorf 121, 307-309.

Aronson, R.B. and Blake, D.B., 1997. Evolutionary paleoecology of dense ophiuroid populations. In: Waters, J.A., Maples, C.G. (Eds.), Geobiology of Echinoderms. Paleontological Society Papers 3, 107-119.

Aronson, R.B. and Blake, D.B., 2001. Global climate change and the origin of modern benthic communities in Antarctica. American Zoologist 41, 27-39.

Ausich, W.I., 2001. Echinoderm taphonomy. In: Jangoux, M., Lawrence, J.M. (Eds.), Echinoderm studies 6, 171-227.

Baird, G. C., Shabica, C.W., Anderson, J.L. and Richard-son, jr. E.S., 1985. The biota of a Pennsylvanian muddy coast: habitats within the Mazonian delta complex, northeastern Illinois. Journal of Paleontology 59:253-281.

Barrett, J.F. and Keat, N., 2004. Artifacts in CT: Recognition and Avoidance. RadioGraphics 24, 1679-1691.

Bartels, C. and Briggs, D.E.G., Brassel, G., 1998. The Fossils of the Hunsrück Slate, Marine Life in the Devonian. Cambridge University Press, Cambridge 3, 1-309.

Behrensmeyer, A.K. and Kidwell, S.M., 1985. Taphonomy's contribution to Paleobiology. Paleobiology, 11, 105-119.

Behrensmeyer, A.K., Kidwell, S.M. and Gastaldo, R.A., 2009. Taphonomy and paleobiology. 26, 103-147.

Bigey, F.P., 1985. Biogeography of Devonian Bryozoa. In: Nielson, C., Larwood, G.P. (Eds.), Bryozoa: Ordovician to Recent. Olsen and Olsen, Fredensborg, pp. 9–23.

Billings, E. 1858. On the Asteridae of the Lower Silurian rocks of Canada, Figures and descriptions of Canadian organic remains. Geological Survey of Canada, 3, 75–85.

Blake, D.B., 2003. Functional morphology and paleoecology of stelleroids of the Hunsrück Slate (Emsian, Lower Devonian). Geological Society of America Abstracts with Programs 35, 162.

Blake, D.B., 2009. Re-evaluation of the Devonian family Helianthasteridae Gregory, 1899 (Asteroidea: Echinodermata). Paläontologische Zeitschrift 83, 293–308.

Blake, D.B., 2013. Early asterozoan (Echinodermata) diversification: a paleontologic quandary. Journal of Paleontology 87, 353–372.

Blake, D.B. and Aronson, R.B., 1998. Eocene stelleroids (Echinodermata) at Seymour Island, Antarctic Peninsula. Journal of Paleontology 72, 339-353.

Blake, D.B., Zamora, S. and García-alcalde, J.L., 2015. A new Devonian asteroid-like ophiuroid from Spain. Geologica Acta 13, 335–343

Boucot, A.J., 1985. Late Silurian-Early Devonian Biogeography, Provincialism, Evolution and Extinction. Philos. Trans. Roy. Soc. B Biol. Sci. 309, 323–339.

Boucot, A.J., 1988. Devonian biogeography: an update. In: McMillan, N.J., Embry, A.F., Glass, D.J. (Eds.), Proceedings, 2nd International Symposium on the Devonian System Canadian Society of Petroleum Geologists Memoir 14, vol. 3, pp. 211–227.

Boucot, A.J. and Gill, E.D., 1956. Australocoelia, a New Lower Devonian Brachiopod from South Africa, South America and Australia. Journal of Palaeontology 30, 1173 – 1178.

Boucot, A.J., Johnson, J.G., Talent, J.A., 1969. Early Devonian brachiopod zoogeography. Geol. Soc. Am. Spec. Pap. 119, 107.

Boucot, A.J., Brunton, C.H.C. and Theron, J.N., 1983. Implications for the age of South African rocks in which Tropidoleptus (Brachiopoda) has been found. Geological Magazine 120, 51-58.

Boucot, A.J. and Theron, J.N., 2001. First Rhipidothyris (Brachiopoda) from southern Africa: Biostratigraphic, paleoecological, biogeographical significance. Journal of the Czech Geological Society 46, 155-160.

Brett, C.E., 1983. Sedimentology, facies and depositional environments of the Rochester shale (Silurian, Wenlockian) in Western New York and Ontario. Journal of Sedimentary Petrology 53 (3), 947-972.

Brett, C.E., 1990. Obrution deposits. In: Briggs, D.E.G., Crowther, P.R. (Eds.), Palaeobiology: A Synthesis. Blackwell Science Publishing, Oxford, 239–243.

Brett, C.E. and Baird, G.C., 1986. Comparative taphonomy: a key to paleoenvironmental interpretation based on fossil preservation. Palaios 1, 207–227.

Brett, C.E., Moffat, H.A. and Taylor, W.L., 1997. Echinoderm taphonomy, taphofacies, and lagerstätten. In: Waters, J.A., Maples, C.G. (Eds.), Geobiology of Echinoderms. The Paleontological Society Papers 3, 147-190.

Bromley, R.G. 1996: Trace Fossils - Biology, Taphonomy and Applications. Chapman and Hall, London, pp. 361.

Broquet, C. A. M., 1992. The sedimentary record of the Cape Supergroup: A review. In: De Wit, M.J. and Ransome, I.G.D. (Eds.): Inversion Tectonics of the Cape Fold Belt, Karoo and Cretaceous Basins of Southern Africa. Balkema, Rotterdam.

Butterfield, N. J., 1990. Organic preservation of non-mineralizing organisms and the taphonomy of the Burgess Shale. Paleobiology 16272-286.

Chatwin, C. P. 1948. British regional geology: the Hampshire Basin and adjoining areas. Second edition. His Majesty's Stationery Office, London, England.

Chauvel, J. 1941. Recherches sur les cystoïdes et les carpoïdes armoricains. Mémoires de la Société géologique et minéralogique de Bretagne 5, 1–286.

Chen, J., Chen, Z.Q. and Tong, J.N., 2010. Palaeoecology and taphonomy of two brachiopod shell beds from the Anisian (Middle Triassic) of Guizhou, Southwest China: recovery of benthic communities from the end-Permian mass extinction. Global and Planetary Change 73(1), 149-160.

Cameron, B., 1969. Paleozoic shell-boring annelids and their trace fossils. Amer. Zool. 9, 689-703.

Caster, K.E., 1952. Concerning Enopleura of the Upper Ordovician and its relation to other carpoid Echinodermata. Bulletins of American Paleontology 34, 1–47.

Caster, K.E., 1954. A new carpoid from the Paraná Devonian. Anais Acad. Brasil. Ciencias 26, 123-147.

Caster, K.E., 1983. A new Silurian carpoid echinoderm from Tasmania and a revision of the Allanicytidiidae. Alcheringa 5, 321–335.

Caster, K.E. and Gill, E.D., 1967. Family Allanicytidiidae, new family. In: Treatise on Invertebrate Paleontology. Part S. Echinodermata 1(2). MOORE, R.C. (Eds.), Geological Society of America, Boulder and University of Kansas Press, Lawrence, 561–564.

Conrad T. A., 1840. Third annual report on the palaeontological department of the survey. New York Geological Survey, Annual Report 4(1), 199-207.

Cooper, M.R., 1982. A revision of the Devonian (Emsian–Eifelian) Trilobita from the Bokkeveld Group of South Africa. Ann. South Afr. Museum 89, 1–174.

Cripps, A.P., 1989. A new genus of stem chordate (Cornuta) from the Lower and Middle Ordovician of Czechoslovakia and the origin of bilateral symmetry in the chordates. Geobios 22, 215–245.

Cripps, A. P., and Daley, P.E.J., 1994 Two new cornutes from the Middle Ordovician (Llandeilo) of Normandy, France, and a reinterpretation of *Milonicystis Kerfornei*. Palaeontographica, Abteilung A 232, 99-132.

Clarke, J.M., 1913. Fosseis Devonianos do Parana. Servicio Geologico e Mineralogico do Brasil, Rio de Janeiro, 353 pp.

Clausen, S. and Smith, A. B., 2005. Palaeoanatomy and biological affinities of a Cambrian deuterostome (Stylophora). Nature 438, 351–354.

Clifton, H. E., 1971. Orientation of empty pelecypod shells and shell fragments in quiet water: Jour. Sed. Petrology 41, 671-682.

Dodd, J.R., Alexander, R.R. and Stanton, R.J., 1985: Population dynamics in Dendraster, Merriamaster, and Anadara from the Neogene of the Kettleman Hills, California. Palaeogeography, Palaeoclimatology, Palaeoecology 52, 61–76.

Donovan, S.K., Sutton, M.D. and Sigwart, J.D., 2010. Crinoids for lunch? An unexpected biotic interaction from the Upper Ordovician of Scotland. Geology 38, 935-938.

Dornbos, S.Q., Bottjer, D.J., 2001. Taphonomy and environmental distribution of helicoplacoid echinoderms. Palaios 16, 197–204.

David, B., Lefebvre, B., Mooi, R. and Parsley, R.L., 2000. Are homalozoans echinoderms? An answer from the extraxial-axial theory. Paleobiology 26, 529–555.

Davies D.J. , Powell E.N. and Stanton R.J.,1989. Relative rates of shell dissolution and net sediment accumulation—a commentary: can shell beds form by the gradual accumulation of biogenic debris on the sea floor? Lethaia 22, 207–212

Dehm, R., 1932. Cystoideen aus dem rheinischen Unterdevon. Neues Jahrbuch fu¨r Mineralogie, Geologie und Pala¨ontologie, Beilagen-Band, Abteilung A 69: 63–93.

Donovan, S.K., 1991. The taphonomy of echinoderms: calcareous multi-element skeletons in the marine environment. In: S.K. Donovan (Eds.), The processes of fossilisation: 241-269. London: Belhaven Press.

Donovan, S.K., Paul, C.R.C., Lewis, D.N., 1996. Echinoderms. In: Harper, D.A.T., Owen, A.W. (Eds.), Fossils of the Upper Ordovician. Field Guide to Fossils, vol. 7. Palaeontological Association, London, pp. 202–267.

du Plessis, A., le Roux, S. G. and Guelpa, A., 2016. The CT Scanner Facility at Stellenbosch University: An open access X-ray computed tomography laboratory. Nuclear Instruments and Methods in Physics Research B 384, 42-49.

Du Toit, A.L., 1956. The Geology of South Africa. Oliver and Boyd, Edinburgh, 611 pp.

Eldredge, N., Ormiston, A.R., 1979. Biogeography of Silurian and Devonian trilobites of the Malvinokaffric Realm. In: Gray, J., Boucot, A.J. (Eds.), Historical Biogeography, Plate Tectonics, and the Changing Environment. Oregon State University Press, Corvallis, pp. 147–167.

Emson, R.H. 1998. Making the best of it: the ecology of deep sea echinoderms. In: Mooi, R. and Telford, M. (Eds.) Echinoderms: San Francisco. Balkema, Rotterdam, pp. 452.

Emson RH and Wilkie IC., 1980. Fission and autotomy in echinoderms. Oceanogr Mar Biol Ann Rev 28,155–250

Fenton, C. L. and Fenton, M. A., 1932 Boring sponges in the Devonian of Iowa. Amer. Mid. Nat. 13, 42-53.

Fourie, P.H., Zimmermann, U., Bukes, N.J., Naidoo, T., Kobayashi, K., Kosler, J., Nakamura, E., Tait, J. and Theron, J.N., 2011. Provenance and reconnaissance study of detrital zircons of the Palaeozoic Cape Supergroup in South Africa: revealing the interaction of the Kalahari and Rio de la Plata cratons. International Journal of Science 100, 527-541.

Fujita, T., 1992. Dense beds of ophiuroids from the Paleozoic to the Recent: the significance of bathyal populations. Otsuchi Marine Research Centre Reports 18, 25–41.

Fujita, T. and Ohta, S., 1989. Spatial structure within a dense bed of the brittle star Ophiura sarsii (Ophiuroidea: Echinodermata) in the bathyal zone off Otsuchi, northeastern Japan. J. Oceanogr. Soc. Jpn. 45, 289–300.

Fujita, T. and Ohta, S., 1990. Size structure of dense populations of the brittle-star Ophiura sarsii (Ophiuroidea: Echinodermata) in the bathyal zone around Japan. Mar. Ecol. Prog. Ser. 64, 113–122.

Fürsich F.T. and Oschmann W., 1993. Shell beds as tools in basin analysis: the Jurassic of Kachchh, western India. J Geol Soc Lond 150,169–185.

Futterer E., 1982. Experiments on the distinction of wave and current influenced accumulations. In: Einsele G, Seilacher A (Eds.) Cyclic and event stratification. Springer, Berlin, pp. 175–179.

Garwood, R.J., Rahman, I.A. and Sutton, M.D., 2010. From clergymen to computers the advent of virtual palaeontology. Geology today 26, 96-100.

Gill, E.D. and Caster, K.E., 1960. Carpoid echinoderms from the Silurian and Devonian of Australia. Bulletins of American Paleontology 41, 1-71.

Gorzelak, P. and Salamon, M., 2013. Experimental tumbling of echinoderms — taphonomic patterns and implications. Palaeogeogr. Palaeoclimatol. Palaeoecol. 386, 569–574.

Gould, S. J., 1989. Wonderful Life: the Burgess Shale and the Nature of History. New York: Norton Press.

Gray, J.E., 1840. A synopsis of the genera and species of the class Hypostoma (Asterias Linnaeus). Annals and Magazine of Natural History 20,193–204.

Gregory, J. W. 1897. On the classification of the Palaeozoic echinoderms of the group Ophiuroidea. Proceedings of the Zoological Society of London, 1896, 1028–1044.

Gresse, P.G. and Theron, J.N., 1992. The geology of the Worcester area. Explanation of geological Sheet 3319. Council for Geoscience, Pretoria, 79pp.

Grisbrook, C.H., 1830. Notes of South African geology. Quart. J. South Africa 1, 446–447.

Glass, A., 2004. The Hunsrück Slate (Lower Devonian, lower Emsian) in the context of the Paleozoic history of the Ophiuroidea (Echinodermata). Geological Society of America Abstracts with Programs 36, 525.

Glass, A., 2006. New observations on some poorly known protasterid ophiuroids from the Lower Devonian Hunsrück Slate of Germany. Paläontologische Zeitschrift 80, 68–87.

Glass, A., 2008. Peculiar and novel morphologies in Paleozoic brittle stars (Echinodermata, Ophiuroidea) from the Lower Devonian Hunsrück Slate of Germany. Geological Society of America Abstracts with Programs 40, 477.

Glass, A. and Blake, D.B., 2002. Soft-tissue preservation in protasteridophiuroids (Echinodermata) from the Kope Formation (Cincinnatian, Upper Ordovician) of North-Western Kentucky and the Hunsrueck Slate (Emsian, Lower Devonian) of Germany. Geological Society of America Abstracts with Programs 34, 36.

Glass, A. and Blake, D.B., 2004. Preservation of tube feet in an ophiuroid (Echinodermata) from the Lower Devonian Hunsrück Slate of Germany and a redescription of Bundenbachiabeneckei and Palaeophiomyxa grandis. Paläontologische Zeitschrift 78, 73–95.

Glass, A. and Poschmann, M., 2006. A new species of brittlestar (Ophiuroidea, Echinodermata) from the Hunsrück Slate (lower Emsian, Lower Devonian) of Germany. Palaeontology 49, 969–981.

Haeckel, E.H., 1866. Generelle Morphologie der Organismen. Zweiter Band: Allgemeine Entwicklungsgeschichte der Organismen. Berlin, Verlag von Georg Reimer, 160pp.

Hall, J., 1868. Contributions to palaeontology. 12. Note on the genus Palaeaster and other fossil starfishes. Annual report of the Regents of the University of the State of New York on the State Cabinet of Natural History and the Historical and Antiquarian collection annexed thereto 20, 282-303.

Hall, J. and Whitfield, R. P., 1869. Preliminary notice of the lamellibranchiate shells of the upper Helderberg, Hamilton and Chemung groups, with others from the Waverly sandstones, part 2, 1-80

Hallam, A., 1972: Models involving population dynamics. In Schopf, J.M. (Eds.): Models in Paleobiology, 62–80. Freeman, Cooper and Co., San Francisco.

Hammer, Ø., Harper, D.A.T. and Ryan, P.D., 2001: PAST (Palaeontological Statistics Software Package for Education and Data Analysis). Palaeontologia Electronica 4, 9.

Harper, J.A. and Morris, R.W., 1978. A new encrinasterid ophiuroid from the Conemaugh Group (Pennsylvanian) of Western Pennsylvania, and revision of the Encrinasteridae. Journal of Paleontology, 52, 155-163.

Haude, R., 1995. Lower Devonian echinoderms from the Precordillera (Argentina). Neues Jahrbuch für Geologie und Paläontologie, Abhandlungen 197, 37–86.

Haude, R., 1999. Der - verzogerte - Ersatz eines Homonyms: Marginaster Haude 1995. Abhandlungen, Neues Jahrbuch für Geologie und Paläontologie, 1999, 292-294.

Haude, R., 2004. Morphology and palaeobiology of echinoderms in the Lower Devonian of the Argentine Precordillera. In Echinoderms: Munchen: Proceedings of the 11th International Echinoderm Conference, 6–10 October 2003, Munich, Germany. Heinzeller, T. and Nebelsick, J.H., (Eds.), CRC Press, USA, 417.

Haude, R., 2010. Ophiuroids in the Lower Devonian of the Argentine Precordillera. In Echinoderm Research 2010: 7th European Conference on Echinoderms, Göttingen, Germany, 2–9 October 2010. Reich, M., Reitner, J., Roden, V. and Thuy, B., (Eds), Universitätsverlag Göttingen, Göttingen, 46–47.

Hess, H. and Meyer, C., 2008: A new ophiuroid (*Geocoma schoentalensis* sp. nov.) from the Middle Jurassic of northwestern Switzerland and remarks on the family Aplocomidae Hess, 1965. Swiss Journal of Geosciences 101, 29-40.

Hiller, N. and Theron, J.N., 1988. Benthic communities in the South African Devonian. In: McMillan, N.J., Embry, A.F., Glass, D.J. (Eds.), Devonian of the World, Vol. III: Paleontology, Paleoecology and biostratigraphy. Memoirs of the Canadian Society of Petroleum Geology 14, 729-740.

Holland S.M., 1988. Taphonomic effects of sea-floor exposure on an Ordovician brachiopod. Palaios 3, 588–597.

Hunter, A.W., Rushton, A.W.A. and Stone, P., 2016. Comments on the ophiuroid family Protasteridae and description of a new genus from the Lower Devonian of the Fox Bay

Formation, Falkland Islands, Alcheringa: An Australasian Journal of Palaeontology 40 (4), 1-14.

Hunter, A.W., Lefebvre, B., Régnault, S., Roussel, P., Claverie, R., 2007. A mixed ophiuroid–stylophoran assemblage (Echinodermata) from the Middle Ordovician (Llandeilian) of western Brittany, France. In: Álvaro, J.J., Aretz, M., Boulvain, F., Munnecke, A., Vachard, D. and Vennin, E. (Eds.), Palaeozoic Reefs and Bioaccumulations: Climatic and Evolutionary Controls. Geological Society, London, Special Publications 275, 71–86.

Isaacson, P.E., 1977. Devonian Stratigraphy and Brachiopod Palaeontology of Bolivia Part B Spiriferida and Terebratulida. Palaeontographica Abteilung A. 156, 168 – 217.

Ishida Y. and Fujita, T., 2001. Escape behaviour of epibenthic ophiuroids buried in the sediment: Observations of extant and fossil *Ophiura sarsii sarsii*. In: Echinoderms 2000: Proceedings of the 10th International Conference, pp. 285-292

Jaekel, O., 1901. Uber Carpoideen; eine neue Klasse von Pelmatozoen. Z. Deutsch. Geol. Gesellsch. 52, 661–677.

Jaekel, O. 1903. Asteriden und Ophiuriden aus dem Silur Bo¨hmens. Zeitschrift der Deutschen Geologischen Gesellschaft 55,106–113.

Jaekel, O. 1918. Phylogenie und System der Pelmatozoen. Paläontologische Zeitschrift 3, 1-124.

Jaekel, O., 1923. Zur morphogenie der Asterozoa. Palaeontologische Zeitschrift 5, 344–350.

Jagt, J.W.M., 2000, Late Cretaceous-Early Palaeogene echinoderms and the K/T boundary in the southeast Netherlands and northeast Belgium - Part 3: Ophiuroids. With a chapter on: Early Maastrichtian ophiuroids from Rügen (northeast Germany) and Møn (Denmark) by Manfred Kutscher and John W.M. Jagt: Scripta Geologica, 121, 1-179.

Jefferies, R. P. S., 1967. Some fossil chordates with echinoderm affinities. Symposium of Zoological Society of London 20, 163-208.

Jefferies, R.P.S., 1968. The subphylum Calcichordata (Jefferies 1967), primitive fossil chordates with echinoderm affinities. Bulletin of the British Museum (Natural History), Geology Series 16, 243-339.

Jefferies, R.P.S., 1984. Locomotion, shape, ornament, and external ontogeny in some mitrate calcichordates. Journal of Vertebrate Paleontology, 4, 292–319.

Jefferies, R.P.S., Brown, N.A and Daley, P.E.F., 1966. The early phylogeny of chordates and echinoderms and the origin of chordate left-right asymmetry and bilateral symmetry. Acta Zoologica, 77,101–122.

Jell, P.A., 1997. Early Carboniferous ophiuroids from Crawfordsville, Indiana. Journal of Paleontology 71, 306-316.

Jell, P.A., 2013. Placocystella in the Early Devonian (Lochkovian) of central Victoria. Alcheringa, 37, 567–569.

Jell, P.A. and Theron, J.N., 1999. Early Devonian echinoderms from South Africa. Memoirs of the Queensland Museum, 43, 115-199.

Jaselli, L., 2014. The first occurrence of ophiuroids (Ophiuroidea, Echinodermata) in the Early Triassic of Lombardy (Northern Italy. Atti della Società Toscana di Scienze Naturali, Memorie, Serie A 121, 47-54.

Johnson, M. R., 1976. Stratigraphy and Sedimentation of the Cape and Karoo Sequences in the Eastern Cape Province. PhD Thesis, Rhodes University, pp. 333.

Kerr, T. J. V. and Twitchett, R. J., 2004. Experimental decay and disarticulation of Ophiura texturata: implications for the fossil record of ophiuroids. In: Heinzeller, T., Nebelsick, J. H. (Eds.), Echinoderms: München. Balkema, Leiden, pp. 439–446.

Kesling, R. V., 1969. A new brittle-star from the Middle Devonian Arkona shale of Ontario. Contributions from the Museum of Paleontology, University of Michigan 23, 37-51.

Kesling, R. V. and Le Vasseur, D., 1971. *Strataster ohioensis,* a new early Mississippian brittle-star, and the paleoecology of its community. Contributions from the Museum of Paleontology, University of Michigan 23, 305-341.

Kidwell, S.M., Füersich, F.T. and Aigner, T., 1986. Conceptual framework for the analysis and classification of fossil concentrations. *Palaios*, pp.228-238.

Kidwell, S.M. and Baumiller, T., 1990. Experimental disintegration of regular echinoids: roles of temperature, oxygen and decay thresholds. Paleobiology 16, 247-271.

Kidwell, S.M. and Bosence, D.W., 1991. Taphonomy and time-averaging of marine shelly faunas. Taphonomy: releasing the data locked in the fossil record. Plenum, New York, pp.115-209.

Kidwell, S.M. and Holland, S.M., 1991. Field description of coarse bioclastic fabrics. *Palaios*, pp.426-434.

Kolata, D. R. and Jollie, M. 1982. Anomalocystitid mitrates (Stylophoran- Echinodermata) from the Champlainian (Middle Ordovician) Guttenberg Formation of the Upper Mississippi Valley region. Journal of Palaeontology 56, 631-653.

Lawrence J., 1987. A functional biology of echinoderms. Baltimore, MD: The Johns Hopkins University Press.

Lawrence, J.M., 2012. Arm loss and regeneration in stellate echinoderms: An organismal view. In: Echinoderms in a Changing World: Proceedings of the 13th International Echinoderm Conference, January 5-9 2009, University of Tasmania, Hobart Tasmania, Australia, p. 53.

Lawrence, J.M. and Vasquez, J., 1996. The effect of sublethal predation on the biology of echinoderms. Oceanologica Acta 19, 431-440.

Lawrence, J.M, Klinger, T.S., McClintock, J.B, Watts, S.A., Chen, C.P., Marsh, A. and Smith, L., 1986. Allocation of nutrient resources to body components by regenerating *Luidia clathrate* (Say) (Echinodermata: Asteroidea). J. Exp. Mar. Biol. Ecol. 102, 47-53.

Lehmann, W.M., 1957. Die Asterozoen in den Dachschiefern des rheinischen Unterdevons. Abhandlungen des Hessischen Landesarntes für Bodenforschung 21, 1–160

Lewis, R., 1980. Taphonomy. In: Broadhead, T.W. and Waters, J.A. (Eds.), Echinoderms, notes for a short course. University of Tennessee, studies in geology 3, 27-39.

Lewis, R.D., 1986. Relative rates of skeletal disarticulation in modern ophiuroids and Paleozoic crinoids. Geol. Soc. Am. Abstr. Programs 18, 672.

Lewis, R.D., 1987. Post-mortem decomposition of ophiuroids from the Mississippi Sound. Geol. Soc. Am. Abstr. Programs 19, 94–95.

Lefebvre, B, 2003. Functional morphology of stylophoran echinoderms. Palaeontology 46, 511-555.

Lefebvre, B., 2007. Early Palaeozoic palaeobiogeography and palaeoecology of stylophoran echinoderms. Palaeogeogr. Palaeoclimatol. Palaeoecol. 245, 156–199.

Lefebvre, B. and Vizcaïno, D., 1999. New Ordovician cornutes (Echinodermata, Stylophora) from Montagne Noire and Brittany (France) and a revision of the Order Cornuta Jaekel 1901. Geobios 32, 421–458.

Makra, A. and Keegan, B.F., 1999, October. Arm regeneration in Acrocnida brachiata (Ophiuroidea) at Little Killary, west coast of Ireland. In Biology and Environment: Proceedings of the Royal Irish Academy, pp. 95-102.

Mángano, M.G., Buatois, L.A., West, R.R. and MapleS, C.G., 1999. The origin and paleoecologic significance of the trace fossil Asteriacites in the Pennsylvanian of Kansas and Missouri. Lethaia 32(1), 17-30.

Martínez, S., Del Rio, C.I., Pérez, D.E., 2010. A brittle star bed from the Miocene of Patagonia, Argentina. Lethaia 43, 1–9.

Martin, E., Lefebvre, B. and Vaucher, R., 2015. Taphonomy of a stylophoran-dominated assemblage in the Lower Ordovician of Zagora Area (Central Anti-Atlas, Morocco). In: Zamora, S. and Rabano, I. (Eds.), Progress in Echinoderm Palaeobiology, Publisher: Cuadernos del Museo Geominero 19, pp.95-100.

Matsumoto, H. 1915. A new classification of the Ophiuroidea; with descriptions of new genera and species. Proceedings of the Academy of Natural Sciences of Philadelphia, 67, 43–92.

McGhee, G.R., 1976. Late Devonian benthic marine communities of the central Appalachian Allegheny Front. Lethia 9, 111-136.

Melo, J.H.G., 1988. The Malvinokaffric Realm in the Devonian of Brazil. In: McMillan, N.J., Embry, A.F., Glass, D.J. (Eds.), Devonian of the World. Canadian Society of Petroleum Geologists, vol. 1, pp. 669–703.

Metaxas, A. and Giffin, B., 2004. Dense beds of the ophiuroid Ophiacantha abyssicola on the continental slope off Nova Scotia, Canada. Deep Sea Research Part I: Oceanographic Research Papers 51, 1307-1317.

Meyer, D.L., 1971. Population palaeoecology and comparative taphonomy of two edriasteroid (Echinodermata) pavements: Upper Ordovician of Kentucky and Ohio. Historical Biology 4, 155-178.

Meyerhoff, A.A., Boucot, A.J., Meyerhoff Hull, D., Dickins, J.M., 1996. Phanerozoic Faunal and Floral Realms of the Earth: the intercalary relations of the Malvinokaffric and Gondwana Faunal Realms with the Tethyan Faunal Realm. Boulder, Colorado, Geological Society of America Memoir 189.

Miller, S.A., 1889. North American Geology and Palaeontology for the use of Amateurs, Students, and Scientists. Western Methodist Book Concern Press, Cincinnati, OH., 662 pp.

Morgan, R. and Jagoux, M., 2004: Juvenile–adult relationship in the gregarious ophiuroid Ophiothrix fragilis (Echinodermata): a behavioural and morphological study. Marine Biology 145, 265–276.

Nebelsick, J.H., 2004, Taphonomy of echinoderms: Introduction and outlook. In: Heinzeller, T., Nebelsick, J.H. (Eds.), Echinoderms: München. Balkema, London, pp. 471-477.

Oji, T. and Okamoto, T., 1994. Arm autotomy and arm branching pattern as anti-predatory adaptations in stalked and stalkless crinoids. Paleobiology, pp.27-39.

Oliver, W.A., 1980. Corals in the Malvinokaffric Realm. Munster Forsch. Geol. Palaont. 52, 13–27.

Oosthuizen, R.D.F., 1984. Preliminary catalogue and report on the biostratigraphy and palaeogeography distribution the Bokkeveld Fauna. Trans. Geol. Soc. South Africa 87, 125–140.

Parsley, R.L., 1988. Feeding and respiratory strategies in Stylophora. In: Paul, C.R.C., Smith, A.B. (Eds.), Echinoderms Phylogeny and Evolutionary Biology. Clarendon Press, Oxford, pp. 347–361.

Parsley, R.L., 1991. Review of selected North American mitrate stylophorans (Homalozoa: Echinodermata). Bull. Am. Paleontol. 100, 5–57.

Parsley, R.L. and Prokop, R.J., 2001. Functional morphology and paleoecology of Middle Cambrian echinoderms from marginal Gondwana basins in Bohemia. Abstr. Programs - Geol. Soc. Am. 33, 247.

Parsley, R.L. and Gutierrez-Marco, 2005. Stylophorans in middle Arenig shallow water siliciclastics: *Vizcainocarpus* from the Imfout Syncline in Morocco's western Meseta. Bulletin of Geosciences 80 (3), 185–192.

Parsley, R.L., Prokop, R.J., Derstler, K., 2000. Kirkocystid ankyroids (Stylophora: Echinodermata) from the Šárka Formation (Ordovician) of Bohemia. Vest. Cesk. geol. úst. 75, 37–47.

Parsons, K. M., Brett, C. E. and Miller, K.B., 1988. Taphonomy and depositional dynamics of Devonian shell-rich mudstone. Palaeogeograghy, Palaeoclimatology, Palaeoecology 63, 109-139.

Paul, C. R. C. and Smith, A.B., 1984. The early radiation and phylogeny of echinoderms. Biological Reviews 59, 444-471.

Philip, G.M., 1979. Carpoids: echinoderms or chordates? Biological Reviews of the Cambridge Philosophical Society 54, 439-471.

Purnell, M., 2003. Casting, replication, and anaglyph stereo imaging of microscopic detail in fossils, with examples from conodonts and other jawless vertebrates. Palaeontologia Electronica 6(2), 11 p.

Rahman, I.A., Jefferies, R.P., Suedkamp, W.H. and Smith, R.D., 2009. Ichnological insights into mitrate palaeobiology. Palaeontology 52, 127-138.

Radwanski, A., 2002. Triassic brittlestar beds of Poland: a case of Aspiduriella ludeni (v. Hagenow, 1846) and Arenorbis squamosus (E. Picard, 1858). Acta Geol. Polon. 52, 395-410.

Rahman, I.A., Jefferies, R.P., Suedkamp, W.H. and Smith, R.D., 2009. Ichnological insights into mitrate palaeobiology. Palaeontology, 52(1), 127-138.

Reid, M., Bordy, E.M. and Taylor, W., 2015. Taphonomy and sedimentology of an echinoderm obrution bed in the Lower Devonian Voorstehoek Formation (Bokkeveld Group, Cape Supergroup) of South Africa. Journal of African Earth Sciences 110, 135-149.

Rennie, J.V.L., 1936. On Placocystella, a new genus of cystids from the Lower Devonian of South Africa. Annals of the South African Museum 31, 269–275.

Reed, F.R.C., 1906. New fossils from the Bokkeveld Beds. Geological Magazine Decade 5, 166–171, 4: 222–232.

Reed, F.R.C., 1925. Revision of the fauna of the Bokkeveld beds. Ann. South African Museum 22, 29–38.

Richter, R., 1941. Devon: Geologische Jahresberichte. Berlin 3A, 31–43.

Richter, R. and Richter, E., 1942. Die Trilobiten der Weismes-Schichten am Hohen Venn, mit Benmerkungen ü ber die Malvinocaffrische Provinz. Seckenbergiana 25,156–179.

Rilett, M.H.P., 1971. Two new fossil ophiuroid species from the Bokkeveld Series, near Ceres, Cape Province. Annales of the Natal Museum 21, 29-35

Roemer, F. 1863. Neue Asteriden und Crinoiden aus devonischem Dachschiefer von Bundenbach bei Birkenfeld. Palaeontographica, 9,143–152.

Roman, J., 1994: Taphonomie des échinodermes des calcaires lithographiques de Canjuers (Tithonien inférieur, Var, France). Geobios 27, 147-155.

Rose, J.J., 1983. A replication technique for scanning electron microscopy: applications for anthropologists. American Journal of Physical Anthropology 62,255- 261.

Rosenkranz, T., 1971: Zur Sedimentologie und Ökologie von Echinodermen- Lagerstätten. Neues Jahrbuch für Geologie und Paläontologie Abhandlungen 138, 221-258.

Rossouw, P.J., 1933. On the geology of Weltevreden, Prince Albert district, with a diagnosis of an ophiuroid, *Ophiurites* sp. Transactions of the Geological Society of South Africa 36, 73-76.

Rousseau, J. and Nakrem, H.A., 2012. An Upper Jurassic Boreal echinoderm Lagerstätte from Janusfjellet, central Spitsbergen. Norw. J. Geol. 92, 133–161.

Rust, I.C., 1973. The Evolution of the Paleozoic Cape Basin, Southern Margin of Africa. In: Nairn, A.E.M. and Stehli, F.G. (Eds.), The Ocean Basins and Margins. 1: The South Atlantic. Plenum Publishing Corp. New York, U.S.A., pp. 247-276.

Ruta, M., 1997. First record of a paranacystid mitrate from the Bokkeveld group of South Africa. Palaeontol. Afr. 34, 15-25.

Ruta, M., 1999. Brief review of the stylophoran debate. Evol. Dev. 1, 123–135.

Ruta, M. and Theron, J.N., 1997. Two Devonian mitrates from South Africa. Palaeontology 40, 201-243.

Ruta, M. and Bartels, C., 1998. A redescription of the anomalocystitid mitrate Rhenocystis latipedunculata from the Lower Devonian of Germany. Palaeontology 41, 771–806.

Salamon, M.A., Niedźwiedzki, R., Lach, R., Brachaniec, T. and Gorzelak, P., 2012. Ophiuroids discovered in the Middle Triassic hypersaline environment. PloS one, 7(11), p.e49798.

Salter, J.W., 1856. Description of Palaeozoic Crustacea and Radiata from South Africa. Trans. Geol. Soc. London 7, 201–243.

Schäfer, W., 1972. Ecology and Paleoecology of Marine Environments. Oliver and Boyd, Edinburgh, 568pp.

Schöndorf, F., 1910. Über einige “Ophiuriden und Asteriden” des englischen Silur und ihre Bedeutung für die Systematik paläozoischer Seesterne. Jahrbüchern des Nassauischen Vereins für Naturkunde in Wiesbaden 63, 206–256.

Schuchert, C. 1914. Fossilium Catalogus I: Animalia, pars 3, Stelleroidea Palaeozoica. 53 pp. W. Junk, Berlin.

Seilacher, A., Reif, W.E., and Westphal, F., 1985. Sedimentological, ecological and temporal patterns of *fossil-Lagerstätten*. Philosophical Transactions of the Royal Society of London 311, 5-23.

Shackleton, J.D., 2005. Skeletal homologies, phylogeny and classification of the earliest asterozoan echinoderms. Journal of Systematic Palaeontology 3, 29–114.

Shin, H.C. and Koh, C.H., 1993. Distribution and abundance of ophiuroids on the continental shelf and slope of the East Sea (southwestern Sea of Japan), Korea. Marine Biol. 115, 393–399.

Shroat-Lewis R A., 2007. Taphonomy of a Pliocene ophiuroid mass mortality lagerstätte in the Tirabuzón Formation, Baja California sur. Master Thesis of the University of North Carolina at Wilmington. 70 pp.

Sköld, M. and Rosenberg, R., 1996. Arm regeneration frequency in eight species of Ophiuroidea (Echinodermata) from European sea areas. Journal of Sea Research 35, 353-362.

Spencer, W.K., 1930. A monograph of the British Palaeozoic Asterozoa. Part 8. Monograph of the Palaeontographical Society, London 82 (for 1928), 389–436.

Spencer, W.K., 1934. A monograph of the British Palaeozoic Asterozoa. Part 9. Monograph of the Palaeontographical Society, London 87 (for 1933), 437–494.

Spencer, W.K., 1950. Asterozoa and the study of Palaeozoic faunas. Geological Magazine 87, 393–408.

Spencer, W.K., 1950a. A new brittle star and eurypterid from the Bokkeveld strata. S. Afr. J. Sci. 46, 300–301.

Spencer, W.K., 1951. Early Palaeozoic starfish. Philosophical Transactions of the Royal Society of London B: Biological Sciences 235, 87–129.

Spencer, W.K. and Wright, C.W., 1966. Asterozoans. In Treatise on Invertebrate Paleontology, Part U, Echinodermata 3. Moore, R.C. (Eds.), The Geological Society of America, Boulder, Colorado and The University of Kansas Press, Lawrence, Kansas, U1–U107.

Speyer, S. E., and Brett, C. E., 1986, Trilobite taphonomy and Middle Devonian taphofacies: Palaios1, 312.

Speyer, S.E. and Brett, C.E., 1991. Taphonomic controls: Background and episodic processes in fossil assemblage preservation. In: Allison, P.A., Briggs, D.E.G. (Eds.), Taphonomy: releasing in the Data Locked in the Fossil Record. Plenum Press, New York, pp. 502-546.

Stöhr, S., O'Hara, T.D. and Thuy, B., 2012. Global diversity of brittle stars (Echinodermata: Ophiuroidea). Plos One 7, 1-14.

Stürtz, B., 1886. Beitrag zur Kenntniss palaeozoischer Seesterne. Palaeontographica, 32,75-98.

Stürtz, B., 1890. Neuer Beitrag zur Kenntniss palaeozoischer Seesterne. Palaeontographica, 36, 203-247.

Sumrall, C.D., 1997. The role of fossils in the phylogenetic reconstruction of Echinodermata. Paleontological Society Papers 3, 267–288.

Sutcliffe, O.E., Südkamp, W. H. and Jefferies, R. P. S., 2000. Ichnological evidence on the behaviour of mitrates: two trails associated with the Devonian mitrate Rhenocystis. Lethaia, 33, 1–12.

Sutton, M.D., Briggs, D.E.G., Siveter, D.J., Siveter, D.J. and Orr, P.J., 2002. The arthropod Offacolus kingi (Chelicerata) from the Silurian of Herefordshire, England: computer based

morphological reconstructions and phylogenetic affinities. Proceedings of the Royal Society B. 269, 1195–1203.

Sutton, M.D., 2008. Tomographic techniques for the study of exceptionally preserved fossils. Proceedings of the Royal Society B. 275, 1587–1593.

Sutton, M., Rahman, I. and Garwood, R., 2014. Techniques for virtual palaeontology. John Wiley and Sons.

Tankard, A.J. and Barwis, J.H., 1982. Wave-dominated deltaic sedimentation in the Devonian Bokkeveld basin of South Africa. Journal of Sedimentary Petrology 52, 959–974.

Theron, J.N., 1970. A stratigraphical study of the Bokkeveld Group (series). Proceedings 2nd IUGS Symposium Stratigraphy Paleontology, Gondwana System, Cape Town, South Africa, pp. 197–204.

Theron, J.N., 1972. The stratigraphy and sedimentation of the Bokkeveld Group. DSc thesis, University Stellenbosch, unpublished.

Theron, J.N., 1999. Lithostratigraphy of the Gydo Formation (Bokkeveld Group), Council for Geoscience, Pretoria pp. 1-11.

Theron, J.N., 2003. Lithostratigraphy of the Voorstehoek Formation (Bokkeveld Group). Lithostratigraphic Series 38, SACS, pp. 11.

Theron, J.N. and Johnson, M.R., 1991. Bokkeveld Group (including the Ceres, Bidouw and Traka Subgroups). Catalogue of South African Lithostratigraphic Units 3, 3-5.

Theron, J.N. and Loock, J.C., 1988. Devonian deltas of the Cape Supergroup, South Africa. In: McMillian N.J., Embry, AF., Glass, D.J. (Eds.), Devonian of the World, Volume 1: Regional Syntheses. Canadian Society of Petroleum Geologists, Memoir No. 14, 729- 740.

Thom, G., 1830. Remarks on the geology of South Africa. South Afr. Quarter. J. 1, 269–271.

Torsvik, T. H. and Cocks, L. R. M., 2013. Gondwana from top to base in space and time, Gondwana Research 24, 999-1030.

Taylor, W.L., and Brett, C.E., 1996, Taphonomy and paleoecology of echinoderm Lagerstätten from the Silurian (Wenlockian) Rochester Shale. Palaios 11, 118–140.

Twitchett, R.J., Feinberg, J.M., O'Connor, D.D., Alvarez, W. and McCollum, L.B., 2005. Early Triassic ophiuroids: their paleoecology, taphonomy, and distribution. Palaios 20, 213–223.

Ubaghs, G., 1961. Un e´chinoderme nouveau de la classe des carpoı¨des dans l'Ordovicien infe´rieur du de´partement de l'He´rault (France). Comptes Rendus des Se´ances de l'Acade´mie des Sciences, 253, 2738–2740.

Ubaghs, G., 1968. Stylophora. In: Moore, R.C. (Eds.), Treatise on Invertebrate Paleontology: Part S. Echinodermata, vol. 1. Geol. Soc. Am. and Univ. Kansas Press, Lawrence, pp. 495-565.

Ubaghs, G., 1975. Early Palaeozoic echinoderms. Annual Review of Earth and Planetary Sciences 3, 70-98.

Ubaghs, G. and Robison, R. A., 1988. Homalozoan echinoderms of the Wheeler Formation (Middle Cambrian) of Western Utah. University of Kansas Paleontological Contributions, 120, 1–18.

Velbel M.A. and Brandt D.S., 1989. Differential preservation of brachiopod valves: Platystrophia ponderosa. Palaios 4, 193–195.

von Schlotheim E.F., 1820. Die Petrfactendunde auf ihrem jetzigen Standpunkte durch die Beshreibung seiner Sammlung versteinerter und fossiler Überreste des Thier- und Pflanzernreichs der Vorwelt erläutert, pp. 1-457.

Walker, K.R., and Bambach, R.K., 1971. The significance of fossil assemblages from fine-grained sediments: Time-averaged communities: Geological Society of America Abstracts with Programs 3, 783–784

Warner, G.F., 1971. On the ecology of a dense bed of the brittle-star Ophiotrix fragilis. J. Marine Biol. Assoc. U.K. 51, 267–282.

Warner, G.F., 1979. Aggregation in echinoderms. In: G. Larwood and B. R. Rosen, editors. Biology and systematics of colonial organisms. Academic Press, London, England, pp. 375-396

Warner, G. 1983. Food and feeding mechanisms: Ophiuroidea. In: Jangoux, M. and Lawrence, J.M. (Eds.) Echinoderm nutrition, pp.161-181.

Warner, G.F. and Woodley, J., 1975. Suspension-feeding in the brittle star Ophiothrix fragilis. Journal of the Marine Biological Association of the United Kingdom 55, 199–210.

Wilkie, I.C., 2001. Autonomy as a prelude to regeneration in echinoderms. Microsc. Res. Tech. 55, 369-396.

Woodley, J., Chornesky, E., Cliffo, P., Jackson, J., Kaufman, L., Knowlton, N., La, J., Pearson, M., Porter, J., Rooney, M. and Rylaarsdz, K.W., 1981. Hurricane Allen's impact on a Jamaican coral reef. Science 214, p.13.

Wright, T. 1863-1880. British fossil Echinodermata of the oolitic formations. Volume II, the Asteroidea and Ophiuroidea. Palaeontographical Society of London Monographs, 3 parts.

Wright, D.K., 1983. Crinoid ossicles in Upper Ordovician benthic marine assemblages from Snowdonia, North Wales. Palaeontology 26, 583-603.

Wyley, A., 1859. Report of the geological surveyor upon a journey made by him, mainly during the year 1858, in two directions across the colony and its results, with appendix. Cape of Good Hope Parliamentary Report G54-59.

Zatoń, M., Salamon, M.A., Boczarowski, A. and Sitek, S., 2008. Taphonomy of dense ophiuroid accumulations from the Middle Triassic of Poland. Lethaia 41, 47–58.

APPENDIX 1

1.1 Details on micro-computed tomography. In order to penetrate dense materials such as fossiliferous rock with X-rays, industrial tomography scanners are used, because these devices operate with high X-rays energies and generate very high-resolution data sets, unlike most medical CT scanners. The following components are common to all industrial and medical CT scanners: (1) an X-ray source; (2) a detector (used to acquire radiographs), and (3) an object to be scanned on a stage (Fig. 1.1) (Sutton *et al*., 2014). The basic principle is an object is exposed to collimated X-rays with parallel beams and the absorbed or scattered radiation is measured with a detector on the opposite side in order to obtain X-ray intensity values over a range of orientations as the sample or source/detector array are rotated. This data is then digitally reconstructed as tomograms, which are a virtual slice or cross-sectional images of the sample, using a filtered back projection algorithm (Sutton *et al*., 2014). Tomograms are orientated perpendicular to the axis of rotation and map the variation of X-ray attenuation (absorbed or scattered) within the sample (i.e. detect small differences in density and atomic number) (Sutton *et al*., 2014). This can allow for distinct mineral phases to be distinguished; in the case of palaeontological investigations, this might include differentiating the fossil specimens from the surrounding matrix. See du Plessis *et al*. (2016), for more details on the specific scanner used at CAF.

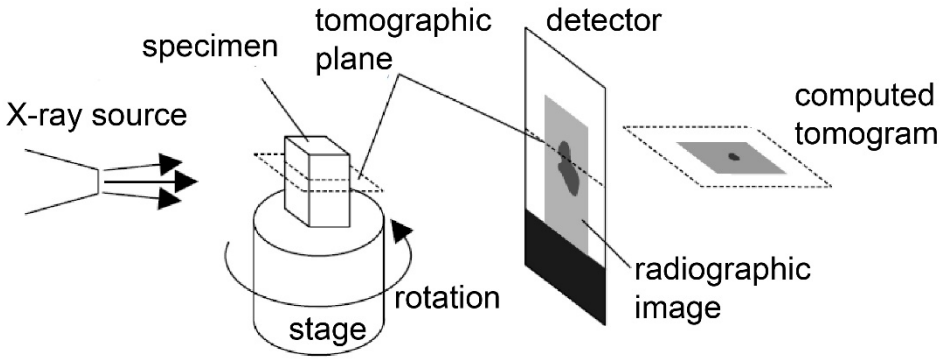

Figure 1.1. Basic components of a typical computed tomography scanner (CT) (taken from Sutton *et al*., 2014).

1.2 Problems encountered during CT scanning. In spite of the general preventative measures (see Methods chapter), a number of the scans had artefacts, which made the interpretation and analysis of the fossils very difficult, and sometimes even impossible.

Artefact is a term used in 3D digital CT scanning to describe any "systematic discrepancy between the CT numbers in the reconstructed image and the true attenuation coefficients of the object" (Barret and Keat, 2004, p. 2), in other words they are errors and mistakes that obscure details of the CT image. This type of problem often occurs in palaeontological samples because of the high density and large size of the fossil specimens, resulting in low transmission and high noise (Sutton *et al*., 2014). The first type of artefact identified is called *beam hardening* which is caused by a variation in the energy of the X-ray beam, a problem that arises when a higher energy X-ray is used to penetrate a dense sample (Abel *et al*., 2012). The result is that the edges of the sample appear to have brighter voxels (i.e., denser because of greater X-ray absorption or greater attenuation) than the centre, or there is artificial darkening at the centre, even though the sample is homogenous (Fig. 1.2A). It can also cause dark streaks along the long axis of a single high attenuation object (in this case pyrite, a common mineral in many rock samples, gives a 'star burst' appearance) (Fig. 1.2C). This made segmenting the ophiuroids (see below for details on segmenting) very difficult and even impossible in some cases, as the details towards the centre of the samples are lost. This is due to the fact that beam hardening changes the grey value of the material (and in this case the voids) depending upon its location in an image (Barret and Keat, 2004). There are a number of technical methods to prevent beam hardening and ring artefacts. As mentioned in the Methods (section 2.2), in this case a copper filter (0.1 mm metal film) was placed in front of the source in order to increase the average energy of the X-ray source by removing lower-energy X-rays, and allowing the remaining higher energy X-rays to penetrate more deeply (Sutton *et al*., 2014). Another artefact identified was *noise*, which gives the sample a grainy appearance and leads to blurring of the boundaries of the imaged object (in this case the large fossil voids versus the sedimentary rock matrix) (Fig. 1.2B). The noise is more pronounced at the centre of the sample (due to lower transmission) and was more prevalent in one direction. Lastly, *partial volume averaging*, which is inherent in all CT data, results from the intensity of any given voxel in a reconstruction, which is proportional to the mean attenuation coefficient within the voxel (Sutton *et al*., 2014). An additional problem during the scanning of the current fossiliferous samples was their large size and high density. A number of the samples had to be rescanned after removing most

of the unfossiliferous sedimentary rock matrix and cutting them fossiliferous bed into smaller fragments.

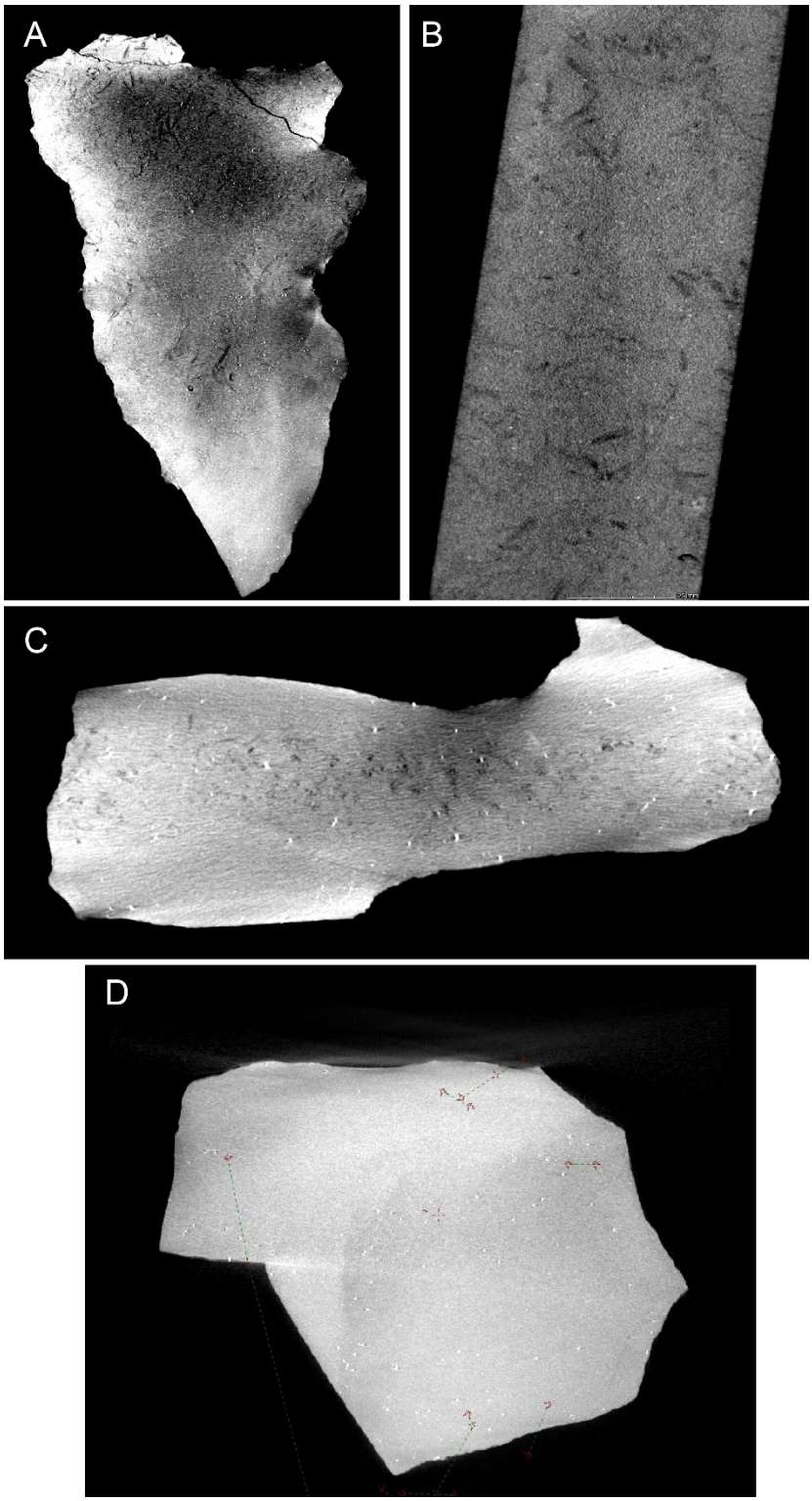

Figure 1.2. (**A**) Beam hardening artefact causing the centre of the sample to appear darker while the edges are much brighter. (**B**) Noise artefact casing the sample to appear grainy. (**C**) Beam hardening artefact causing the pyrite minerals to give a 'star burst' appearance. (**D**) Beam hardening artefact causing streaks across the sample.

1.3 Step by step process on virtual preparation. Virtual preparation and dissection of the specimens involves a series of modified steps outlined by Abel *et al.* (2012): (1) *Density contrast enhancement*: generation of a larger contrast between the grey scale values that represent the rock and surrounding air, by optimizing the grey value range on the histogram (Fig. 1.3). The x-axis denotes the grey values and the y-axis their count, thus showing how often certain grey values appear in the data set, more than one peak suggests a range of distinct attenuation materials; (2) *Register object*: aliment of the sample to a specific coordinate system so that the top-down 2D viewer of the slices cuts through the sample parallel to the bedding plane; (3) *Surface determination*: defining the material boundary of interest. This is generally the quickest and easiest way to separate a region of interest (ROI), however this was not possible due to the nature of the fossils having the same density (or grey scale value) as the permeating cracks in the samples and the surrounding air. It is for this reason that the region growing tool was predominantly used; (4) *Region growing*: generating a selection using a region growing algorithm. This is called *segmentation*, which essentially establishes the ROI (i.e., subparts of the volume data). After selecting a 'seed' point (in this case the 'black' voxel of a fossil or the voids within the rock sample), the algorithm will expand the selection to all voxels connected to that seed point based on a defined tolerance of voxel grey values relative to the selected seed point. The threshold (selection of voxels with grey values within the selected grey value interval) changed from sample to sample but was generally around ±5000 in this study. Region growing was the most time-consuming step as each individual fossil had to be segmented out in order to make the 3D volume rendering. Detection of the fossils was performed after careful macroscopic analysis of the sample and checking in the 3D live view on demand; (5) *Volume rendering*: generation of a 3D volume from the segmented 2D ROI's using a specific rendering algorithm (in this case, the isosurface render). Isosurfaces are mathematically defined surfaces calculated from a volume along points of interest (Sutton *et al*., 2014). The dataset is treated as a volume comprising cubic voxels (3D pixels that contain measurements of colour) instead of 2D pixels. Once the volume is created, the appearance of the volume objects can be manipulated (e.g., colour, transparency) to visualise the fossils in 3D. Each echinoderm specimen (as well as different orientations and decay stages) was given a colour and, by setting the surrounding matrix to transparent, their posture and orientation could be studied relative to one another. Switching the 3D volume 'on' and 'off' for each individual further helped to identify their position relative to each other in space. Lastly, once the fossils were segmented out, rendered in 3D and coloured

accordingly, the fossiliferous rock samples were 'stitched' together in order to recreate the entire bed. Using the volume import tool, each sample had to be manually aligned and placed in 3D space (Fig.1.3.1). This however proved to be a very difficult task as the available computing power was only a standard desktop PC Windows 7 64-bit operating system with an Intel Core processor and 100 GB of RAM, which only permitted the digital stitching of half of the scanned samples, and thus only half of the fossiliferous bed could be reconstructed digitally (Fig. 9 in methods section).

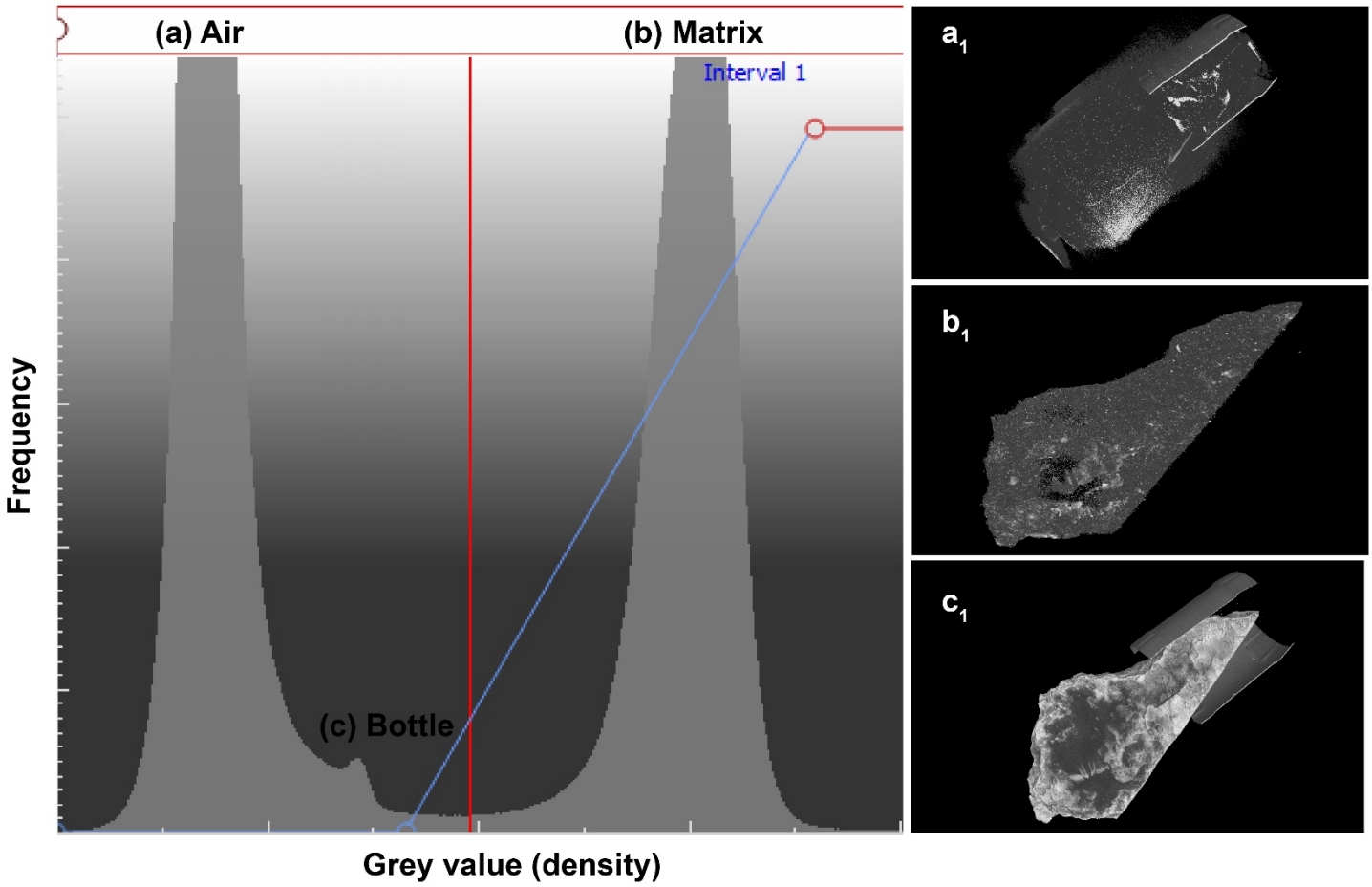

Figure 1.3. Micro-CT grey value frequency distribution plot. The histogram shows three peaks: (a) represents surrounding and internal air, as shown in the 3D view of a sample (a_1); (b) represents the matrix of the rock sample, as shown in the 3D view of a sample (b_1); (c) represents the plastic bottle used to hold the sample in place, as shown in the 3D view of a sample (c_1).

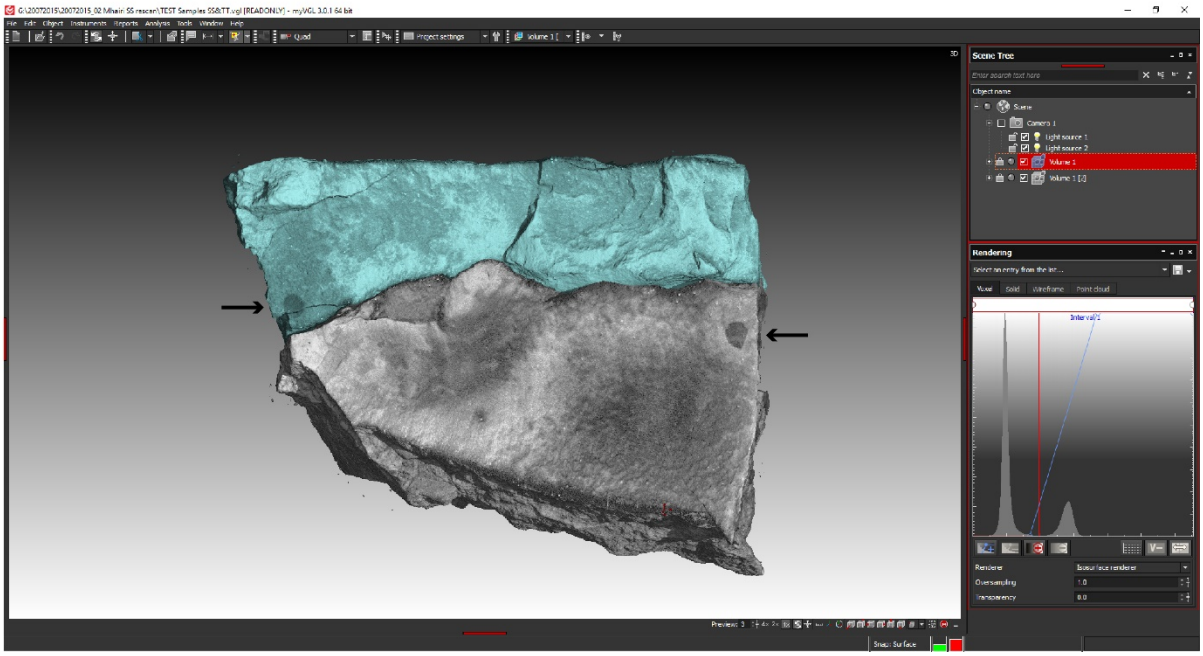

Figure 1.3.1. An example of two samples 'stitched' together within the 3D space. Black arrows point towards wax balls stuck to the upper surface of the samples to indicate right way up and relative positions.

1.4 Casting method. silicone rubber moulds were made from selected specimens. Detailed moulds were made using a low viscosity, two-part component silicone rubber (Mold Star® Smooth-On, Inc.). It is general convention for palaeontologists to use latex based rubber however due to the unavailability of a good product, room temperature vulcanization (RTV) silicone rubber was opted for instead. Silicone rubber has a major advantage over latex in that it has a very long shelf life (low levels of shrinkage), high strength and flexibility. There is however the misconception that silicone rubber does not provide the same high level of detail that latex does. Work by Rose (1983), Purnell (2003) and others disproved this notion. To check the quality of the moulds in this study, sample moulds were examined under the SEM at the University of Curtin where delicate features such as spine bases identified on the adambulacrals could be seen. The basic steps in the mould making process are as follows: prior to moulding, the specimens are cleaned with water, lightly brushed with a toothbrush and then dried naturally. Generally, a consolidant or release agent is applied in order to prevent loose parts of the specimen from being detached when the mould is removed, however in this case, because the specimens were initially pyritised and weathered to iron oxide, the moulding itself was used to clean out any remaining iron oxide in the fossil voids. The disadvantage to doing this is that the silicone fluid penetrates

the surface leaving a dark stain and can leave fragments of rubber in the undercuts or worse, it may destroy the specimen in the process. Each specimen was surrounded by a retaining wall of non-curing modelling clay in order to prevent the silicone from spilling beyond the specimen, but more importantly, to stop any movement of the silicone while curing. Parts A and Part B of the rubber were mixed together with black pigment powder, then placed into a vacuum chamber for a few minutes to eliminate all air bubbles trapped in the liquid. The silicone mixture was then poured onto the specimen. After approximately four hours (at 25 °C), the rubber was firm enough to peel off the specimen. Finally, the black silicone moulds were whitened with ammonium chloride and photographed using a 100 mm lens attached to Nikon DSLR camera.

APPENDIX 2. Surface area of the samples versus the number of ophiuroids and stylophorans in the Karbonaatjies obrution bed.

Sample no.	Surface area (mm)	Ophiuroid count (no. of disks)	*Placocystella africana* count (no. of thecae)	Paranacystid count (no. of thecae)
A	177 × 86	18	0	0
BC	164 × 85	64	1	14
D	125 × 102	33	0	16
E	86 × 83	21	0	12
E2	Not measured	1	0	8
F	102 × 226	32	0	8
F1	232 × 115	26	1	0
G	143 × 55	23	0	17
G2	70 × 27	0	0	2
F2	117 × 38	23	0	3
F	85 × 31	3	0	1
M	129 × 113	23	0	2
K	182 × 100	32	0	13
WW	114 × 116	32	0	3
WW2	75 × 40	10	0	1
VV3	97 × 57	16	0	4
VV2	86 × 80	26	1	7
X	110 × 47	6	0	1
W	156 × 140	47	0	4
R	242 × 58	46	3	6
P	210 × 135	66	1	3
O	220 × 170	34	0	7
UU	169 × 80	39	1	9
TT3	70 × 90	6	0	0
TT	149 × 75	46	0	8
SS	150 × 70	24	0	5
Total	**75 × 45 cm**	**714**	**8**	**145**

APPENDIX 3. Taphonomic parameters of ophiuroids from Karbonaatjies obrution bed. Missing data is recorded as n/a, and are due to scans being too faint and/or obscured by artefacts and/or 3D model unclear for measurements.

Sample No.	Ophiuroid arm length (mm)	Ophiuroid disc diameter (mm)	Orientation: oral side up (u), down (d), oblique (o)	Taphonomic grade
A	17,55	6,8	d	1
	17,33	7,21	u	1
	8,95	n/a	n/a	1
	9,66	n/a	d	1
	14,35	7,06	d	1
	17,31	6,95	d	2
	14,8	9,17	d	1
	13,51	7,19	u	1
	14,22	7,75	u	1
	14	7	u	1
	10,2	6,37	u	1
	12,25	6,05	u	1
	19,19	9,62	u	1
	10,24	8,2	u	2
	n/a	7,61	d	2
	13,41	7,16	u	1
	10,44	n/a	u	2
	16,6	8,02	d	1
BC	8,14	9,79	u	1
	18,34	9,26	d	1
	n/a	n/a	o	n/a
	12,48	6,03	d	1
	9,36	4,54	d	1
	n/a	n/a	n/a	n/a
	15,62	4,9	u	1
	n/a	n/a	n/a	n/a
	11,14	5,48	d	2
	7,69	4,93	d	2
	13,46	5,83	n/a	2
	13	n/a	d	1
	18	9,21	d	1
	15,57	7,77	d	1
	n/a	n/a	d	2
	12,82	7,43	u	1
	n/a	n/a	d	2
	23,36	9,33	d	1
	6,2	3,55	d	1
	n/a	6,83	d	2

n/a	n/a	n/a	3
n/a	n/a	n/a	3
11,45	9,96	u	2
12,79	n/a	d	1
11,79	7,69	d	1
n/a	n/a	o	2
n/a	n/a	d	1
15,25	6,25	d	1
n/a	n/a	n/a	2
n/a	n/a	d	n/a
14,48	n/a	d	1
n/a	n/a	n/a	n/a
4,44	2,39	o	1
12,13	7,4	d	1
13,01	5,95	d	2
9,17	n/a	d	2
n/a	n/a	n/a	3
6,05	3,13	d	1
17,62	n/a	d	1
n/a	6,37	d	2
15,3	5,95	d	1
13,59	9	d	2
10,73	4	u	2
14,55	6	d	1
11,68	4,92	d	1
17,89	55,42	d	1
n/a	7,12	u	1
13,14	8,21	d	1
n/a	n/a	u	2
13,05	7,54	d	1
14,98	n/a	d	2
n/a	n/a	o	1
12	2,72	d	2
16,15	8,06	d	1
n/a	n/a	d	2
n/a	9,01	u	1
12	n/a	u	2
14,09	8,56	d	1
n/a	n/a	d	2
n/a	9,11	u	1
11	9,03	u	1
12,41	n/a	u	1
n/a	n/a	n/a	2
n/a	n/a	o	1

D	n/a	n/a	n/a	2
	15,38	7,64	u	1
	n/a	n/a	d	2
	n/a	n/a	n/a	2
	n/a	7,64	u	1
	n/a	n/a	n/a	1
	13,79	7,86	d	2
	11	5,5	d	2
	n/a	n/a	n/a	2
	n/a	n/a	u	2
	n/a	7,64	u	2
	13,54	5,12	d	1
	n/a	7,19	d	2
	21,26	7,09	u	1
	n/a	n/a	u	2
	16,29	6,37	d	1
	17,14	8,01	d	2
	17,83	10,83	d	2
	6,77	5,35	u	2
	11,69	6,14	n/a	2
	n/a	6,64	d	2
	n/a	n/a	o	1
	n/a	8,44	d	2
	n/a	8,59	d	2
	15,82	8,16	d	1
	13,46	4,23	d	1
	13,57	6,02	u	1
	23,36	9,87	u	1
	n/a	7,28	d	2
	n/a	n/a	o	1
	n/a	n/a	o	2
	n/a	n/a	d	2
	17,1	9,08	u	1
E	6,34	2,16	d	1
	3,36	3,3	d	1
	16,17	5,7	u	2
	n/a	n/a	d	n/a
	n/a	n/a	u	n/a
	n/a	n/a	u	n/a
	9,41	6,23	d	2
	15,48	6,23	d	1
	13,52	6,5	u	2
	n/a	n/a	d	n/a
	n/a	n/a	u	n/a

	n/a	3,23	d	2
	n/a	n/a	o	2
	19,75	5,34	u	2
	n/a	n/a	n/a	n/a
	n/a	n/a	n/a	n/a
	n/a	5,78	d	2
	n/a	5,34	d	2
	n/a	n/a	o	2
	n/a	4,27	d	1
E2	n/a	n/a	n/a	1
F	11,23	6,58	u	1
	11,38	4,38	d	2
	10,83	8,17	d	1
	16,19	5,59	u	1
	9,63	5,95	d	1
	7,35	3,35	d	1
	7,08	3,45	d	1
	10,26	8,05	u	2
	12,67	3,75	u	n/a
	18,58	5,38	u	1
	11,77	6,22	u	2
	n/a	3,18	u	2
	10,62	4,62	d	n/a
	5,11	2,1	d	1
	19,21	8,46	d	1
	n/a	n/a	u	2
	n/a	n/a	d	1
	n/a	n/a	d	2
	n/a		o	2
	n/a	n/a	n/a	3
	n/a	n/a	n/a	2
	n/a	n/a	n/a	2
	15,83	7,65	d	1
	n/a	n/a	n/a	2
	n/a	n/a	n/a	2
F1	22,29	10,2	u	2
	20	8,3	u	2
	14,23	4,62	u	2
	14,23	6,88	u	1
	14,7	8,03	u	1
	17,84	5,53	d	1
		5,8	u	3
	17,13	4,84	d	1

	16,18	7,68	d	1
	13,22	7,41	d	2
	n/a	n/a	o	1
	n/a	n/a	o	1
	n/a	n/a	u	2
	n/a	7,07	u	2
	n/a	n/a	d	2
	20,38	10,52	d	1
	n/a	n/a	d	2
	n/a	n/a	d	1
	n/a	n/a	d	2
	n/a	n/a	d	1
	n/a	n/a	o	1
	n/a	6,41	d	1
	16,05	4,42	d	1
G	14,81	6,62	d	1
	13,42	6,57	d	1
	19,57	8,83	d	1
	21,83	11,24	u	1
	16	8	d	1
	18,85	9,56	d	1
	14,96	7,88	d	1
	n/a	n/a	d	1
	n/a	4,17	d	2
	n/a	n/a	d	2
	n/a	n/a	d	1
	17,81	7,81	u	1
	21,31	6,28	u	1
	5,01	2,88	d	1
	n/a	n/a	d	2
	14,87	n/a	u	
	n/a	7,02	u	2
	7,59	5,4	d	1
	n/a	n/a	d	2
	15,33	8,74	u	1
	16,94	8	u	1
F2	n/a	n/a	o	1
	13,9	6,7	d	1
	10,09	5,45	u	1
	7,17	3,74	u	1
	n/a	n/a	o	1
	n/a	7,39	u	2
	n/a	n/a	d	2
	n/a	7,68	u	2

	n/a	n/a	o	1
	18,32	7,67	u	1
	n/a	n/a	n/a	2
	n/a	n/a	n/a	2
	11,77	3,67	n/a	1
	n/a	n/a	u	3
	n/a	n/a	o	1
	n/a	n/a	o	1
	17,77	6,37	u	1
	7,72	4,05	u	1
	n/a	6,12	d	2
	n/a	n/a	n/a	2
	n/a	n/ n/a a	o	1
	1,24	2,61	d	1
	n/a	n/a	o	1
F bottom	n/a	n n/a /a	u	2
	8,04	n/a n/a	d	1
M	14,12	8,59	u	2
	13,57	9,9	u	2
	16,81	n/a	d	1
	9,46	6,01	u	2
	12,611	7,14	u	1
	n/a	n/a	d	2
	n/a	n/a	u	1
	14,88	5,31	u	1
	n/a	n/a	o	1
	n/a	n/a	o	1
	11,54	n/a	u	1
	15,71	8,27	u	1
	n/a	n/a	d	1
	n/a	7,12	d	1
	15,2	n/a	o	1
	n/a	n/a	u	3
	n/a	8,07	u	1
	n/a	n/a	o	1
	20	6,18	d	1
	n/a	7,43	u	2
	n/A	n/a	n/a	3
	10,78	4,48	d	1
	N/A	n/a	n/a	3
k	20,7	9,58	u	1
	n/a	5,43	u	1
	14,95	5,48	u	1
	n/a	5,15	u	3

	14,31	n/a	d	2
	n/a	n/a	d	2
	n/a	9,8	u	1
	n/a	8,73	d	2
	n/a	6,12	d	1
	n/a	3,8	d	2
	n/a	n/a	d	1
	17,54	4,9	u	1
	16,93	n/a	d	1
	n/a	4,43	u	3
	10,08	n/a	d	1
	n/a	3,91	u	1
	n/a	4,22	d	2
	n/a	n/a	d	1
	12,79	n/a	u	1
	n/a	n/a	d	1
	17,8	8,77	u	2
	14,57	8,57	u	1
	16,58	8,9	d	1
	n/a	8,47	d	2
	16,34	8,83	u	2
	n/a	n/a	d	2
	n/a	n/a	d	3
	19,29	7,2	u	1
	6,54	3,04	d	1
WW	n/a	n/a	o	1
	17,7	6,37	d	1
	n/a	n/a	o	1
	n/a	n/a	o	1
	17,02	9,95	d	1
	n/a	n/a	o	1
	n/a	n/a	u	2
	17,66	9,84	u	1
	17,66	9,84	u	1
	n/a	5,62	d	2
	n/a	6,47	d	1
	n/a	4,61	d	2
	12,84	6,99	u	1
	23,73	10,3	d	1
	n/a	n/a	u	1
	19,84	11,27	d	1
	16	6,9	u	2
	n/a	6,27	n/a	2

	n/a	6,1	u	2
	n/a	n/a	o	1
	n/a	n/a	d	2
	n/a	n/a	d	1
	n/a	n/a	n/a	1
	n/a	n/a	o	1
	n/a	n/a	o	1
	17,02	9,95	d	1
	11,89	n/a	d	1
	n/a	n/a	o	1
WW2	n/a	14,52	o	2
	n/a	n/a	n/a	2
	n/a	n/a	d	1
	n/a	n/a	d	1
	n/a	n/a	d	2
	n/a	n/a	n/a	1
	17,86	5,44	u	1
	21,58	5,46	d	1
	n/a	n/a	o	1
	n/a	n/a	o	1
VV3	15,83	5,01	d	1
	n/a	n/a	d	2
	14,6	6,86	d	1
	n/a	n/a	o	1
	n/a	n/a	d	2
	14,88	6,67	d	1
	22,06	8,23	d	1
	n/a	n/a	d	1
	n/a	n/a	o	1
	n/a	2,29	u	2
	n/a	n/a	u	2
	n/a	n/a	d	1
	n/a	n/a	u	1
	n/a	n/a	d	2
	n/a	2,45	u	1
	7,67	2,96	d	1
VV2	n/a	n/a	o	1
	11,4	4,84	d	1
	12	8,22	d	1
	n/a	5,57	d	1
	16,49	7,19	d	2
	n/a	n/a	d	2
	16,93	6,78	d	1
	n/a	6,85	d	2

	n/a	n/a	o	1
	n/a	n/a	n/a	2
	15,39	6,25	d	1
	n/a	n/a	d	2
	n/a	n/a	n/a	3
	n/a	n/a	d	2
	n/a	n/a	n/a	2
	n/a	n/a	d	2
	n/a	n/a	o	1
	18,21	n/a	d	2
	4,22	2,57	d	1
	5,74	2,95	d	1
	n/a	7,22	u	3
	n/a	5	u	2
	n/a	7	d	2
	16	7,18	u	1
	13	6,39	d	1
	16	5,15	d	1
X	n/a	6,65	u	2
	17,54	n/a	u	1
	n/a	n/a	u	2
	18,72	9,39	d	1
	10,4	n/a	d	1
	n/a	5,53	u	1
W	20,91	8,5	u	1
	n/a	7,16	u	3
	n/a	7	u	3
	n/a	8,82	u	1
	19	7,12	d	1
	n/a	7,12	o	1
	n/a	n/a	d	1
	16,72	6,49	d	2
	13,24	5,81	d	1
	14,98	5,11	u	2
	6	3,04	d	1
	n/a	7,37	u	2
	n/a	n/a	o	1
	n/a	n/a	u	2
	15	5,2	d	2
	n/a	n/a	o	1
	n/a	n/a	d	2
	12	6	d	1
	15,46	8,03	u	2
	13,56	7,31	d	2

	n/a	7,65	u	2
	n/a	n/a	d	3
	n/a	6,38	d	2
	n/a	7,91	u	2
	20	9,1	u	2
	17	8,29	u	1
	19	9,07	d	1
	n/a	7,65	d	2
	n/a	7,62	d	2
	n/a	n/a	n/a	3
	n/a	7,71	d	1
	n/a	10,14	d	2
	n/a	7,81	d	2
	19	7,59	d	1
	16,44	8,13	d	2
	18	7,08	u	1
	18	9,55	d	1
	n/a	n/a	n/a	3
	n/a	n/a	n/a	2
	n/a	n/a	d	2
	n/a	9,25	d	2
	15,75	8,57	d	2
	n/a	n/a	d	3
	n/a	n/a	o	1
	n/a	7,37	u	2
	n/a	6,44	d	2
	4	1,67	n/a	1
R	18,97	9,44	d	1
	n/a	7,9	d	2
	n/a	10,04	d	2
	n/a	4,67	u	2
	n/a	6,29	u	2
	n/a	7,06	u	2
	n/a	7,02	u	1
	n/a	n/a	d	?
	12,49	6,05	d	1
	n/a	n/a	d	2
	n/a	9,31	d	2
	18,99	8,29	u	1
	n/a	6,01	o	1
	13,99	n/a	u	1
	n/a	7,11	d	2
	n/a	6,9	u	1
	17,72	7,71	d	1

	n/a	6	u	2
	n/a	n/a	o	2
	n/a	n/a	n/a	2
	17,83	6,19	u	2
	n/a	n/a	d	2
	n/a	n/a	d	3
	n/a	n/a	d	2
	n/a	n/a	d	2
	17,04	6	d	1
	7,01	2,51	d	1
	n/a	8,04	d	2
	4,76	2,35	d	1
	n/a	n/a	n/a	2
	6,18	2,43	d	1
	n/a	n/a	d	1
	n/a	n/a	o	1
	7,5	1,9	u	1
	n/a	n/a	d	2
	n/a	n/a	o	1
	n/a	n/a	d	1
	n/a	5,38	d	3
	n/a	n/a	d	2
	n/a	4,01	d	2
	n/a	5,63	d	1
	n/a	n/a	o	1
P	n/a	6,91	u	3
	17,25	8,27	u	1
	5,33	3,06	d	1
	6,24	n/a	o	1
	n/a	n/a	d	2
	18,82	8,43	u	1
	18,25	8,31	d	1
	n/a	8,04	d	3
	8,9	4,37	d	1
	n/a	8,49	u	2
	n/a	n/a	d	2
	n/a	8,38	u	2
	n/a	n/a	d	2
	n/a	n/a	u	2
	18,68	7,25	d	1
	3,98	2,1	d	1
	17	9,11	d	1
	15,74	6,92	d	1

19,22	9,1	u	1
15,28	7,44	u	2
n/a	n/a	d	2
17,96	6,74	d	2
n/a	7,52	u	2
n/a	9,53	d	2
n/a	8,36	d	1
8,56	4,15	d	2
n/a	8	u	2
n/a	8	u	2
n/a	8,3	d	3
n/a	n/a	d	2
n/a	n/a	d	3
n/a	7,56	d	1
n/a	n/a	u	2
5,78	2,7	d	1
2,27	1,45	d	1
n/a	n/a	u	2
16,44	8,5	d	1
n/a	n/a	u	2
8,54	4,89	d	1
15,57	8,26	u	1
15,57	n/a	d	1
n/a	n/a	d	1
n/a	n/a	d	1
n/a	n/a	o	1
n/a	n/a	u	2
n/a	n/a	d	1
n/a	n/a	d	2
n/a	n/a	o	1
n/a	n/a	o	1
n/a	n/a	o	1
n/a	n/a	o	1
n/a	2,21	d	1
n/a	n/a	o	1
5,71	3,14	d	1
7,88	3,52	d	1
3,02	1,77	d	1

	6,54	n/a	o	1
	n/a	n/a	o	1
	n/a	2,32	d	1
	n/a	n/a	o	2
	2,53	1,78	d	1
	n/a	n/a	o	1
	n/a	n/a	o	1
O	21,23	10,93	d	1
	14,28	7,37	d	1
	n/a	n/a	o	2
	n/a	5,58	u	2
	17,92	6,58	u	2
	6,37	3,06	d	1
	8,23		o	1
	16,25	9,71	d	1
	4,63	2,65	d	1
	19,26	6,87	d	2
	9,85	4,97	d	2
	16,02	6,38	d	1
	n/a	n/a	d	2
	n/a	n/a	o	1
	n/a	n/a	o	2
	17,19	7,39	u	1
	15,76	8,03	d	1
	n/a	7,93	u	1
	n/a	n/a	u	2
	n/a	n/a	o	2
	n/a	6,84	u	1
	n/a	n/a	o	1
	n/a	n/a	u	2
	n/a	n/a	d	2
	n/a	n/a	u	2
	n/a	n/a		2
	n/a	n/a	o	1
	n/a	n/a	u	2
	n/a	n/a		3
	n/a	n/a	o	1
	13,45	n/a	o	1

	16,65	n/a	d	1
	n/a	2,72	u	1
	n/a	5,93		3
UU	n/a	7,11	u	2
	n/a	6,27	u	2
	n/a	2,99	d	2
	n/a	8,39	d	2
	n/a	6,8	o	2
	n/a	7,72	d	2
	n/a	7,23	d	2
	n/a	9,98	u	2
	n/a	n/a	o	1
	n/a	n/a	o	1
	n/a	n/a	o	2
	n/a	n/a	u	2
	n/a	6,4	d	2
	n/a	6,37	d	2
	n/a	5,87	u	2
	n/a	n/a	d	2
	n/a	n/a	d	3
	n/a	9.84	u	2
	n/a	n/a	d	2
	n/a	6.38	d	2
	n/a	n/a	d	2
	n/a	n/a	o	2
	17.04	6.44	d	1
	n/a	7.06	u	2
	n/a	n/a	o	2
	16.80	6,16	u	1
		3,62	d	2
	6,26	3,35	d	1
	n/a	n/a	o	2
	n/a	7,27	d	2
	n/a	n/a	o	1
	n/a	n/a	d	2
	n/a	5,22	d	1
	n/a	6,16	u	2

	n/a	n/a	d	3
	2,51	2,38	d	1
	n/a	n/a	d	2
	n/a	8,28	u	2
	3,48	2,68	d	1
UU2	16,84	7,12	d	1
	n/a	n/a	d	2
	n/a	n/a	o	1
	n/a	5,28	d	2
	n/a	n/a	o	1
	n/a	6,93	u	2
	n/a	7,11	u	2
	n/a	8,96	u	2
	n/a	6,83	u	2
	19,67	6	d	1
TT3	n/a	6,66	d	1
	n/a	n/a	d	2
	n/a	n/a	d	2
	n/a	6	u	2
	n/a	n/a	o	1
	n/a	3,02	d	1
TT2	n/a	8,32	u	2
	n/a		d	1
	5,1	2,85	d	1
	17,08		d	1
	7,47	3,57	d	1
	16,92	6,77	u	1
	3,27	1,9	d	1
TT	n/a	7,14	u	1
	n/a	n/a	d	1
	n/a	6,54	d	2
	n/a	7,26	u	1
	19	8,41	u	1
	n/a	n/a	o	1
	n/a	6,94	d	1
	17	8,3	u	1
	n/a	n/a	d	1
	n/a	9,35	d	2

	n/a	7,99	d	1
	n/a	n/a	d	
	n/a	6,09	d	1
	n/a	6,42	d	2
	n/a	7,18	d	1
	n/a	6,09	d	1
	n/a	6,81	u	1
	n/a	6,54	u	2
	5,88	2,36	d	1
	n/a	n/a	o	1
	n/a	n/a	o	1
	17,73	8,23	d	1
	n/a	n/a	d	3
	19,52	8,05	u	2
	n/a	7,24	d	2
	n/a	6,66	u	2
	n/a	10,37	d	2
	17	8,18	d	1
	9,1	3,39	d	1
	4,57	3,37	d	1
	18,57	8,1	d	2
	20,14	8,82	d	1
	20,14	8,82	d	1
	3,04	1,89	d	1
	n/a	6,64	d	1
	n/a	8,89	d	2
	n/a	5,39	o	1
	n/a	n/a	d	1
	n/a	7,26	d	2
	n/a	8,72	u	2
	n/a	6,15	d	2
	n/a	8,4	u	2
	n/a	n/a	o	2
	n/a	7,41	d	1
	n/a	7,35	d	2
	n/a	n/a	o	1
SS	n/a	7,79	u	3
	n/a	3,46	d	2
	15,63	8,66	u	2

22,17	8,86	u	1
3	2,98	d	1
3,54	2,84	d	1
n/a	n/a	u	2
8,09	3,41	d	1
n/a	6,47	d	2
n/a	n/a	o	2
n/a	n/a n/a	u	2
16,05	7,04	u	1
n/a		d	2
n/a	n/a	d	2
23,47	n/a	d	2
7	3,45	d	1
18	8,45	u	2
8,31	5	d	1
20,2	7,93	u	1
n/a	7,47	u	1
n/a	11,11	u	2
n/a		d	2
n/a	n/a	o	2
2,73	2,15	d	1

APPENDIX 4. Measured thecal width versus length of the paranacystids in each sample as well as orientation of the aulacophore and taphonomic grade. Missing data recorded as n/a and are due to scans being too faint and/or obscured by artefacts and/or 3D model unclear for measurements.

Sample No.	Thecal width (mm)	Thecal length (mm)	Orientation of aulacophore	Taphonomic grade
BC	2,51	4,2		1
	1,71	4	over theca (top)	1
	2,15	4,08		1
	1,79	4,37	curved to side	1
	1,89	3,87		1
	2,36	3,7	over theca (top)	1
	1,73	3,49	over theca (bottom)	1
	2,11	3,8		1
	n/a	n/a		2
	2,2	3,74	over theca (bottom)	1
	2,1	4		1
	1,35	4,03	curved to side	1
	1,36	3,18	stretch out	1
	2,38	3,21		1
D	2,15	3,78	over theca (top)	1

	2,13	4,35		2
	2,39	3,79		1
	1,79	3,55		1
	2,03	4,35		1
	n/a	n/a		2 (too faint)
	1,84	3,98		2 (too faint)
	2,01	4,08		1
	2,42	4,61	curved to side	1
	2,07	3,82		1
	2,08	3,79		1
	n/a	n/a		2 (no theca)
	2,49	4,57	curved to the side	1
	2,27	4,55	curved to side	
	n/a	n/a		2 (no theca)
E	n/a	n/a		2
	1,64	3,55	arm over theca (top)	1
	1,86	3,75		1
	n/a	n/a		2
	1,25	3,94	arm curved to side	1
	2,35	4,52	arm over theca (bottom)	1
	n/a	3,94	arm curved to side	1
	n/a	n/a		2
	3,47	2,24		
	2,14	4,99	arm stretch out	1
	2,65	4,82		1
E2	2,29	3,78	arm curved to side	1
	1,68	3,6		1
	1,78	3,6		1
	n/a	n/a		2(no theca)
	1,62	2,69		1
	2,09	3,26		1
	1,7	2,98	arm curved to side	1
	2,13	3,37	arm curved to side possible digit??	1
F	0,99	1,95		1
	2,28	4,79	arm curved to side	1
	n/a	3,59		2
	2,07	3,49		1
	1,35	3,18		1
	1,7	3,99		1
	1,9	2,89		1
	2,01	4,25		1
G	2,11	3,49	arm curved to side	1
	2,61	5,23	arm flexed up (top)	1

	1,33	3,14	no arm	2
	1,72	3,59	no arm	2
	n/a	n/a	no theca just aulco	2
	1,82	3,83		1
	2,71	4,81		1
	1,38	3,75		1
	n/a	4,21		2
	1,96	4,8	arm curved to side	1
	1,93	3,8	arm curved to side	1
	1,11	3,13	on its side	1
	2,25	4,01	arm stretched out	1
	n/a	n/a	no theca	2
	1,61	2,27	no arm but aulco	1
	1,97	2,88		1
	2,48	4,22		1
G2	1,91	3,34		1
	3,28	5,37		1
F2	2,37	3,91	arm curved to side	1
	1,5	3,12		1
	2,09	4,97	arm flexed up (top)	1
F bottom	1,59	3,42	no auclophore	2
M	1,19	4,4		1
	2,81	5,5		1
K	1,55	2,87		1
	1,87	4,38	arm flexed up (bottom)	1
	2,37	4,68		1
	n/a	4,78		1
	1,88	3,85	flexed up top	1
	2,43	4,3		1
	1,34	3,27		1
	2,16	3,53		1
	n/a	4,51		1
	n/a	n/a		2
	2,4	4,95	flexed up top	1
WW	2,3	4,95		1
	1,87	4,95	curved to side	1
	2,1	4,53	flexed over theca (up)	1
WW2	2,14	4,95	flexed under	1
VV3	1,85	4,81	curved under	1
	n/a	n/a		2
	1,65	3,27	curved under	1
	n/a	3,98	curved to side	1
VV2	1,91	4,14	curved up	1

	2,38	5,56	curved to side	1
	2,19	4,3		1
	2,18	5,51	curved under	1
	2,03	3,1	curved arm	1
	2,51	5,38	curved arm	1
	1,91	3,47		1
X	2,17	4,41		1
W	2,48	4,92		1
	1,89	3,26	arm	1
	2,19	3,85		1
	2,11	5,01		1
R	2,12	5,27	flexed over theca top	1
	2,03	4,53		1
	1,98	4,78		2
	2,44	4,75	curved under theca	1
	2,81	4,8	curved to the side	1
	n/a	2,57		2
P	n/a	5,71	on its side, arm on side	1
	2,27	4,61	curved to side	1
	1,92	5,41		1
O	2,3	5,53	curved under	1
	2,71	4,85	curved to the side	1
	n/a	4,78		1
	2,3	4,38	curved up	1
	2,22	4,18		1
	1,79	3,58	curved to side	1
	1,69	3,39		1
UU	2	3,96		1
	2,36	4,4	curved up	1
	2,17	4,87	curved up	1
	2,13	5,87		1
	1,41	2,54		1
	2,65	4,15		2
	1,66	3,99		1
	2,36	4,73	curved to side	1
	2,68	4,66	curved up	1
TT2	1,92	4,81	curved to side	1
TT	2,54	4,93	curved to side	1
	2,64	4,41	flexed up top	1
	2,37	3,39		1
	1,73	3,08		1
	1,96	3,2	flexed up top	1
	1,93	3,16		1

	2,2	4,57	curved to side	1
	2,16	4,08	curved to side	1
SS	1,73	3,89		1
	1,88	3,85		1
	2,5	5	curved up	1
	1,98	4,68	curved to side	1
	1,37	2,86		1

APPENDIX 5. Measured thecal width versus length of the *Placocystella* in each sample as well as orientation defined by the position of the brachial and taphonomic grade. Missing data recorded as n/a and are due to scans being too faint and/or obscured by artefacts and/or 3D model unclear for measurements

Sample No.	Thecal width (mm)	Thecal length (mm)	Orientation	Taphonomic grade
BC	10,41	13,14	brachial down	1
F1	8,83	13,42	brachial down	2
VV2	10,21	13,32	brachial down	1
W	9,13	12,15	n/a	1
R	8,73	13,77	n/a	2
	9,37	12,79	n/a	1
P	9,46	11,72	n/a	2
UU2	6,45	6,18	brachial up	1

APPENDIX 6. Basic statistics and results of normality tests.

	Ophiuroids	Paranacystids
N	415	139
Min	1,45	1,95
Max	14,52	5,87
Mean	6,577831	4,078489
Median	6,88	4,01
Std. error	0,1052746	0,066476
Stand. dev	2,144606	0,783736
Skewness	-0,2998331	-0,1185
Kurtosis	-0,05621089	-0,31847
Shapiro-Wilk W	0.9754	0.9921
Shapiro-Wilk Probability	1.769E-06	0.6274

APPENDIX 7. Taphonomic parameters of brachiopods extracted from Karbonaatjies obrution bed. All shells are disarticulated. Missing data recorded as n/a and are due to scans being too faint and/or obscured by artefacts and/or 3D model unclear for measurements.

Sample no.	Fragmentation	Brachial (b) or pedical (p) valve	Convex up (u) or down (d)	Orientation	Borings	Valve length (mm)	Valve width (mm)
Z	low	p	n/a	v		65	n/a
XX	high	p	u	h		n/a	n/a
	high	p	d	h	yes	n/a	n/a
F1	moderate	p	d	h		54,1	22,48
	high	n/a	u	h		n/a	n/a
	moderate	p	u	h		n/a	n/a
G	moderate	p	u	h		n/a	n/a
	high	p	u	h		n/a	n/a
UU	high	n/a	n/a	n/a	yes	n/a	n/a
F	high	b	d	h		n/a	30
	high	p	u	h		n/a	n/a
OO	high	p	d	h		n/a	n/a
RR	moderate	p	u	h		43,15	n/a
	high	p	u	h		33,53	n/a
Fb	moderate-h	p	d	h		3,5	2
	m-h	b	u	h		n/a	n/a
P	mod	p	d	h		61,34	n/a
CC	m-h	b	u	h		n/a	n/a
PP	m-h	p	d	h		n/a	n/a
	m-h	p	d	h		n/a	n/a
Q	m-h	b	u	h	yes	n/a	n/a
J	m-h	p	u	h		n/a	n/a
	m-h	b	u	h	yes	n/a	n/a
HH	m-h	p	u	h		n/a	n/a
	m-h	p	d	h		n/a	n/a
EE	m-h	p	u	h		n/a	n/a
	m-h	b	u	h		n/a	n/a
QQ	m-h	p	d	h		n/a	n/a
K	high	n/a	u	sub-h	yes	n/a	n/a

	high	n/a	u	h	yes	n/a	n/a
	high	n/a	u	h	yes	n/a	n/a
AA	m	p	u	h	yes	55	n/a
LT	m	p	d	h		18,35	7,18
CC2	L-m	p	d	h		63	34
	L-M	p	d	h		42	22,3
W2	m	p	d	h	yes	23,84	n/a
N	m	p	d	h		33,7	n/a
SS	m	p	u	h	yes	30,26	23,57
	m	p	d	h		52,98	40,47
Y	l-m	p	d	h		62,97	32,86
JJ	m	p	u	h	yes	52,64	17.59
GG	m-h	p	u	h		n/a	n/a

APPENDIX 8. Taphonomic parameters of bivalves extracted from Karbonaatijies obrution bed. All shells are disarticulated. Missing data recorded as n/a and are due to scans being too faint and/or obscured by artefacts and/or 3D model unclear for measurements.

Sample no.	**Fragmentation**	**Right (R) or left (L) valve**	**Convex up (u) or down (d)**	**Orientation**	**valve length (cm)**	**valve width (cm)**
F1	high	n/a	n/a	h	n/a	n/a
	high	R	u	h	n/a	
G	high	n/a	d	h	n/a	n/a
UU	low	R	u	h	4	3
F	moderate	L	u	h	n/a	n/a
ZZ	moderate	R	u	h	n/a	n/a
RR	low	L	u	h	3	2
XX	low	L	u	h	n/a	n/a

APPENDIX 9.

Our Ref: HM\CAPE WINELANDS\BREEDE VALLEY\TOUWS RIVER\BOKKEVELD STARFISH PALAEO PERMIT

iLifa leMveli iePhondo Kolony Erfenis Wes-Kaap Heritage Western Cape

Enquiries	Guy Thomas	**Date:**	12 June 2015
Tel:	021 483 9685	**Case No:**	15060901GT0610E
Email:	guy.thomas@westerncape.gov.z	**Auto IDs:**	3383 - 4086

PERMIT
In terms of section 35(4) of the National Heritage Resources Act (Act 25 of 1999) and the Western Cape Provincial Gazette 6061, Notice 298 of 2003

Attention: Dr Wendy Taylor
Department of Geological Sciences
University of Cape Town
13 University Avenue, Rondebosch
7701

CASE NUMBER: 15060901GT0610E
SECTION 35 PERMIT: PROPOSED PALAEONTOLOGY EXCAVATION IN A ROAD CUTTING OF THE N1, APPROXIMATELY 16KM SOUTH WEST OF TOUWSRIVIER

The matter above has reference.

To: DR W. Taylor
of: Department of Geological Sciences, University of Cape Town
for: Excavation and collection
of: Fossil Material
from: N1 Road reserve, in vicinity of 33.400992 S and 19.878514 E

1. This permit is valid until 30 June 2015.

Terms and Conditions:

1. If the permit holder is not to be present on the site at all times then HWC must be provided with the names and qualifications of the authorized representatives.
2. Adequate recording methods as specified in the Regulations and Guidelines pertaining to the National Heritage Resources Act must be used.
3. A final report, in both digital and hardcopy format, MUST be submitted to HWC on or before 12 June 2018. An extension to this permit can be granted on submission of a progress report (if work was initiated) and a letter stating reasons for the extension. HWC reserves the right to withhold further permits if progress is not deemed satisfactory.
4. All material collected and excavated, as well as field notes and records, will be curated by the Iziko: South African Museum.
5. Reprints of all published papers or copies of theses or reports resulting from this work must be lodged with HWC.
6. If a published report has not appeared within three years of the lapsing of this permit, the report in terms of the permit will be made available to researchers on request.
7. It is the responsibility of the permit holder to obtain permission from the landowner for each visit, and conditions of access imposed the landowner must be observed.
8. HWC shall not be liable for any losses, damages or injuries to persons or properties as a result of any activities in connection with this permit.
9. HWC reserves the right to cancel this permit by notice to the permit holder.

Should you have any further queries, please contact the official above and quote the case number above.

Yours faithfully

Signed

Dr Errol Myburg
Interim Chief Executive Officer
Heritage Western Cape

www.capegateway.gov.za/culture_sport

Street Address: Protea Assurance Building, Green Market Square, Cape Town, 8000 • **Postal Address:** Private Bag X9067, Cape Town, 8001 • **Tel.** +27 (0)21 483 5959 • **E-mail:** hwc.hwc@westerncape.gov.za

Straatadres: Protea Assuransie-gebou, Groentemarkplein, Kaapstad, 8000 • **Posadres:** Privaatsak X9067, Kaapstad, 8001 • **Tel:** +27 (0)21 483 5959 • **E-pos:** hwc.hwc@westerncape.gov.za